7

COMPTON SCATTERING

7.1 CROSS SECTION AND ENERGY TRANSFER FOR THE FUNDAMENTAL PROCESS

Scattering from Electrons at Rest

For low photon energies, $h\nu \ll mc^2$, the scattering of radiation from free charges reduces to the classical case of Thomson scattering, discussed in Chapter 4. Recall that for Thomson scattering, when the incident photons are approximated as a continuous electromagnetic wave [cf. Eq. (3.40)],

$$\epsilon = \epsilon_1, \tag{7.1a}$$

$$\frac{d\sigma_T}{d\Omega} = \tfrac{1}{2} r_0^2 (1 + \cos^2\theta), \tag{7.1b}$$

$$\sigma_T = \frac{8\pi}{3} r_0^2. \tag{7.1c}$$

Here ϵ and ϵ_1 are the incident and scattered photon energy, respectively, $d\sigma_T/d\Omega$ is the differential Thomson cross section for unpolarized incident radiation, and r_0 is the classical electron radius. When $\epsilon = \epsilon_1$, the scattering is called *coherent* or *elastic*.

Quantum effects appear in two ways: First, through the kinematics of the scattering process, and, second, through the alteration of the cross sections. The kinematic effects occur because a photon possesses a momentum $h\nu/c$ as well as an energy $h\nu$. The scattering will no longer be elastic ($\epsilon_1 \neq \epsilon$) because of the recoil of the charge. Let us set up the conservation of energy and momentum relations. The initial and final four-momenta of the photon are $\vec{P}_{\gamma i} = (\epsilon/c)(1, \mathbf{n}_i)$ and $\vec{P}_{\gamma f} = (\epsilon_1/c)(1, \mathbf{n}_f)$ and the initial and final momenta of the electron are $\vec{P}_{ei} = (mc, \mathbf{0})$ and $\vec{P}_{ef} = (E/c, \mathbf{p})$, where $\mathbf{n}_i$ and $\mathbf{n}_f$ are the initial and final directions of the photons (see Fig. 7.1). Conservation of momentum and energy is expressed by $\vec{P}_{ei} + \vec{P}_{\gamma i} = \vec{P}_{ef} + \vec{P}_{\gamma f}$. Rearranging terms and squaring gives $|\vec{P}_{ef}|^2 = |\vec{P}_{ei} + \vec{P}_{\gamma i} - \vec{P}_{\gamma f}|^2$, which eliminates the final electron momentum. We thus finally obtain

$$\epsilon_1 = \frac{\epsilon}{1 + \dfrac{\epsilon}{mc^2}(1 - \cos\theta)}. \tag{7.2}$$

In terms of wavelength, this can be written:

$$\lambda_1 - \lambda = \lambda_c(1 - \cos\theta) \tag{7.3a}$$

where the *Compton wavelength* is defined by

$$\lambda_c \equiv \frac{h}{mc} = 0.02426 \text{ Å for electrons.} \tag{7.3b}$$

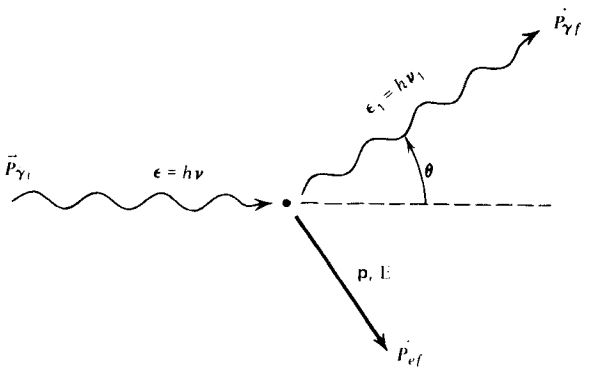

Figure 7.1 Geometry for scattering of a photon by an electron initially at rest.

We see that there is a wavelength change of the order of λ_c upon scattering. For long wavelengths $\lambda \gg \lambda_c$ (i.e., $h\nu \ll mc^2$) the scattering is closely elastic. When this condition is satisfied, we can assume that there is no change in photon energy in the rest frame of the electron.

Although a derivation is outside the scope of this text, let us briefly describe the quantum effect on the cross section. The differential cross section for unpolarized radiation is shown in quantum electrodynamics (Heitler, 1954) to be given by the *Klein–Nishina* formula

$$\frac{d\sigma}{d\Omega} = \frac{r_0^2}{2}\frac{\epsilon_1^2}{\epsilon^2}\left(\frac{\epsilon}{\epsilon_1} + \frac{\epsilon_1}{\epsilon} - \sin^2\theta\right). \tag{7.4}$$

Note that for $\epsilon_1 \sim \epsilon$ Eq. (7.4) reduces to the classical expression. The principal effect is to *reduce* the cross section from its classical value as the photon energy becomes large. Thus Compton scattering becomes less efficient at high energies. The total cross section can be shown to be

$$\sigma = \sigma_T \cdot \frac{3}{4}\left[\frac{1+x}{x^3}\left\{\frac{2x(1+x)}{1+2x} - \ln(1+2x)\right\} + \frac{1}{2x}\ln(1+2x) - \frac{1+3x}{(1+2x)^2}\right] \tag{7.5}$$

where $x \equiv h\nu/mc^2$. In the nonrelativistic regime we have approximately

$$\sigma \approx \sigma_T\left(1 - 2x + \frac{26x^2}{5} + \cdots\right), \qquad x \ll 1, \tag{7.6a}$$

whereas for the extreme relativistic regime we have

$$\sigma = \frac{3}{8}\sigma_T x^{-1}\left(\ln 2x + \frac{1}{2}\right), \qquad x \gg 1. \tag{7.6b}$$

Scattering from Electrons in Motion: Energy Transfer

In the rest of this section we assume that in the rest frame of the electron $h\nu \ll mc^2$, so that the relativistic corrections in the Klein–Nishina formula may be neglected. Whenever the moving electron has sufficient kinetic energy compared to the photon, net energy may be transferred from the electron to the photon, in contrast to the situation indicated in Eq. (7.2). In such a case the scattering process is called *inverse Compton*.

Let us call K the lab or observer's frame, and let K' be the rest frame of the electron. The scattering event as seen in each frame is given in Fig. 7.2.

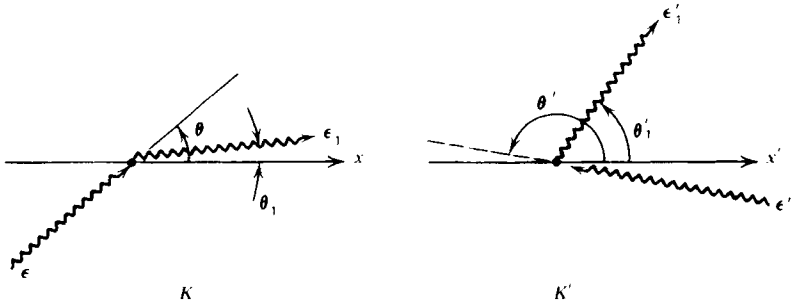

***Figure 7.2** Scattering geometries in the observer's frame K and in the electron rest frame K'.*

Note that our previous formulas for scattering from electrons at rest should now be written in primed notation, since they hold in the electron rest frame. From the Doppler shift formulas, [cf. (4.12)],

$$\epsilon' = \epsilon\gamma(1 - \beta\cos\theta), \tag{7.7a}$$

$$\epsilon_1 = \epsilon_1'\gamma(1 + \beta\cos\theta_1'). \tag{7.7b}$$

Now, we also know, from Eq. (7.2) that

$$\epsilon_1' \approx \epsilon'\left[1 - \frac{\epsilon'}{mc^2}(1 - \cos\Theta)\right] \tag{7.8a}$$

$$\cos\Theta = \cos\theta_1'\cos\theta' + \sin\theta'\sin\theta_1'\cos(\phi' - \phi_1'), \tag{7.8b}$$

where ϕ_1' and ϕ' are the azimuthal angles of the scattered photon and incident photon in the rest frame.

In the case of relativistic electrons, $\gamma^2 - 1 \gg h\nu/mc^2$, the energies of the photon before scattering, in the rest frame of the electron, and after scattering are in the approximate ratios

$$1 : \gamma : \gamma^2,$$

providing that the condition for Thomson scattering in the rest frame $\gamma\epsilon \ll mc^2$ is met. This follows from Eqs. (7.7), since θ and θ_1' are characteristically of order $\pi/2$.

This process therefore converts a low-energy photon to a high-energy one by a factor of order γ^2. Since the intermediate photon energy can be as high as, say, 100 keV and still be in the Thomson limit, it can be seen that photons of enormous energies ($\gamma \times 100$ keV) can be produced. If the

intermediate energy is too high, then both quantum effects mentioned in the previous section act to reduce the effectiveness of the process, by making $\epsilon_1' < \epsilon$ and by reducing the probability of scattering. Kinematical effects alone limit the energy attainable: From the conservation of energy we can write $\epsilon_1 < \gamma mc^2 + \epsilon$. Fixing ϵ and letting γ become large, we see that photon energies larger than $\sim \gamma mc^2$ cannot be obtained.

7.2 INVERSE COMPTON POWER FOR SINGLE SCATTERING

In the preceding section the formulas referred to Compton scattering of a single photon off a single electron. Now we want to derive average formulas for the case of a given isotropic distribution of photons scattering off a given isotropic distribution of electrons. An elegant way to average Eqs. (7.7) and (7.8) over angles, due to Blumenthal and Gould (1970), is sketched below. Let the photon phase space distribution function be $n(p)$, which is a Lorentz invariant. Let $v\,d\epsilon$ be the density of photons having energy in range $d\epsilon$. Then v and n are related by

$$v\,d\epsilon = n\,d^3p. \tag{7.9}$$

Recall that d^3p transforms in the same way as energy under Lorentz transformations [cf. Eq. (4.106b)]. Thus $v\,d\epsilon/\epsilon$ is a Lorentz invariant:

$$\frac{v\,d\epsilon}{\epsilon} = \frac{v'\,d\epsilon'}{\epsilon'}. \tag{7.10}$$

The total power emitted (i.e., scattered) in the electron's rest frame can be found from

$$\frac{dE_1'}{dt'} = c\sigma_T \int \epsilon_1' v'\,d\epsilon', \tag{7.11}$$

where $v'\,d\epsilon'$ is the number density of incident photons. We now assume that the change in energy of the photon in the rest frame is negligible compared to the energy change in the lab frame, $\gamma^2 - 1 \gg \epsilon/mc^2$; thus we can equate $\epsilon_1' = \epsilon'$. Now, we also know

$$\frac{dE_1}{dt} = \frac{dE_1'}{dt'} \tag{7.12}$$

by the invariance of emitted power. Thus we have the result

$$\frac{dE_1}{dt} = c\sigma_T \int \epsilon'^2 \frac{v'\, d\epsilon'}{\epsilon'} = c\sigma_T \int \epsilon'^2 \frac{v\, d\epsilon}{\epsilon}. \tag{7.13}$$

In Eqs. (7.12) and (7.13) we have again made the assumption that $\gamma\epsilon \ll mc^2$, so that the Thomson cross section is applicable. As is seen in Problem 7.3, a variety of scattering processes might be expected to satisfy this criterion.

Now, since $\epsilon' = \epsilon\gamma(1 - \beta\cos\theta)$, Eq. (7.13) becomes

$$\frac{dE_1}{dt} = c\sigma_T \gamma^2 \int (1 - \beta\cos\theta)^2 \epsilon v\, d\epsilon, \tag{7.14}$$

which now referes solely to quantities in frame K. For an isotropic distribution of photons we have

$$\langle (1 - \beta\cos\theta)^2 \rangle = 1 + \frac{1}{3}\beta^2,$$

since $\langle \cos\theta \rangle = 0$ and $\langle \cos^2\theta \rangle = \frac{1}{3}$. Thus we obtain

$$\frac{dE_1}{dt} = c\sigma_T \gamma^2 \left(1 + \frac{1}{3}\beta^2\right) U_{\text{ph}}, \tag{7.15a}$$

where

$$U_{\text{ph}} \equiv \int \epsilon v\, d\epsilon, \tag{7.15b}$$

is the initial photon energy density. The rate of decrease of the total initial photon energy is

$$\frac{dE_1}{dt} = -c\sigma_T \int \epsilon v\, d\epsilon = -\sigma_T c U_{\text{ph}}.$$

Thus the net power lost by the electron, and thereby converted into increased radiation, is

$$\frac{dE_{\text{rad}}}{dt} = c\sigma_T U_{\text{ph}} \left[\gamma^2 \left(1 + \frac{1}{3}\beta^2\right) - 1 \right]$$

Since $\gamma^2 - 1 = \gamma^2\beta^2$, we finally have

$$P_{\text{compt}} = \frac{dE_{\text{rad}}}{dt} = \tfrac{4}{3}\sigma_T c \gamma^2 \beta^2 U_{\text{ph}}. \tag{7.16a}$$

When the energy transfer in the electron rest frame is not neglected, Eq. (7.16a) becomes (cf. Blumenthal and Gould, 1970, but subtract out incoming energy)

$$P_{\text{compt}} = \frac{4}{3}\sigma_T c\gamma^2\beta^2 U_{\text{ph}}\left[1 - \frac{63}{10}\frac{\gamma\langle\epsilon^2\rangle}{mc^2\langle\epsilon\rangle}\right], \tag{7.16b}$$

where $\langle\epsilon^2\rangle$ and $\langle\epsilon\rangle$ are mean values integrated over U_{ph}. Note that Eq. (7.16b) allows energy to be either given or taken from the photons.

Recall that the formula for the synchrotron power emitted by each electron is [cf. Eq. (6.7b)]

$$P_{\text{synch}} = \frac{4}{3}\sigma_T c\gamma^2\beta^2 U_B. \tag{7.17}$$

Using Eq. (7.16a), we have the general result:

$$\frac{P_{\text{synch}}}{P_{\text{compt}}} = \frac{U_B}{U_{\text{ph}}}, \tag{7.18}$$

that is, the radiation losses due to synchrotron emission and to inverse Compton effect are in the same ratio as the magnetic field energy density and photon energy density. Note that this result also holds for *arbitrary* values of the electron's velocity, not just for ultrarelativistic values. It does, however, depend on the validity of Thomson scattering in the rest frame so that $\gamma\epsilon \ll mc^2$.

From Eq. (7.16) one can compute the total Compton power, per unit volume, from a medium of relativistic electrons. Let $N(\gamma)d\gamma$ be the number of electrons per unit volume with γ in the range γ to $\gamma + d\gamma$. Then

$$P_{\text{tot}}(\text{erg s}^{-1}\text{ cm}^{-3}) = \int P_{\text{compt}} N(\gamma)\, d\gamma. \tag{7.19}$$

For example, if

$$N(\gamma) = \begin{cases} C\gamma^{-p}, & \gamma_{\min} \leqslant \gamma \leqslant \gamma_{\max} \\ 0, & \text{otherwise,} \end{cases} \tag{7.20}$$

then, with $\beta \sim 1$, we obtain

$$P_{\text{tot}}(\text{erg s}^{-1}\text{ cm}^{-3}) = \frac{4}{3}\sigma_T c U_{\text{ph}} C(3-p)^{-1}\left(\gamma_{\max}^{3-p} - \gamma_{\min}^{3-p}\right). \tag{7.21}$$

From Eq. (7.16a) we can also compute the total power from a thermal distribution of nonrelativistic electrons of number density n_e. Taking $\gamma \approx 1$, $\langle \beta^2 \rangle = \langle v^2/c^2 \rangle = 3kT/mc^2$, we obtain

$$P_{\text{tot}}(\text{erg s}^{-1}\ \text{cm}^{-3}) = \left(\frac{4kT}{mc^2}\right) c\sigma_T n_e U_{\text{ph}}. \tag{7.22}$$

We show below, in Eq. (7.36), that the factor in parentheses is the fractional photon energy gain per scattering, when $\epsilon \ll 4kT$.

7.3 INVERSE COMPTON SPECTRA FOR SINGLE SCATTERING

The spectrum of inverse Compton scattering depends on both the incident spectrum and the energy distribution of the electrons. However, it is only necessary to determine the spectrum for the scattering of photons of a given energy ϵ_0 off electrons of a given energy γmc^2, because the general spectrum can then be found by averaging over the actual distributions of photons and electrons. We consider here cases in which both the photons and electrons have isotropic distributions; the scattered photons are then also isotropically distributed, and it only remains to find their energy spectrum.

To demonstrate the techniques involved without being burdened by excessive detail, we treat the case $\gamma\epsilon_0 \ll mc^2$, implying Thomson scattering in the rest frame. The small energy shift given by Eq. (7.2) is also ignored. In addition, we make the assumption that the scattering in the rest frame is *isotropic*, that is, we assume that

$$\frac{d\sigma'}{d\Omega'} = \frac{1}{4\pi}\sigma_T = \frac{2}{3}r_0^2,$$

instead of the more exact Eq. (7.1b). This will give the correct qualitative behavior of the results.

It is convenient when dealing with such problems of scattering to use an intensity I based on photon number rather than energy. The number of photons crossing area dA in time dt within solid angle $d\Omega$ and energy range $d\epsilon$ is, then, $I\,dA\,dt\,d\Omega\,d\epsilon$. This intensity can be found from the monochromatic specific intensity by dividing by the energy. A similar definition holds for the emission functions.

Suppose that the isotropic incident photon field is monoenergetic:

$$I(\epsilon) = F_0\delta(\epsilon - \epsilon_0),$$

where F_0 is the number of photons per unit area, per unit time per steradian. Let us determine the scattering off a beam of electrons of density N and energy γmc^2 traveling along the x axis (see Fig. 7.2). The incident intensity field in the rest frame K' is

$$I'(\epsilon',\mu') = F_0\left(\frac{\epsilon'}{\epsilon}\right)^2 \delta(\epsilon - \epsilon_0),$$

using Eq. (4.110) and remembering the extra factor of ϵ implied by the present definition of I. From the Doppler formulas (4.12) we have

$$\begin{aligned} I'(\epsilon',\mu') &= \left(\frac{\epsilon'}{\epsilon_0}\right)^2 F_0 \delta(\gamma\epsilon'(1+\beta\mu') - \epsilon_0) \\ &= \left(\frac{\epsilon'}{\epsilon_0}\right)^2 \frac{F_0}{\gamma\beta\epsilon'} \delta\left(\mu' - \frac{\epsilon_0 - \gamma\epsilon'}{\gamma\beta\epsilon'}\right), \end{aligned}$$

where μ' is the cosine of the angle between the photon direction in the rest frame and the x axis. The emission function in K' is given by Eqs. (1.84) and (1.85):

$$j'(\epsilon_1') = N'\sigma_T \frac{1}{2} \int_{-1}^{+1} I'(\epsilon_1',\mu')\, d\mu',$$

where j' is the number of emitted photons per unit volume per unit per steradian. We have here introduced the elastic scattering assumption that the scattered photon energy ϵ_1' equals the incident energy ϵ'. It follows that

$$\begin{aligned} j'(\epsilon_1') &= \frac{N'\sigma_T \epsilon_1' F_0}{2\epsilon_0^2 \gamma\beta}, \quad \text{if } \frac{\epsilon_0}{\gamma(1+\beta)} < \epsilon_1' < \frac{\epsilon_0}{\gamma(1-\beta)} \\ &= 0, \qquad\qquad \text{otherwise.} \end{aligned}$$

The emission function in frame K can be found from Eq. (4.113)

$$\begin{aligned} j(\epsilon_1,\mu_1) &= \frac{\epsilon_1}{\epsilon_1'} j'(\epsilon_1'), \\ &= \frac{N\sigma_T \epsilon_1 F_0}{2\epsilon_0^2 \gamma^2 \beta}, \quad \text{if } \frac{\epsilon_0}{\gamma^2(1+\beta)(1-\beta\mu_1)} < \epsilon_1 < \frac{\epsilon_0}{\gamma(1-\beta)(1-\beta\mu_1)} \\ &= 0, \qquad\qquad \text{otherwise.} \end{aligned} \tag{7.23}$$

Here we have used $N = \gamma N'$, relating the densities in the two frames, and also Eq. (4.12).

The above results hold for a beam of electrons. To obtain the results for an isotropic distribution of electrons we must average over the angle between the electron and emitted photon:

$$j(\epsilon_1) = \frac{1}{2}\int_{-1}^{+1} j(\epsilon_1, \mu_1)\, d\mu_1.$$

The quantity $j(\epsilon_1, \mu_1)$ is nonzero only for a certain interval of μ_1:

$$\frac{1}{\beta}\left[1 - \frac{\epsilon_0}{\epsilon_1}(1+\beta)\right] < \mu_1 < \frac{1}{\beta}\left[1 - \frac{\epsilon_0}{\epsilon_1}(1-\beta)\right],$$

which follows from the restriction on Eq. (7.23). When ϵ_1/ϵ_0 is less than $(1-\beta)/(1+\beta)$ or greater than $(1+\beta)/(1-\beta)$, there is no overlap between this interval and $(-1, 1)$, so $j(\epsilon_1)$ vanishes. The other cases for the limits of the μ_1 integral are:

$$-1 < \mu_1 < \frac{1}{\beta}\left[1 - \frac{\epsilon_0}{\epsilon_1}(1-\beta)\right], \quad \text{for } \frac{1-\beta}{1+\beta} < \frac{\epsilon_1}{\epsilon_0} < 1,$$

$$\frac{1}{\beta}\left[1 - \frac{\epsilon_0}{\epsilon_1}(1+\beta)\right] < \mu_1 < 1, \qquad \text{for } 1 < \frac{\epsilon_1}{\epsilon_0} < \frac{1+\beta}{1-\beta}.$$

Therefore, we obtain the result:

$$j(\epsilon_1) = \frac{N\sigma_T F_0}{4\epsilon_0 \gamma^2 \beta^2} \begin{cases} (1+\beta)\dfrac{\epsilon_1}{\epsilon_0} - (1-\beta), & \dfrac{1-\beta}{1+\beta} < \dfrac{\epsilon_1}{\epsilon_0} < 1 \quad (7.24a) \\ (1+\beta) - \dfrac{\epsilon_1}{\epsilon_0}(1-\beta), & 1 < \dfrac{\epsilon_1}{\epsilon_0} < \dfrac{1+\beta}{1-\beta}, \quad (7.24b) \\ 0, & \text{otherwise.} \quad (7.24c) \end{cases}$$

It may easily be checked that

$$\int_0^\infty j(\epsilon_1)\, d\epsilon_1 = N\sigma_T F_0,$$

$$\int_0^\infty j(\epsilon_1)(\epsilon_1 - \epsilon_0)\, d\epsilon_1 = N\sigma_T \frac{4}{3}\gamma^2\beta^2\epsilon_0 F_0.$$

Since $N\sigma_T F_0$ is the rate of photon scattering per unit volume, per unit solid

angle, the first of these simply expresses the conservation of number of photons upon scattering. The second expresses the average increase in photon energy per scattering [cf. Eq. (7.16a)].

The function $j(\epsilon_1)$ is plotted for several values of β in Fig. 7.3*a*. For small β the curves are symmetrical about the initial photon energy ϵ_0. As β increases, the portion of the curve for $\epsilon \gg \epsilon_0$ becomes more and more dominant, expressing the upward shift of average energy of the scattered photon.

For values of β near unity ($\gamma \gg 1$) it is convenient to rescale the energy variable and write

$$x \equiv \frac{\epsilon_1}{4\gamma^2 \epsilon_0}. \tag{7.25}$$

The emission function, in our isotropic approximation, is dominated by Eq. (7.24b) and can be written as

$$j(\epsilon_1) = \frac{3N\sigma_T F_0}{4\gamma^2 \epsilon_0} f_{\text{iso}}(x), \tag{7.26a}$$

where

$$f_{\text{iso}}(x) \equiv \frac{2}{3}(1-x), \qquad 0 < x < 1, \tag{7.26b}$$

and zero otherwise. Note that the vanishing of $f_{\text{iso}}(x)$ for $x > 1$ comes about from the restriction $\epsilon_1/\epsilon_0 < (1+\beta)/(1-\beta)$ on Eq. (7.24), which for $\gamma \gg 1$ becomes $\epsilon_1/\epsilon_0 < 4\gamma^2$.

When the exact angular dependence in $d\sigma'/d\Omega'$ is included, the expression for $f(x)$ in the limit $\gamma \gg 1$ is given by (see Blumenthal and Gold, 1970):

$$f(x) = 2x \ln x + x + 1 - 2x^2, \qquad 0 < x < 1. \tag{7.27}$$

A comparison of these two forms for $f(x)$ is given in Fig. 7.3*b*. Notice that most qualitative features of the exact result are preserved by the approximate one.

The spectrum resulting from the scattering of an arbitrary initial spectrum off a power law distribution (Eq. 7.20) of relativistic electrons can now be found. Let us use $v(\epsilon)$, the initial photon number density

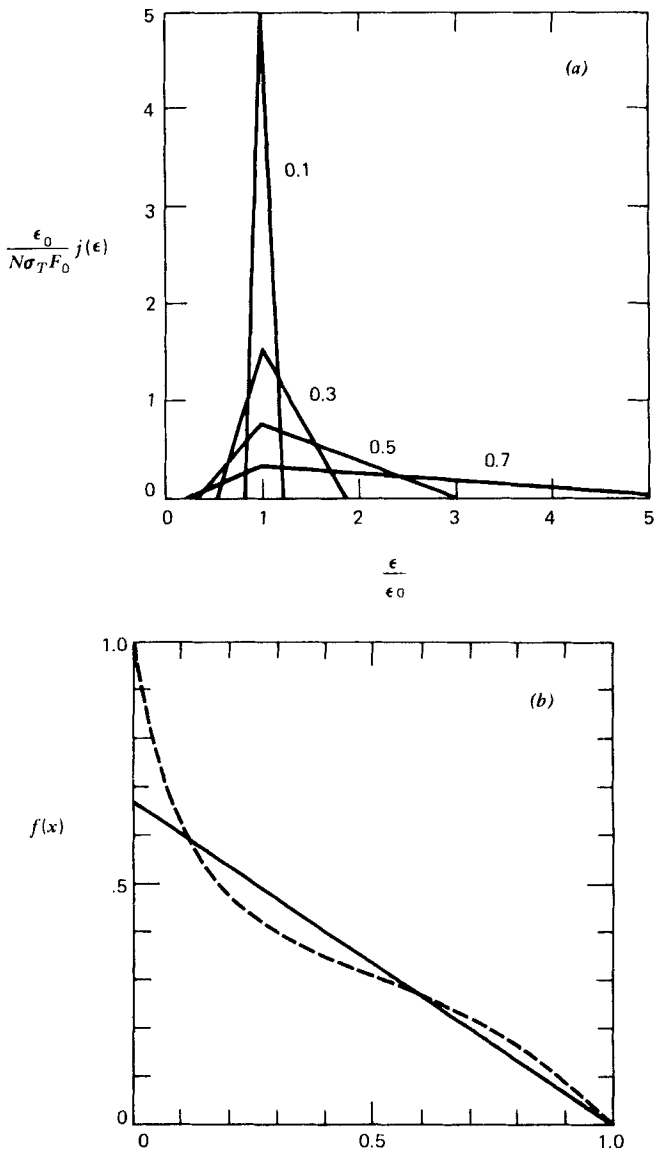

Figure 7.3 Functions describing the inverse Compton spectrum from a single scattering. (a) Emission function for various values of β within isotropic approximation (b) Comparisons of exact (dashed) and isotropic (solid) approximations for f(x).

introduced in Eq. (7.9), related to the isotropic intensity by $v(\epsilon) = 4\pi c^{-1} I(\epsilon)$. Then the total scattered power per volume per energy is

$$\frac{dE}{dV\,dt\,d\epsilon_1} = 4\pi\epsilon_1 j(\epsilon_1)$$

$$= \frac{3}{4} c\sigma_T C \int d\epsilon \left(\frac{\epsilon_1}{\epsilon}\right) v(\epsilon) \int_{\gamma_1}^{\gamma_2} d\gamma\, \gamma^{-p-2} f\left(\frac{\epsilon_1}{4\gamma^2\epsilon}\right). \quad (7.28a)$$

Changing the variable of integration from γ to x in the second integral yields

$$\frac{dE}{dV\,dt\,d\epsilon_1} = 3\sigma_T c C 2^{p-2} \epsilon_1^{-(p-1)/2} \int d\epsilon\, \epsilon^{(p-1)/2} v(\epsilon) \int_{x_1}^{x_2} dx\, x^{(p-1)/2} f(x), \quad (7.28b)$$

where $x_1 \equiv \epsilon_1/(4\gamma_1^2\epsilon)$ and $x_2 \equiv \epsilon_1/(4\gamma_2^2\epsilon)$. Now, suppose that $\gamma_2 \gg \gamma_1$ and that $v(\epsilon)$ peaks at some value $\bar{\epsilon}$. The second integral in Eq. (7.28b) is then independent of ϵ_1 and can be removed. The final result is then

$$\frac{dE}{dV\,d\epsilon_1\,dt} = \pi c r_0^2 C A(p) \epsilon_1^{-(p-1)/2} \int d\epsilon\, \epsilon^{(p-1)/2} v(\epsilon) \quad (7.29a)$$

where

$$A(p) \equiv 2^{p+1} \int_0^\infty dx\, x^{(p-1)/2} f(x) = 2^{p+3} \frac{p^2+4p+11}{(p+3)^2(p+5)(p+1)}. \quad (7.29b)$$

We point out that Eq. (7.29) is valid only over a range in ϵ_1 such that the upper and lower limits in the integral of Eq. (7.28b) can be extended to zero and infinity. If $\bar{\epsilon}$ is the typical energy of a photon in the distribution of incident photons, then this range is approximately given by $4\gamma_1^2\bar{\epsilon} \ll \epsilon_1 \ll 4\gamma_2^2\bar{\epsilon}$. In particular, Eq. (7.29) cannot be integrated over all ϵ_1 to obtain the total power—instead, one must return to Eqs. (7.28a) or (7.28b) in their exact forms. The spectral index is seen to be

$$s = \frac{p-1}{2} \quad (7.30)$$

identical to the case of synchrotron emission (cf. §6.3).

When $v(\epsilon)$ is the blackbody distribution, that is,

$$v(\epsilon)=\frac{8\pi\epsilon^2}{h^3c^3}\frac{1}{\exp(\epsilon/kT)-1},$$

we obtain from (7.29), and 23.2.7 of Abramovitz and Stegun (1965),

$$\frac{dE}{dV\,dt\,d\epsilon_1}=\frac{C8\pi^2r_0^2}{h^3c^2}(kT)^{(p+5)/2}F(p)\epsilon_1^{-(p-1)/2} \tag{7.31}$$

where

$$F(p)\equiv A(p)\Gamma\left(\frac{p+5}{2}\right)\zeta\left(\frac{p+5}{2}\right)$$

and ζ denotes the Riemann zeta function, defined by

$$\zeta(s)\equiv\sum_{n=1}^{\infty}n^{-s}.$$

The general problem of scattering of an isotropic photon field from an isotropic electron distribution, including the Compton effect and Klein–Nishina cross section, has been solved by Jones (1968), and the interested reader should look there for details.

7.4 ENERGY TRANSFER FOR REPEATED SCATTERINGS IN A FINITE, THERMAL MEDIUM: THE COMPTON *Y* PARAMETER

Before discussing in some detail the effect of repeated Compton scattering on the spectrum and total energy of the photon distribution, it is useful to determine the conditions under which the scattering process significantly alters the total photon energy. We restrict our considerations to situations in which the Thomson limit applies: $\gamma\epsilon\ll mc^2$.

In finite media one may define a Compton y parameter, to determine whether a photon will significantly change its energy in traversing the medium:

$$y\equiv\left[\begin{array}{l}\text{average fractional}\\ \text{energy change per}\\ \text{scattering}\end{array}\right]\times\left(\begin{array}{l}\text{mean number of}\\ \text{scatterings}\end{array}\right). \tag{7.32}$$

The quantities in parentheses are evaluated below. In general when $y \gtrsim 1$, the total photon energy and spectrum will be significantly altered; whereas for $y \ll 1$, the total energy is not much changed.

It is convenient to evaluate the first term in Eq. (7.32) for a thermal distribution of electrons. Consider first the nonrelativistic limit. Averaging Eq. (7.8a) over angles, we obtain

$$\frac{\Delta\epsilon'}{\epsilon'} \equiv \frac{\epsilon_1' - \epsilon'}{\epsilon'} = -\frac{\epsilon'}{mc^2}. \tag{7.33}$$

Now, in the lab frame to lowest order in the two small parameters ϵ/mc^2 and kT/mc^2, this must be of the form

$$\frac{\Delta\epsilon}{\epsilon} = -\frac{\epsilon}{mc^2} + \frac{\alpha kT}{mc^2}, \tag{7.34}$$

where α is some coefficient to be determined. To calculate α, imagine that the photons and electrons are in complete equilibrium but interact only through scattering. We assume that the photon density is sufficiently small that stimulated processes can be neglected. The photons thus have a Bose–Einstein distribution with a chemical potential rather than a Planck distribution because photons cannot be created or destroyed by scattering. In the nondegenerate limit (where stimulated effects are negligible) the appropriate distribution is Eq. (6.51), and we have the averages

$$\langle\epsilon\rangle = \int \epsilon \frac{dN}{d\epsilon}\, d\epsilon \Big/ \int \frac{dN}{d\epsilon}\, d\epsilon = 3kT, \tag{7.35a}$$

$$\langle\epsilon^2\rangle = 12(kT)^2. \tag{7.35b}$$

For this hypothetical case no net energy can be transferred from photons to electrons, so

$$\langle\Delta\epsilon\rangle = 0 = \frac{\alpha kT}{mc^2}\langle\epsilon\rangle - \frac{\langle\epsilon^2\rangle}{mc^2}$$

$$= \frac{3kT}{mc^2}(\alpha - 4)kT,$$

giving the result $\alpha = 4$. Thus for nonrelativistic electrons in thermal equilibrium, the expression for the energy transfer per scattering is

$$(\Delta\epsilon)_{NR} = \frac{\epsilon}{mc^2}(4kT - \epsilon). \tag{7.36}$$

Note that if the electrons have high enough temperature relative to incident photons, the photons may gain energy. This is called *inverse Compton scattering*. If $\epsilon > 4kT$, on the other hand, energy is transferred from photons to electrons.

In the ultrarelativistic limit, $\gamma \gg 1$, ignoring the energy transfer in the electron rest frame, Eqs. (7.7) show that

$$(\Delta\epsilon)_R \sim \frac{4}{3}\gamma^2\epsilon, \tag{7.37}$$

where the 4/3 results from angle averaging Eqs. (7.37) and is derived in §7.2. For a thermal distribution of ultrarelativistic electrons, we have, using arguments analogous to those leading to Eq. (7.35),

$$\langle \gamma^2 \rangle = \frac{\langle E^2 \rangle}{(mc^2)^2} = 12\left(\frac{kT}{mc^2}\right)^2.$$

Thus Eq. (7.37) becomes

$$(\Delta\epsilon)_R \sim 16\epsilon\left(\frac{kT}{mc^2}\right)^2, \tag{7.38}$$

Now, the second term in Eq. (7.32) may be evaluated using Eqs. (1.89a) and (1.89b). For a pure scattering medium we have

$$\begin{pmatrix}\text{mean number of}\\ \text{scatterings}\end{pmatrix} \approx \text{Max}(\tau_{es}, \tau_{es}^2), \tag{7.39a}$$

where τ_{es} is given by

$$\tau_{es} \sim \rho\kappa_{es}R. \tag{7.39b}$$

Here κ_{es} is the electron scattering opacity, which for ionized hydrogen is

$$\kappa_{es} = \frac{\sigma_T}{m_p} = 0.40 \text{ cm}^2 \text{ g}^{-1} \tag{7.40}$$

and where R is the size of the finite medium. Combining Eqs. (7.32), (7.36), (7.37), and (7.39), we then obtain expressions for the Compton y parameter for relativistic and nonrelativistic thermal distributions of electrons:

$$y_{NR} = \frac{4kT}{mc^2}\text{Max}(\tau_{es}, \tau_{es}^2), \tag{7.41a}$$

$$y_R = 16\left(\frac{kT}{mc^2}\right)^2 \text{Max}(\tau_{es}, \tau_{es}^2). \tag{7.41b}$$

We have assumed that the energy transfer in the electron rest frame is negligible, that is, $4kT \gg \epsilon$ in the nonrelativistic case. The importance of the y parameter is illustrated in Problem 7.1. There it is shown that input photons of initial energy ϵ_i emerge with average energy $\epsilon_f \sim \epsilon_i e^y$ after scattering in a cloud of nonrelativistic electrons (as long as $\epsilon_f \ll 4kT$).

In media in which absorption is important, it is convenient to define a frequency-dependent Compton parameter, $y(\nu)$. For this parameter the relevant $\tau_{es}(\nu)$ must be measured from an effective absorption optical depth, $\tau_*(\nu)$, of order unity. Thus $\tau_{es}(\nu) = \rho \kappa_{es} l_*(\nu)$ (cf. §1.7), and using Eqs. (1.96), we obtain

$$\tau_{es}(\nu) \sim \left(\frac{\kappa_{es}/\kappa_a(\nu)}{1 + \kappa_a(\nu)/\kappa_{es}} \right)^{1/2} \tag{7.42}$$

where $\kappa_a(\nu)$ is the absorption opacity. Equation (7.42) gives the scattering optical depth to the surface from the characteristic point of emission of a photon of frequency ν. The definitions for $y_{NR}(\nu)$ and $y_R(\nu)$ are identical to Eqs. (7.41a) and (7.41b) with τ_{es} replaced by $\tau_{es}(\nu)$ of Eq. (7.42).

7.5 INVERSE COMPTON SPECTRA AND POWER FOR REPEATED SCATTERINGS BY RELATIVISTIC ELECTRONS OF SMALL OPTICAL DEPTH

In §7.3 it has been shown that a power-law spectrum results from inverse Compton scattering off a power-law distribution of relativistic electrons. This is not surprising, since any quantity scaled by a factor that has a power-law distribution will itself have a power-law distribution. However, as we now show here, for relativistic electrons, and below for nonrelativistic electrons, a power-law photon distribution can also be produced from *repeated* scatterings off a nonpower-law electron distribution of small scattering depth.

Let A be the mean amplification of photon energy per scattering, that is,

$$A \equiv \frac{\epsilon_1}{\epsilon} \sim \frac{4}{3}\langle \gamma^2 \rangle = 16 \left(\frac{kT}{mc^2} \right)^2, \tag{7.43}$$

where the second equation follows for a thermal electron distribution, (cf. §7.4). Consider an initial photon distribution of mean photon energy ϵ_i,

such that $\epsilon_i \ll \langle\gamma^2\rangle^{-1/2} mc^2$, and intensity $I(\epsilon_i)$ at ϵ_i. Then, after k scatterings, the energy of a mean initial photon will be

$$\epsilon_k \sim \epsilon_i A^k. \tag{7.44}$$

If the medium is of small scattering optical depth (and much smaller absorption depth), then the probability $p_k(\tau_{es})$ of a photon undergoing k scatterings before escaping the medium is approximately $p_k(\tau_{es}) \sim \tau_{es}^k$. The intensity of emergent radiation at energy ϵ_k is roughly proportional to $p_k(\tau_{es})$, since the bandwidth of the Compton produced spectrum is comparable to the frequency. Thus the emergent intensity at energy ϵ_k has the power-law shape

$$I(\epsilon_k) \sim I(\epsilon_i)\tau_{es}^k \sim I(\epsilon_i)\left(\frac{\epsilon_k}{\epsilon_i}\right)^{-\alpha}, \tag{7.45a}$$

where

$$\alpha \equiv \frac{-\ln \tau_{es}}{\ln A}. \tag{7.45b}$$

The above qualitative derivation of Eq. (7.45) was first given by Ya. B. Zeldovich and has been verified in numerical Monte Carlo calculations by L. A. Pozdnyakov, I. M. Sobol, and R. A. Sunyaev (1976).

Equation (7.45) only holds for emergent photons satisfying $\epsilon_k/\langle\gamma^2\rangle^{1/2} \lesssim mc^2$, so that the energy amplification at the last scattering is correctly described by Eq. (7.43). Note, however, that such photons are just those that emerge at energies $\sim kT$ in a thermal distribution of relativistic electrons.

The total Compton power in the output spectrum is given by

$$P \propto \int_{\epsilon_i}^{A^{1/2}mc^2} I(\epsilon_k)\, d\epsilon_k = I(\epsilon_i)\epsilon_i \left[\int_1^{A^{1/2}mc^2/\epsilon_i} x^{-\alpha}\, dx\right]. \tag{7.46}$$

The factor in square brackets is approximately the factor by which the initial power $\propto I(\epsilon_i)\epsilon_i$ is amplified in energy. Clearly, this amplification will be important if $\alpha < 1$. From Eq. (7.45b) we conclude that energy amplification of a soft photon input spectrum is therefore important when

$$A\tau_{es} \sim 16(kT/mc^2)^2 \tau_{es} \gtrsim 1, \tag{7.47}$$

where the intermediate step holds if the electrons are thermal. Note that Eq. (7.47) is equivalent to $y_R \gtrsim 1$ [cf. Eq. (7.41b)] for $\tau_{es} \lesssim 1$.

7.6 REPEATED SCATTERINGS BY NONRELATIVISTIC ELECTRONS: THE KOMPANEETS EQUATION

Consider now the evolution of the photon phase space density $n(\omega)$ due to scattering from electrons. We assume that $n(\omega)$ is isotropic. If $f_e(\mathbf{p})$ is the phase density of electrons of momentum $\mathbf{p}$, then the *Boltzmann equation* for $n(\omega)$ is

$$\frac{\partial n(\omega)}{\partial t} = c\int d^3p \int \frac{d\sigma}{d\Omega}\, d\Omega \big[f_e(\mathbf{p}_1) n(\omega_1)(1+n(\omega)) - f_e(\mathbf{p}) n(\omega)(1+n(\omega_1)) \big] \tag{7.48}$$

where we consider the scattering events

$$p+\omega \leftrightarrows p_1+\omega_1.$$

The first term in Eq. (7.48) represents scattering into frequency ω by photons of frequency ω_1, whereas the second term represents scattering out of frequency ω into frequencies ω_1. The relationship between ω and ω_1 is given by Eqs. (7.50), (7.53) and Problem 7.4 and is a function of the scattering angles. The dependence on angles disappears after integration over $d\Omega$. The factors $1+n(\omega)$ and $1+n(\omega_1)$ take into account stimulated scattering effects; that is, the probability of scattering from frequency ω_1 to ω is increased by the factor $1+n(\omega)$ because photons obey Bose–Einstein statistics and tend toward mutual occupation of the same quantum state [cf. Eqs. (1.68) and (1.74) and §1.5]. Aside from these quantum mechanical correction factors, Eq. (7.48) is a standard form in kinetic theory. In general, the Boltzmann equation can be solved only for special cases or with approximations. We give approximate solutions in the nonrelativistic limit below.

A detailed analysis of the evolution of the spectrum in the presence of repeated scatterings off relativistic electrons is difficult because the energy transfer per scattering is large and one must solve the full integrodifferential equation, (7.48). However, when the electrons are nonrelativistic, the fractional energy transfer per scattering is small. In particular, the Boltzmann equation may be expanded to second order in this small quantity, yielding an approximation called the *Fokker–Planck equation*. For photons scattering off a nonrelativistic, thermal distribution of electrons, the Fokker–Planck equation was first derived by A. S. Kompaneets (1957) and is known as the Kompaneets equation.

For a thermal distribution of nonrelativistic electrons, the phase space density $f_e(E)$, where $E=p^2/2m$, is given by

$$f_e(E) = n_e(2\pi mkT)^{-3/2} e^{-E/kT}, \tag{7.49}$$

where n_e is the electron space density. We define the dimensionless energy transfer to the photons as

$$\Delta \equiv \frac{\hbar(\omega_1 - \omega)}{kT}. \tag{7.50}$$

We now consider situations in which the energy transfer is small, $\Delta \ll 1$, and expand $f_e(E_1)$ and $n(\omega_1)$ for this regime. For example, for $n(\omega_1)$ this expansion, *to second order*, is

$$n(\omega_1) = n(\omega) + (\omega_1 - \omega)\frac{\partial n(\omega)}{\partial \omega} + \frac{1}{2}(\omega_1 - \omega)^2 \frac{\partial^2 n(\omega)}{\partial \omega^2} + \cdots \tag{7.51}$$

Now letting

$$x \equiv \frac{\hbar\omega}{kT},$$

we obtain, to second order in Δ,

$$c^{-1}\frac{\partial n}{\partial t} = \left[n' + n(1+n)\right]\int\int d^3p \frac{d\sigma}{d\Omega} d\Omega f_e \Delta + \left[\frac{1}{2}n'' + n'(1+n) + \frac{1}{2}n(1+n)\right]\int\int d^3p \frac{d\sigma}{d\Omega} d\Omega f_e \Delta^2, \tag{7.52}$$

where $n' \equiv \partial n/\partial x$ and so on. The term in Δ gives the "secular" shift in energy, and the term in Δ^2 gives the "random walk" change in energy.

Let us first compute the second integral, I_2, in Eq. (7.52), which gives the random walk contribution to $\partial n/\partial t$. Using a derivation completely analogous to that leading to Eq. (7.2) but with the electron not initially at rest, one finds (Problem 7.4),

$$\Delta = \frac{x\mathbf{p}\cdot(\mathbf{n}_1 - \mathbf{n})}{mc} + O\left(\frac{kT}{mc^2}\right), \tag{7.53}$$

where $\mathbf{p}$ is the electron momentum before collision and $\mathbf{n}$ and $\mathbf{n}_1$ are unit vectors along the photon direction before and after collision, respectively. Now, using the formula for $d\sigma/d\Omega$, Eq. (7.1b), and the above equations, one obtains (Problem 7.4),

$$I_2 = 2x^2 n_e \sigma_T \left(\frac{kT}{mc^2}\right) + O\left(\frac{kT}{mc^2}\right)^2. \tag{7.54}$$

We can similarly evaluate the integral I_1, but this is more difficult than I_2. A simpler method uses photon conservation and detailed balancing. Since n is the photon phase space density and x is proportional to momentum, then the change in number of photons per unit volume, which must vanish, is proportional to

$$\frac{d}{dt}\int nx^2\,dx = \int \frac{\partial n}{\partial t}\,x^2\,dx = 0.$$

It is thus clear that $\partial n/\partial t$ must be of the form (Problem 7.4)

$$\frac{\partial n}{\partial t} = -\frac{1}{x^2}\frac{\partial}{\partial x}\left[x^2 j(x)\right]. \tag{7.55a}$$

By comparison with Eq. (7.52), j must be of the form

$$j = g(x)\left[n' + h(n,x)\right], \tag{7.55b}$$

with h and g two functions to be determined. Now, we know that a Bose–Einstein photon distribution with finite chemical potential,

$$n = (e^{\alpha + x} - 1)^{-1}, \tag{7.56}$$

must be in thermal equilibrium with the electrons, with $j = 0$. Requiring $n' + h(n,x) = 0$ for n given by Eq. (7.56) then determines

$$h(n,x) = n(1+n). \tag{7.57a}$$

Comparison of Eqs. (7.57a) and (7.55) with (7.54) and (7.52) then yields the two desired results:

$$g(x) = -cx^2 n_e \sigma_T \left(\frac{kT}{mc^2}\right), \tag{7.57b}$$

$$I_1 = n_e \sigma_T x(4-x)\left(\frac{kT}{mc^2}\right). \tag{7.58}$$

Note that the "secular term" of the Fokker–Planck equation, proportional to I_1, states that energy is gained or lost depending on the sign of $4-x$, in agreement with Eq. (7.36).

Substitution of Eqs. (7.57) into (7.55) then yields the Kompaneets equation, describing the evolution of the photon distribution function due to repeated, nonrelativistic, inverse Compton scattering:

$$\frac{\partial n}{\partial t_c} = \left(\frac{kT}{mc^2}\right)\frac{1}{x^2}\frac{\partial}{\partial x}\left[x^4(n' + n + n^2)\right]. \tag{7.59}$$

Here, the quantity

$$t_c \equiv (n_e \sigma_T c) t$$

is the time measured in units of mean time between scatterings.

In general, Eq. (7.59) must be solved by numerical integration. However, several important limiting cases can be pointed out here. First, note that the spectrum reaches equilibrium after photons have been "scattered up" to energies forming the Bose–Einstein distribution, Eq. (7.56). This steady-state, "saturated" spectrum is approximated by a *Wien law* [cf. Eq. (1.54)]

$$n(x) \propto e^{-x} \tag{7.60}$$

when the occupation number is small; that is, $\alpha \gg 1$. Note also that for times short compared to that required to reach saturation, so that the mean $h\nu$ of an initially low energy photon distribution is still small compared to kT, $x \ll 1$, the total energy density of the photons increases with time according to

$$\frac{dE}{dt_c} = \frac{8\pi}{c^3 h^3} (kT)^4 \frac{d}{dt_c} \int_0^\infty n x^3 dx \approx \left(\frac{4kT}{mc^2} \right) E . \tag{7.61a}$$

Here we have neglected the n and n^2 terms compared to the n' on the right-hand side of Eq. (7.59) and have performed two integrations by parts. From Eq. (7.61a) it can be seen that the total energy in a soft input spectrum increases initially as

$$E(t) \approx E(0) \exp\left(\frac{4kT}{mc^2} t_c \right). \tag{7.61b}$$

Note the similarity between this expression and that for the energy gain of a single photon in scattering out of a finite medium, Problem 7.1:

$$\epsilon_f = \epsilon_i e^y, \tag{7.62}$$

where $\text{Max}(\tau_{es}, \tau_{es}^2)$ plays the role of t_c.

7.7 SPECTRAL REGIMES FOR REPEATED SCATTERING BY NONRELATIVISTIC ELECTRONS

A detailed analysis of Compton spectra requires a solution of the Kompaneets equation, Eq. (7.59), with a photon source term. For

frequencies where $y \ll 1$ (modified blackbody) or $y \gg 1$ (saturated Comptonization), approximate analyses are usually adequate. For intermediate cases (unsaturated Comptonization) we return to the more detailed treatment required by the Kompaneets equation.

To delineate regimes it is convenient to introduce several characteristic frequencies. We are concerned with thermal media in which absorption and emission arise from free-free (bremsstrahlung) processes, (see §5.3). In such media the relative importance of absorption is greatest at low frequencies. Consider first the frequency, ν_0, at which the scattering and absorption coefficients are equal: From Eqs. (1.22), (5.18), and (7.40), we have

$$\kappa_{es} = \kappa_{ff}(\nu_0), \tag{7.63a}$$

$$\frac{x_0^3}{1-e^{-x_0}} \sim 4\times 10^{25} T^{-7/2} \rho \bar{g}_{ff}(x_0), \tag{7.63b}$$

where $x_0 \equiv h\nu_0/kT$ and $\bar{g}_{ff}(x)$ is the free-free Gaunt factor. In the range of interest, $\bar{g}_{ff}$ is approximated by, (Fig. 5.2)

$$\bar{g}_{ff}(x) \sim 3\pi^{-1/2} \ln\left(\frac{2.25}{x}\right).$$

For $x \equiv h\nu/kT < x_0$, scattering will be unimportant; whereas for $x > x_0$, scattering will modify the spectrum. Note that if $x_0 \gtrsim 1$, scattering is unimportant over most of the spectrum. In all the following discussion we assume $x_0 \ll 1$.

Consider next the frequency ν_t at which the medium becomes effectively thin. From Eqs. (1.97) and (5.18) we have

$$\kappa_{es} = \kappa_{ff}(\nu_t)\tau_{es}^2, \tag{7.64a}$$

$$\frac{x_t^3}{1-e^{-x_t}} \sim 4\times 10^{25} T^{-7/2} \rho \bar{g}_{ff}(x_t)\tau_{es}^2, \tag{7.64b}$$

where $x_t \equiv h\nu_t/kT$ and τ_{es} is the total optical depth to electron scattering, Eq. (7.39b). For values of $x > x_t$, absorption is unimportant. Note that in the range $x_0 < x < x_t$ both scattering and absorption are important.

Finally, we introduce the frequency ν_{coh} for which incoherent scattering (inverse Compton effects) can be important. This frequency is so defined that $y(\nu_{coh}) = 1$, that is, for $\nu > \nu_{coh}$ inverse Compton is important between emission and escape from the medium. Note that this frequency is defined only if the y parameter for the full thickness of the medium, Eqs. (7.39)–(7.41), exceeds unity. Otherwise, inverse Compton scattering is unim-

portant at all frequencies. From Eqs. (7.41), (7.42), and (5.18), for $x_{coh} \ll 1$,

$$\kappa_{es} = \left(\frac{mc^2}{4kT}\right)\kappa_{ff}(\nu_{coh}), \tag{7.65a}$$

$$x_{coh} \sim 2.4 \times 10^{17} \rho^{1/2} T^{-9/4} \left[\bar{g}_{ff}(x_{coh})\right]^{1/2}. \tag{7.65b}$$

From Eqs. (7.64) and (7.65), we see that inverse Compton is important, and x_{coh} is defined, only when $x_{coh} < x_t$.

Modified Blackbody Spectra; $y \ll 1$

For $y \ll 1$, only coherent scattering is important. Then, from Problem 1.10, we have for the emergent intensity in a scattering and absorbing medium

$$I_\nu = \frac{2B_\nu}{1 + \sqrt{(\kappa_{ff} + \kappa_{es})\kappa_{ff}^{-1}}}. \tag{7.66}$$

The functional form of Eq. (7.66), in the limit $\kappa_{es} \gg \kappa_{ff}(\nu)$, may also be derived by the simple random-walk considerations leading to Eq. (1.102). We see that at values of $x \ll x_0$ Eq. (7.66) reduces to the blackbody intensity, whereas at values of $x \gg x_0$ Eq. (7.66) becomes a "modified blackbody spectrum,"

$$I_\nu^{MB} \equiv 2B_\nu \sqrt{\kappa_{ff}/\kappa_{es}} \tag{7.67a}$$

$$= 8.4 \times 10^{-4} T^{5/4} \rho^{1/2} \bar{g}_{ff}^{1/2} x^{3/2} e^{-x/2} (e^x - 1)^{-1/2}$$

$$\times \text{erg s}^{-1} \text{ cm}^{-2} \text{ Hz}^{-1} \text{ ster}^{-1}. \tag{7.67b}$$

For $x_0 \ll 1$ Eq. (7.63b) gives the approximate equation for x_0:

$$x_0 \sim 6.3 \times 10^{12} T^{-7/4} \rho^{1/2} \left[\bar{g}_{ff}(x_0)\right]^{1/2}. \tag{7.68}$$

Note that at frequencies $x_0 \ll x \ll 1$, $I_\nu^{MB} \propto \nu$ instead of the Rayleigh–Jeans law $I_\nu^{RJ} \propto \nu^2$. The total flux in a modified blackbody spectrum is approximately

$$F^{MB} \sim \sigma T^4 \left(\frac{\kappa_R}{\kappa_{es}}\right)^{1/2}$$

$$\sim 2.3 \times 10^7 T^{9/4} \rho^{1/2} \text{ erg s}^{-1} \text{ cm}^{-2}, \tag{7.69}$$

where we have taken the Rosseland mean, κ_R, for the frequency-averaged κ_{ff} [cf. Eq. (5.20)].

Equation (7.66) actually applies only to a medium that is an infinite half-space. For finite media it is necessary to determine the value of x_t [cf. Eq. (7.64b)]. For $x_t < x_0$ the emission is blackbody at $x < x_t$ and optically thin bremsstrahlung for $x > x_t$, with scattering never important. For $x_0 < x_t < 1$, the emission is correctly described by Eq. (7.66) for $x < x_t$ and is then optically thin bremsstrahlung for $x > x_t$. For $x_t > 1$ the medium behaves as if it were infinite, and Eq. (7.66) may be used for the entire spectrum.

The above relations for the modified blackbody spectrum were first discussed by Felten and Rees (1972) and by Illarionov and Sunyaev (1972).

Wien Spectra; $y \gg 1$

When $y \gg 1$, inverse Compton may be important, depending on whether $x_{coh} \ll 1$ or $x_{coh} \gg 1$. In the latter case, inverse Compton may be neglected, since the majority of the photons and energy, that is, the spectrum in the region $x \lesssim 1$, undergo coherent scattering. The preceding subsection may be used to describe the spectrum. We therefore consider only the case $x_{coh} \ll 1$.

For $x_{coh} \ll 1$, Eqs. (7.63) and (7.65) give

$$x_{coh} = \left(\frac{mc^2}{4kT}\right)^{1/2} x_0. \tag{7.70}$$

The spectrum is correctly described by Eq. (7.66) for $x \ll x_{coh}$, but for $x \gtrsim x_{coh}$ we must consider inverse Compton effects, (see Fig. 7.4). In this region of the spectrum, if $x_{coh} \ll 1$, inverse Compton will go to saturation, and §7.6 shows that a Wien intensity will be produced [cf. Eq. (1.54)]:

$$I_\nu^W = \frac{2h\nu^3}{c^2} n = \frac{2h\nu^3}{c^2} e^{-\alpha} e^{-h\nu/kT}, \tag{7.71}$$

where the factor $e^{-\alpha}$ is related to the rate at which photons are produced. (Recall that the photon number is conserved in the scattering process.) The total flux in a spectrum of the form of Eq. (7.71) is

$$F^W(\text{erg s}^{-1}\text{ cm}^{-2}) = \pi \int I_\nu^W \, d\nu = \frac{12\pi e^{-\alpha} k^4 T^4}{c^2 h^3}, \tag{7.72}$$

while the mean photon has an energy $\overline{h\nu} = 3kT$.

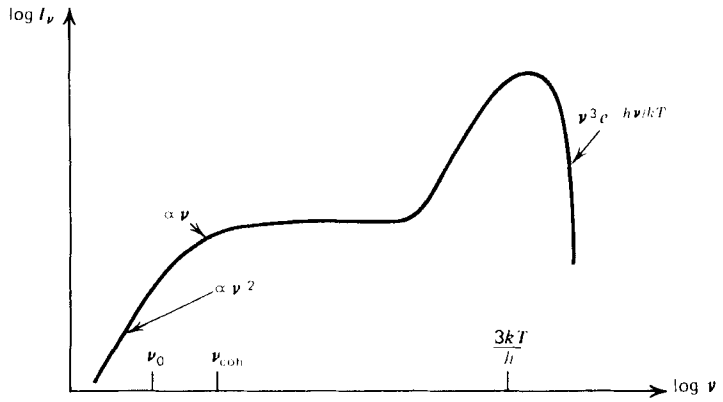

***Figure 7.4** Spectrum from a thermal, nonrelativistic medium characterized by free-free emission and absorption and by saturated inverse Compton scattering. At low frequencies the spectrum is blackbody then becomes modified blackbody and, at high frequencies, becomes a Wien spectrum.*

The rate at which energy is generated in the Comptonized spectrum can be calculated approximately by shifting all of the bremsstrahlung photons to energies kT:

$$\frac{dW^W}{dt\,dV}(\text{erg s}^{-1}\text{ cm}^{-3}) \sim kT\int\left(\frac{\epsilon_\nu^{ff}}{h\nu}\right)d\nu$$

$$\sim \epsilon^{ff}\int_{\nu_{coh}}^{\infty}\bar{g}_{ff}(\nu,T)e^{-h\nu/kT}\frac{d\nu}{\nu}. \tag{7.73}$$

Here $\epsilon_\nu^{ff}(\text{erg s}^{-1}\text{ cm}^{-3}\text{ Hz}^{-1})$ is the bremsstrahlung (free-free) energy generation rate given by Eq. (5.14), and $\epsilon^{ff}(\text{erg s}^{-1}\text{ cm}^{-3})$ given by Eq. (5.15) is the total energy per unit time per unit volume. This integral may be approximated by evaluating $\bar{g}$ at the lower limit, ν_{coh}, and letting $e^{-h\nu/kT}$ be a step function that is unity for $h\nu < kT$ and then zero for $h\nu > kT$. The result is, using the analytical approximation to $\bar{g}$ given in Fig. 5.2,

$$\frac{dW^W}{dt\,dV} \sim A(\rho,T)\epsilon^{ff}, \tag{7.74a}$$

$$A(\rho,T) \equiv \frac{3}{4}\left[\ln(2.25/x_{coh})\right]^2. \tag{7.74b}$$

Here $A(\rho,T)$ is the factor by which inverse Compton amplifies the

bremsstrahlung power. Equation (7.74), including the more exact overall numerical factor, was first derived by Kompaneets (1957).

To calculate the emergent flux from Eq. (7.74), and hence the normalization of Eqs. (7.71) and (7.72), we must multiply Eq. (7.74) by a characteristic depth. If $x_t \ll 1$, then the medium is effectively thin for most photons and $F^W \sim RA\epsilon^{ff}$, where R is the size of the medium. If $x_t \gg 1$ then, since photons at energies $x > x_{coh}$ amplify quickly to $x \sim 1$, R is replaced by $\bar{R}$, where $\tau_*(\bar{R}, x = 1) \sim 1$. The emergent intensity is shown in Fig. 7.4.

Unsaturated Comptonization with Soft Photon Input

Finally, we must consider situations in which $y \gg 1$, but in which $x_{coh} \sim 1$; that is, media for which the inverse Compton process is important but does not saturate to the Wien spectrum for most photons. In this case an analysis of the Kompaneets equation is required.

Let us consider a steady-state solution to this equation, under certain idealizations. For steady-state solutions in a finite medium it is necessary to consider both the input and the escape of photons. Denote the photon source by $Q(x)$. The photon escape is a spatial diffusion process. However, for photons which have scattered many times, it is a fair approximation to assume that the probability for a photon to escape per Compton scattering time is equal to the inverse of the mean number of scatterings, $\mathrm{Max}(\tau_{es}, \tau_{es}^2)$. With this approximation, one may consider a modified, steady-state Kompaneet's equation of the form

$$0 = \left(\frac{kT}{mc^2}\right) \frac{1}{x^2} \frac{\partial}{\partial x} \left[x^4 (n' + n) \right] + Q(x) - \frac{n}{\mathrm{Max}(\tau_{es}, \tau_{es}^2)}, \qquad (7.75)$$

where the n^2 term, usually small in astrophysical applications, has been dropped.

Assume now that $Q(x)$ is nonzero only for $x \leqslant x_s$, where $x_s \ll 1$; that is, we have an input of "soft" photons, rather than the bremsstrahlung input considered previously. For $x \gg 1$, the term in brackets shows that an approximate solution is

$$n \propto e^{-x}; \qquad (7.76a)$$

that is, the spectrum falls roughly exponentially at photon energies much above the electron temperature, as would be expected for a thermal spectrum. On the other hand, for $x_s \ll x \ll 1$, the n term in brackets may be neglected in comparison with the n' term, and one obtains the approximate

power-law solution:

$$n \propto x^m, \tag{7.76b}$$

$$m(m+3) - \frac{4}{y} = 0, \tag{7.76c}$$

$$m = -\frac{3}{2} \pm \sqrt{\frac{9}{4} + \frac{4}{y}}\ , \tag{7.76d}$$

where the Compton y parameter is given in Eq. (7.41a). The + root in Eq. (7.76d) is appropriate if $y \gg 1$ (leading to the low-frequency limit of the Wien law in the limit $y \to \infty, I_\nu \propto x^3 n \propto x^3$); for $y \ll 1$, the minus root is appropriate. For $y \sim 1$, one must take a linear combination of the two solutions, and no power law exists.

Figure 7.5 illustrates the spectrum resulting from unsaturated Comptonization. Note that measurement of only the shape of an unsaturated Compton spectrum with soft photon source determines both the electron temperature and the scattering optical depth of the source. The emergent intensity in the power-law regime satisfies

$$I_\nu \sim I_{\nu_s} \left(\frac{\nu}{\nu_s} \right)^{3+m}. \tag{7.77}$$

The spectrum is clearly sensitive to y. The input energy is significantly amplified for $m \geqslant -4$, that is, $y \geqslant 1$. This result is quite analogous to that for the relativistic case considered previously in §7.5. Unsaturated Compton spectra are treated in some detail in Shapiro, Lightman, and Eardley (1976) and Katz (1976).

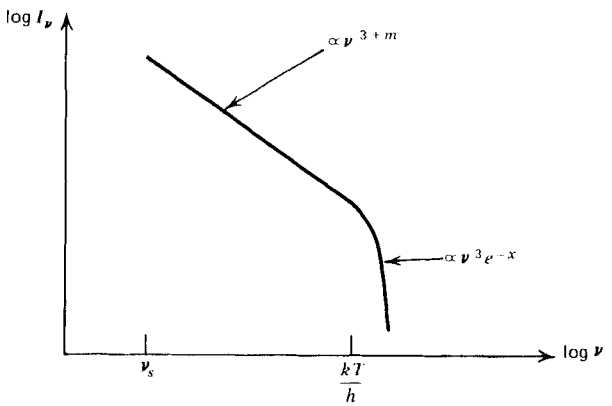

Figure 7.5 Spectrum produced by unsaturated Comptonization of low energy photons by thermal electrons.

PROBLEMS

7.1—A cloud of nonrelativistic electrons is maintained at temperature T. The cloud is thick to electron scattering, $\tau_{es} \gg 1$, but very thin to absorption, $\tau_*(h\nu = kT) \ll 1$. A copious supply of "soft" photons, each of characteristic energy $\epsilon_i \ll kT$, is injected into the cloud. As a result of inverse Compton scattering, these initially soft photons emerge from the cloud with characteristic energies $\epsilon_f \gg \epsilon_i$. It is found that ϵ_f increases rapidly with increasing τ_{es} as the latter is varied, until τ_{es} reaches a critical value τ_{crit}, above which the Comptonization process "saturates."

a. Find an approximate expression for ϵ_f as a function of ϵ_i, τ_{es}, T, and fundamental constants.

b. Find an approximate expression for τ_{crit}.

c. Find a single parameter of the fixed medium that determines whether inverse Compton is a significant effect.

7.2—Consider the observed X-ray source of Problem 5.2. From the deduced characteristics of the source, determine a lower limit to the central mass M such that inverse Compton effects in the emission mechanism are negligible.

7.3—Show that the photon energy in the electron rest frame is small compared to mc^2 for the following cases:

a. Electrons with $\gamma \sim 10^4$ scattering synchrotron photons produced in a magnetic field $B \sim 0.1$ G (typical of compact radio sources).

b. Electrons with $\gamma \sim 10^4$ scattering the 3 K photons of the cosmic microwave background.

7.4—Derive Eqs. (7.53) to (7.55) for the Kompaneets equation.

REFERENCES

Abramowitz, M., and Stegun, I. A., *op. cit.*
Blumenthal, G. R., and Gould, R. J., 1970, *Rev. Mod. Phys.*, **42**, 237.
Felten, J. E., and Rees, M. J., 1972, *Astron. Astrophys.*, **17**, 226.
Heitler, W., 1954, *The Quantum Theory of Radiation*, (Oxford, London).
Illarionov, A. F., and Sunyaev, R. A., 1972, *Sov. Astron. A. J.*, **16**, 45.
Jones, F. C., 1968, *Phys. Rev.*, **167**, 1159.
Katz, J. I., 1976, *Astrophys. J.*, **206**, 910.
Kompaneets, A. S., 1957, *Sov. Phys. JETP*, **4**, 730.
Pozdnyakov, L. A., Sobol, I. M., and Sunyaev, R. A., 1976, *Sov. Astron. Lett.*, **2**, 55.
Shapiro, S. L., Lightman, A. P., and Eardley, D. M., 1976, *Astrophys. J.*, **204**, 187.

Let us assume that our plasma consists of electrons with density n. The ions are neglected here, because they are very much less mobile than the electrons and contribute negligibly to the current. (They are important for certain wave motions other than radiation, however, and they do keep the plasma neutral globally.) We also assume that there is no external magnetic field; thus the plasma is *isotropic*. Each electron responds to the electric field according to Newton's law (for an electron charge $q = -e$)

$$m\dot{\mathbf{v}} = -e\mathbf{E}. \tag{8.2}$$

The magnetic force, being of order v/c, has been neglected. In terms of oscillating quantities $\mathbf{v}$ becomes

$$\mathbf{v} = \frac{e\mathbf{E}}{i\omega m}. \tag{8.3}$$

Since the current density is given by $\mathbf{j} = -ne\mathbf{v}$, we have

$$\mathbf{j} = \sigma\mathbf{E}, \tag{8.4}$$

where the *conductivity*, σ, satisfies

$$\sigma = \frac{ine^2}{\omega m}. \tag{8.5}$$

By means of the charge conservation equation we find:

$$-i\omega\rho + i\mathbf{k}\cdot\mathbf{j} = 0,$$

so that

$$\rho = \omega^{-1}\mathbf{k}\cdot\mathbf{j} = \sigma\omega^{-1}\mathbf{k}\cdot\mathbf{E}. \tag{8.6}$$

Using these expressions for $\mathbf{j}$ and ρ and introducing the *dielectric constant* ϵ, defined by

$$\epsilon \equiv 1 - \frac{4\pi\sigma}{i\omega}, \tag{8.7}$$

we find that Maxwell's equations become

$$\begin{aligned} i\mathbf{k}\cdot\epsilon\mathbf{E} &= 0, & i\mathbf{k}\cdot\mathbf{B} &= 0, \\ i\mathbf{k}\times\mathbf{E} &= i\frac{\omega}{c}\mathbf{B}, & i\mathbf{k}\times\mathbf{B} &= -i\frac{\omega}{c}\epsilon\mathbf{E}. \end{aligned} \tag{8.8}$$

These equations are now "source-free" and can be solved in precisely the same way as before. We find again that **k**, **E**, and **B** form a mutually orthogonal right-hand vector triad, but now the relation between k and ω becomes

$$c^2k^2 = \epsilon\omega^2. \tag{8.9}$$

Substituting in Eq. (8.5) for σ, we obtain an alternate expression for the dielectric constant

$$\epsilon = 1 - \left(\frac{\omega_p}{\omega}\right)^2, \tag{8.10}$$

where we have introduced the *plasma frequency* ω_p, defined by

$$\omega_p^2 = \frac{4\pi ne^2}{m}. \tag{8.11}$$

Numerically, we obtain

$$\omega_p = 5.63 \times 10^4 n^{1/2}\, s^{-1}, \tag{8.12}$$

where n is given in cm^{-3}. The dispersion relation connecting k and ω can now be written:

$$k = c^{-1}\sqrt{\omega^2 - \omega_p^2}\,, \tag{8.13a}$$

$$\omega^2 = \omega_p^2 + k^2c^2. \tag{8.13b}$$

We see immediately from these equations that for $\omega < \omega_p$, the wave number is *imaginary*

$$k = \frac{i}{c}\sqrt{\omega_p^2 - \omega^2}\,. \tag{8.14}$$

In this case the amplitude of the wave decreases exponentially on a scale of the order of $2\pi c/\omega_p$. Thus ω_p defines a *plasma cutoff frequency* below which there is no electromagnetic propagation. For example, the earth's ionosphere prevents extraterrestrial radiation at frequencies less than about 1 MHz from being observed at the earth's surface (corresponding to $n_{\text{average}} \sim 10^4\ \text{cm}^{-3}$).

Note from the purely imaginary nature of σ, Eq. (8.5), that **j** and **E** are 90° out of phase with each other ($i = e^{i\pi/2}$). Thus there is no time-averaged

mechanical work done on the particles by the field in an isotropic plasma, and no dissipation.

The existence of the plasma cutoff yields an important method of probing the ionosphere. Let a pulse of radiation in a narrow range about ω be directed straight upward from the earth's surface. When there is a layer at which n is large enough to make $\omega_p > \omega$, the pulse will be *totally reflected* from the layer. The time delay of the pulse provides information on the height of the layer. By making such measurements at many different frequencies, the electron density can be determined as a function of height.

Group and Phase Velocity and the Index of Refraction

When $\omega > \omega_p$, there is propagation of electromagnetic radiation with *phase velocity*

$$v_{ph} \equiv \frac{\omega}{k} = \frac{c}{n_r}, \tag{8.15}$$

where n_r is the *index of refraction*

$$n_r \equiv \sqrt{\epsilon} = \sqrt{1 - \frac{\omega_p^2}{\omega^2}}\ . \tag{8.16}$$

The phase velocity always exceeds the speed of light. The *group velocity*

$$v_g \equiv \frac{\partial \omega}{\partial k} = c\sqrt{1 - \frac{\omega_p^2}{\omega^2}}\ , \tag{8.17}$$

on the other hand, is always less than c. The wave energy travels at the group velocity, as does any modulation of the wave (information coding). See Jackson (1975) for a standard discussion of v_{ph} and v_g and Problem 8.2 for an alternative treatment.

In a medium with variable electron density, and hence variable index of refraction, radiation travels along curved paths rather than in straight lines. Radio propagation in the ionosphere and solar corona is affected by such curved paths. The curved trajectories in inhomogeneous media may be obtained straightforwardly from application of Snell's law for ray bending (see e.g., Rossi, 1957) and are given by

$$\frac{d(n\hat{\mathbf{k}})}{dl} = \nabla n, \tag{8.18}$$

where n, $\hat{\mathbf{k}}$, and l are the index of refraction, ray direction, and ray path length, respectively. It can be shown (Problem 8.1) that it is the quantity I_ν/n_r^2 that is constant along the ray, rather than I_ν. This is a generalization of Liouville's theorem, Eq. (1.12).

An important application of the formula for group velocity is to pulsars. Each individual pulse from the pulsar has a spectrum covering a wide band of frequency. Therefore, the pulse will be *dispersed* by its interaction with the interstellar plasma, since each small range of frequencies travels at a slightly different group velocity and will reach earth at a slightly different time.

Suppose the pulsar is a distance d away. Then the time required for a pulse to reach earth at frequency ω is

$$t_p = \int_0^d \frac{ds}{v_g},$$

where s measures the line-of-sight distance from the pulsar to earth. The plasma frequencies in interstellar space are usually quite low ($\sim 10^3$ Hz), so we can assume $\omega \gg \omega_p$ and expand

$$v_g^{-1} = \frac{1}{c}\left(1 - \frac{\omega_p^2}{\omega^2}\right)^{-1/2} \approx \frac{1}{c}\left(1 + \frac{1}{2}\frac{\omega_p^2}{\omega^2}\right).$$

Thus we obtain

$$t_p \approx \frac{d}{c} + (2c\omega^2)^{-1}\int_0^d \omega_p^2\, ds. \tag{8.19}$$

The first term is the transit time for a vacuum; the second term is the plasma correction. What is usually measured is the rate of change of arrival time with respect to frequency, $dt_p/d\omega$. With the formula for ω_p^2 this can be written

$$\frac{dt_p}{d\omega} = -\frac{4\pi e^2}{cm\omega^3}\mathcal{D}, \tag{8.20a}$$

where

$$\mathcal{D} \equiv \int_0^d n\, ds \tag{8.20b}$$

is the *dispersion measure* of the ray. By assuming a typical value for the electron density in interstellar space ($n \sim 0.03$ cm^{-3}) an estimate of the pulsar's distance can be obtained.

8.2 PROPAGATION ALONG A MAGNETIC FIELD; FARADAY ROTATION

We now want to extend somewhat the above discussion of plasma propagation effects by considering the effect of an external, fixed magnetic field $\mathbf{B}_0$. The properties of the waves will then depend on the direction of propagation relative to the direction of $\mathbf{B}_0$. For this reason the plasma is called *anisotropic*. We also make the cold plasma approximation here, and treat only the special case of propagation along the magnetic field.

Because of the magnetic field, a new frequency enters the problem, namely, the *cyclotron frequency*

$$\omega_B = \frac{eB_0}{mc}, \tag{8.21}$$

which is the frequency of gyration for an electron about the field lines. Numerically we obtain, for B_0 in gauss,

$$\omega_B = 1.67 \times 10^7 B_0 \, s^{-1}, \tag{8.22a}$$

$$\hbar\omega_B = 1.16 \times 10^{-8} B_0 \, eV. \tag{8.22b}$$

The dielectric constant is no longer a scalar; it becomes a tensor and has different effective values for waves of different directions. The medium now also discriminates between different polarizations. Only waves with special polarizations have the simple exponential forms we have been assuming, $\mathbf{E}\exp i(\mathbf{k}\cdot\mathbf{r} - \omega t)$ where $\mathbf{E}$ is *constant*.

If the fixed magnetic field $\mathbf{B}_0$ is much stronger than the field strengths of the propagating wave, then the equation of motion of an electron in the plasma is approximately

$$m\frac{d\mathbf{v}}{dt} = -e\mathbf{E} - \frac{e}{c}\mathbf{v}\times\mathbf{B}_0. \tag{8.23}$$

Assume that the propagating wave is circularly polarized and sinusoidal:

$$\mathbf{E}(t) = Ee^{-i\omega t}(\boldsymbol{\epsilon}_1 \mp i\boldsymbol{\epsilon}_2), \tag{8.24}$$

where the $-$ corresponds to right circular polarization and the $+$ corresponds to left circular polarization. Assume further, for simplicity, that the wave propagates along the fixed field $\mathbf{B}_0$:

$$\mathbf{B}_0 = B_0 \epsilon_3. \tag{8.25}$$

Substituting Eqs. (8.24) and (8.25) into (8.23), one finds that the steady-state velocity $\mathbf{v}(t)$ has the form

$$\mathbf{v}(t) = \frac{-ie}{m(\omega \pm \omega_B)} \mathbf{E}(t), \tag{8.26}$$

where ω_B is given in Eq. (8.21).

Comparison of Eq. (8.26) with Eqs. (8.3)–(8.5) and (8.7) then gives an expression for the dielectric constant

$$\epsilon_{R,L} = 1 - \frac{\omega_p^2}{\omega(\omega \pm \omega_B)}, \tag{8.27}$$

where the R,L corresponds to the $+$ and $-$ signs, respectively. These waves travel with different velocities. Therefore, a plane polarized wave, which is a linear superposition of a right-hand and a left-hand polarized wave, will not keep a constant plane of polarization, but this plane will *rotate* as it propagates. This effect is called *Faraday rotation*.

The phase angle ϕ through which the electric vector of a circularly polarized wave moves in traveling a distance d is simply $\mathbf{k}\cdot\mathbf{d}$. More generally, if the wave number is not constant along the path, the phase angle is

$$\phi_{R,L} = \int_0^d k_{R,L}\, ds, \tag{8.28a}$$

where

$$k_{R,L} = \frac{\omega}{c} \sqrt{\epsilon_{R,L}}\,. \tag{8.28b}$$

A plane-polarized wave is rotated through an angle $\Delta\theta$, equal to one-half the difference between ϕ_R and ϕ_L, as can be seen from Fig. 8.1. We assume that $\omega \gg \omega_p$ and $\omega \gg \omega_B$ so that

$$k_{R,L} \approx \frac{\omega}{c}\left[1 - \frac{\omega_p^2}{2\omega^2}\left(1 \mp \frac{\omega_B}{\omega}\right)\right]. \tag{8.29}$$

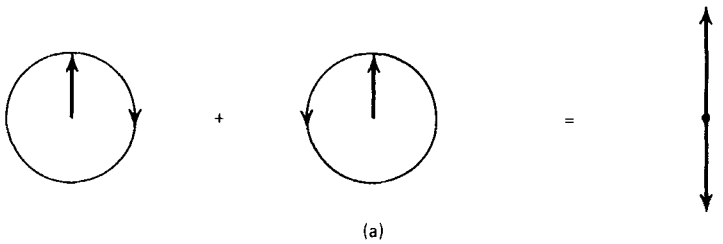

Figure 8.1a Decomposition of linear polarization into components of right and left circular polarization.

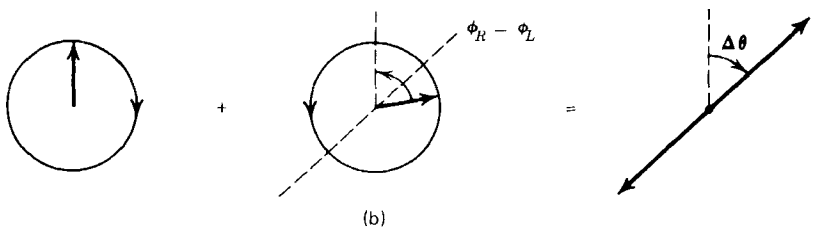

Figure 8.1b Faraday rotation of the plane of polarization.

Thus we have the result

$$\Delta\theta = \tfrac{1}{2}\int_0^d (k_R - k_L)\, ds$$
$$= \tfrac{1}{2}\int_0^d (c\omega^2)^{-1}\omega_p^2\omega_B\, ds, \tag{8.30}$$

or, substituting for ω_p^2 and ω_B, we obtain the formula for Faraday rotation:

$$\Delta\theta = \frac{2\pi e^3}{m^2c^2\omega^2}\int_0^d nB_{\|}\, ds. \tag{8.31}$$

As derived here, this formula holds only if the direction of **B** is always along the line of sight. However, it can be shown that this formula holds in general if we use $B_{\|}$, the component of **B** along the line of sight.

Since $\Delta\theta$ varies with frequency (as ω^{-2}) for the same line of sight, we can determine the value of the integral $\int nB_{\|}\, ds$ by making measurements at several frequencies. This can be used to deduce information about the interstellar magnetic field. However, if this field changes direction often along the line of sight (as we believe it does), then this method gives only a lower limit to actual field magnitudes.

8.3 PLASMA EFFECTS IN HIGH-ENERGY EMISSION PROCESSES

When fast particles radiate by means of a high-energy emission mechanism —like synchrotron, inverse Compton, or bremsstrahlung emission—this radiation is subject to all the plasma propagation effects mentioned previously. In particular, we can expect little observable radiation below the cutoff frequency ω_p, whereas above ω_p the phenomena of pulse dispersion and path curvature may occur. When magnetic fields are present, Faraday rotation will degrade the degree of polarization of synchrotron sources.

In addition, however, there are some specific effects on the high-energy emission processes themselves that can change the entire character of the emitted radiation. We shall describe two such effects, *Cherenkov radiation* and the *Razin effect*. Both of these require us to consider the induced motions and subsequent emission from the particles comprising the medium through which the fast particles are moving. Since we are only interested in the collective response of the medium, it is permissible to treat the medium in terms of a macroscopic dielectric constant ϵ. For certain parts of the following discussion we make the assumption that the dielectric constant is independent of frequency and wave number. This is not strictly true, as we have seen, but it allows us to obtain the principal results quickly. For more detailed derivations, without use of this assumption, see Ginzburg and Syrovatskii (1965) and Razin (1960). For our assumption, Maxwell's equations can be written as

$$\begin{aligned} \nabla\cdot\mathbf{E} &= \frac{1}{\epsilon}4\pi\rho, \qquad \nabla\cdot\mathbf{B}=0, \\ \nabla\times\mathbf{E} &= \frac{1}{c}\frac{\partial\mathbf{B}}{dt}, \qquad \nabla\times\mathbf{B}=\frac{4\pi}{c}\mathbf{j}+\frac{\epsilon}{c}\frac{\partial\mathbf{E}}{\partial t}. \end{aligned} \tag{8.32}$$

It can easily be shown that these equations *formally* result from Maxwell's equation in vacuum by the substitutions

$$\begin{aligned} &\mathbf{E}\to\sqrt{\epsilon}\,\mathbf{E}, \qquad c\to c/\sqrt{\epsilon}\,, \\ &\mathbf{B}\to\mathbf{B}, \qquad \phi\to\sqrt{\epsilon}\,\phi, \\ &e\to e/\sqrt{\epsilon}\,, \qquad \mathbf{A}\to\mathbf{A}. \end{aligned} \tag{8.33}$$

These equations may be solved in the same manner as before for the retarded and Liénard–Wiechert potentials, using Eqs. (3.7a), (3.7b), and (3.10), and then making the substitutions indicated in Eqs. (8.33).

Cherenkov Radiation

A charge moving uniformly in a vacuum cannot radiate, as such radiation would violate the results of relativity theory. The same conclusion holds for a charge moving uniformly through a dielectric medium, providing the velocity of the charge is less than the phase velocity of light in the medium. This can be proved directly from the modified Liénard–Wiechert potentials. These potentials differ from the vacuum case only in the scale of some of the parameters, according to the substitutions in Eqs. (8.33); thus these changes do not affect the conclusion that the fields fall off as $1/R^2$ and do not carry energy over large distances.

If the medium has an index of refraction greater than unity, $n_r > 1$, the velocity of the charge can exceed the phase velocity. In this case the potentials differ qualitatively from those of the vacuum. From Eqs. (8.33) the factor $\kappa = 1 - \beta\cos\theta$ in Eqs. (3.7) becomes

$$\kappa = 1 - \beta n_r \cos\theta, \tag{8.34}$$

and this can *vanish* for an angle θ such that $\cos\theta = (n_r\beta)^{-1}$. The potentials become infinite at certain places, and this invalidates the usual arguments concerning the $1/R^2$ behavior of the fields. In consequence, the particle can now radiate.

Another qualitatively different effect appears when $v > c/n_r$, namely, that the potentials at a point may be determined by *two* retarded positions of the particle, rather than just one. This can be seen from Fig. 8.2. The points 1, 2, 3, and 4 denote successive positions of the particle, and the spheres represent "information spheres" generated at these positions, which move outward with the velocity c/n_r.

Looking at the case $v > c/n_r$ we note that space is divided into two distinct regions by a cone, the *Cherenkov cone*, such that points outside the cone feel no potentials as yet; inside the cone each point is intersected by two spheres, and thus each point feels the potentials due to two retarded positions of the particle.

The resulting radiation, called *Cherenkov radiation*, is confined within the cone and moves outward in a direction normal to the cone with the velocity c/n_r. Notice the similarity of this pattern with a shock pattern generated by a supersonic airplane; both are due to motion of a body at a velocity greater than that of wave propagation in the medium. The relation $\cos\theta = (\beta n_r)^{-1}$ can be understood from Fig. 8.3. Since $\cos\theta < 1$ and $v/c < 1$ it follows that

$$\frac{c}{n_r} < v < c \tag{8.35}$$

for Cherenkov radiation.

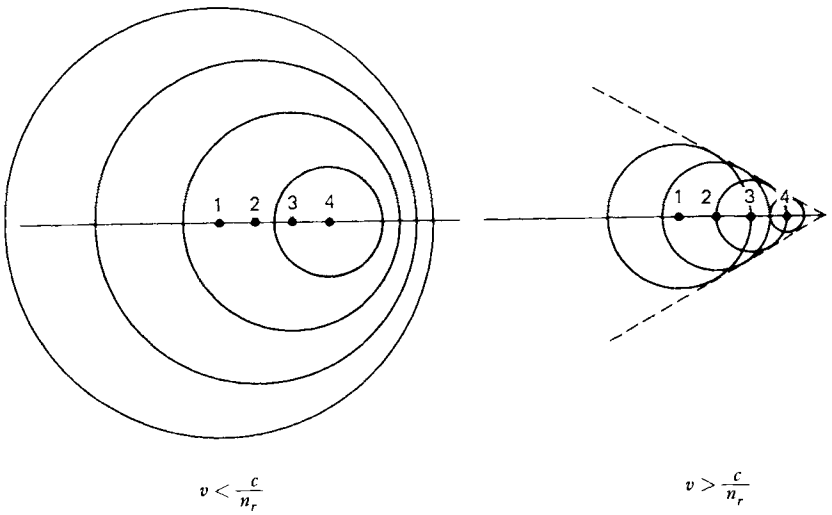

Figure 8.2 Propagation of wave fronts generated by a particle moving with velocity v through a refractive medium.

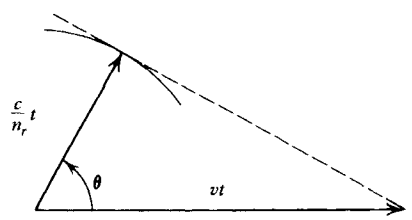

Figure 8.3 Geometry of Cherenkov cone.

The precise direction of the radiation can be used as an energy measurement for fast particles in the laboratory or observatory. Cherenkov radiation due to high energy cosmic rays has been observed in the earth's atmosphere. Since the radiation is quite intense for fast particles, it acts as an effective mechanism for energy loss.

Razin Effect

When $n_r < 1$, as it is in a cold plasma, Cherenkov radiation cannot occur. In this case there is an effect that has important implications for synchrotron emission. The "beaming" effect associated with emission from a fast

particle can be attributed to the factor $\kappa = 1 - \beta\cos\theta$ appearing in the denominators of the Liénard–Wiechert potentials. Making the above substitutions, this factor is now given by Eq. (8.34).

For $n_r < 1$, as in a plasma, the beaming effect is suppressed, for now there is no velocity and angle combination for which κ is small. This can be seen as follows: The critical angle defining the beaming effect has been shown to be given by $\theta_b \sim 1/\gamma = \sqrt{1-\beta^2}$ in a vacuum. Therefore, in a medium we have

$$\theta_b \sim \sqrt{1 - n_r^2\beta^2}\ , \tag{8.36}$$

using the substitutions of Eqs. (8.33). There are two cases of this formula that can be identified, depending on which factor, n_r or β, dominates in keeping θ_b from being small. If n_r is sufficiently close to unity, then θ_b is determined by β, as in the vacuum case. On the other hand, if n_r differs substantially from unity, then we have

$$\theta_b \sim \sqrt{1 - n_r^2}\ = \frac{\omega_p}{\omega}\,. \tag{8.37}$$

From this it can be seen that the medium will dominate beaming at low frequencies. At higher frequencies θ_b decreases until it becomes of order of the vacuum value $1/\gamma$, and thereafter the vacuum results apply. Therefore, the medium is unimportant when

$$\omega \gg \gamma\omega_p,$$

and the medium is important when

$$\omega \ll \gamma\omega_p.$$

This suppression of the beaming effect at low frequencies has a profound effect on synchrotron emission, as can be appreciated from the dominant role beaming has in the physical explanation of this process. Below the frequency $\gamma\omega_p$ the synchrotron spectrum will be cut off because of the suppression of beaming. This is called the *Razin effect*. It is obvious that this effect dominates the ordinary plasma cutoff, which occurs at the much lower frequency ω_p.

PROBLEMS

8.1—In a medium with dielectric constant n_r, show that I_ν/n_r^2 is constant along a ray.

8.2—Consider a traveling wave packet of amplitude

$$\psi(r,t)=\int_{-\infty}^{\infty} A(k)e^{i[kr-\omega(k)t]}dk,$$

where $\omega(k)$ is a real function of k. Define the centroid of the wave packet, $\langle r(t)\rangle$ by

$$\langle r(t)\rangle \equiv \frac{\int r|\psi(r,t)|^2 dr}{\int |\psi(r,t)|^2 dr}.$$

Show that the wave centroid travels with the velocity $\langle \partial\omega/\partial k\rangle$,

$$\frac{d}{dt}\langle r(t)\rangle = \langle \partial\omega/\partial k\rangle,$$

where

$$\langle \partial\omega/\partial k\rangle \equiv \frac{\int \partial\omega/\partial k|A(k)|^2 dk}{\int |A(k)|^2 dk}.$$

8.3—The signal from a pulsed, polarized source is measured to have an arrival time delay that varies with frequency as $dt_p/d\omega = 1.1\times10^{-5}$ s^2, and a Faraday rotation that varies with frequency as $d\Delta\theta/d\omega = 1.9\times10^{-4}$ s. The measurements are made around the frequency $\omega = 10^8$ s^{-1}, and the source is at unknown distance from the earth. Find the mean magnetic field, $\langle B_\parallel\rangle$, in the interstellar space between the earth and the source:

$$\langle B_\parallel\rangle \equiv \frac{\int nB_\parallel ds}{\int n\, ds}.$$

REFERENCES

Ginzburg, V. L. and Syrovatskii, S. I., 1965, *Ann. Rev. Astron. Astrophys.*, **3**, 297.
Jackson, J. D., 1975, *Classical Electrodynamics*, (Wiley, New York).
Pacolczyk, A. G., 1970, *Radio Astrophysics*, (Freeman, San Francisco).
Razin, V. A., 1960, *Izvestiya Vys. Ucheb. Zaved. Radiofiz.*, **3**, 921.
Rossi, B., 1957, *Optics*, (Addison-Wesley, Reading, Mass.).

9

ATOMIC STRUCTURE

The classical theory of radiation is unable to treat physical processes in which the interaction between matter and radiation takes place by means of single (or a few) photons. We have already dealt with some elementary aspects of this interaction when we discussed the Planck law and the Einstein coefficients. However to really solve problems we need to find explicit expressions for the A and B coefficients or equivalents. This must involve detailed investigation of the structure of the matter that interacts with the radiation, its energy levels, and other physical properties. In this chapter we treat the structure of atoms, and in the next chapter we consider the radiative transitions of these atoms.

9.1 A REVIEW OF THE SCHRODINGER EQUATION

We begin with the *time-dependent Schrodinger equation* for a system with Hamiltonian H:

$$i\hbar \frac{\partial \Psi}{\partial t} = H\Psi. \tag{9.1}$$

Often we are interested in the stationary solutions found by separating the

time and space parts of the wave function Ψ, which is possible if H is independent of time:

$$\Psi(\mathbf{r},t)=\psi(\mathbf{r})e^{iEt/\hbar}. \tag{9.2}$$

It follows that ψ satisfies the *time-independent Schrodinger equation*

$$H\psi=E\psi. \tag{9.3}$$

Here E is the energy and ψ is the wave function of the corresponding energy state. In the case of electrons surrounding a nucleus of charge Ze, neglecting spin, relativistic effects and nuclear effects, the Hamiltonian is

$$H=-\frac{\hbar^2}{2m}\sum_j \nabla_j^2 - Ze^2\sum_j \frac{1}{r_j}+\sum_{i>j}\frac{e^2}{r_{ij}}. \tag{9.4}$$

Here the first term in H is the sum over electron kinetic energy, the second term is the Coulomb interaction energy between nucleus and electrons, and the third term is the Coulomb energy of the electrons interacting with themselves. We then obtain the equation

$$\left(-\frac{\hbar^2}{2m}\sum_j \nabla_j^2 - E - Ze^2\sum_j \frac{1}{r_j}+\sum_{i>j}\frac{e^2}{r_{ij}}\right)\psi=0. \tag{9.5}$$

This determines an approximation to the atomic states. This equation can be put into dimensionless form by using the electron mass and charge as units of mass and charge, and using the first Bohr radius,

$$a_0\equiv\frac{\hbar^2}{me^2}=0.529\times10^{-8}\text{ cm} \tag{9.6}$$

as the unit of length. With this unit of length, the energy E is measured in units

$$\frac{e^2}{a_0}=4.36\times10^{-11}\text{ erg}=27.2\text{ eV}. \tag{9.7}$$

(This unit of energy equals two Rydbergs.) Characteristic sizes and binding energies of atoms will be of the order of the above values. In dimensionless form, the Schrodinger equation becomes

$$\left(\frac{1}{2}\sum_j \nabla_j^2 + E + Z\sum_j \frac{1}{r_j}-\sum_{i>j}\frac{1}{r_{ij}}\right)\psi=0. \tag{9.8}$$

9.2 ONE ELECTRON IN A CENTRAL FIELD

Even in complete atoms with N electrons it is useful to consider single-electron states. We assume that each electron moves in the potential of the nucleus plus the averaged potential due to the other $N-1$ electrons. This is called the *self-consistent field approximation*. When, in addition, this averaged potential is assumed to be spherically symmetric, it is called the *central field approximation* and represents one of the most powerful concepts in atomic theory. It provides a useful classification of atomic states and also a starting point for treating correlations as perturbations.

In the central field approximation each electron feels a different potential, which may be regarded as a shielded nuclear charge. When the electron is far from the nucleus and outside the cloud of other electrons, the potential is

$$V(r)\to\frac{Z-N+1}{r}, \qquad r\to\infty.$$

When the electron is close to the nucleus, so that all the other electrons are further away, we have

$$V(r)\to-\frac{Z}{r}+C, \qquad r\to 0.$$

Wave Functions

In classical mechanics a central potential implies the constancy of orbital angular momentum. The same is true in quantum mechanics. If H depends only on the magnitude of r, we can make the separation

$$\psi(r,\theta,\phi)=r^{-1}R(r)\,Y(\theta,\phi). \tag{9.9}$$

The functions $Y(\theta,\phi)$ are the *spherical harmonics*, defined by

$$Y=Y_{lm}(\theta,\phi)=\left[\frac{(l-|m|)!}{(l+|m|)!}\,\frac{2l+1}{4\pi}\right]^{1/2}(-1)^{(m+|m|)/2}P_l^{|m|}(\cos\theta)e^{im\phi}, \tag{9.10}$$

where P_l^m is the associated Legendre function, and l and m are integers. The functions Y_{lm} are eigenfunctions of the orbital angular momentum

operator $\mathbf{L}=\mathbf{r}\times\mathbf{p}$. That is,

$$\mathbf{L}^2 Y_{lm} = l(l+1)\, Y_{lm}, \tag{9.11a}$$

$$L_z\, Y_{lm} = m Y_{lm}, \tag{9.11b}$$

where angular momentum is in units of $\hbar$. The values of l are $l=0,1,2,3,4,\ldots,$ called s states, p states, d states, f states, g states, and so on, respectively. The value m ranges from $-l$ to $+l$ in integer steps. The functions Y_{lm} are orthonormal:

$$\int d\Omega\, Y^*_{lm}(\theta,\phi)\, Y_{l'm'}(\theta,\phi) = \delta_{l,l'}\delta_{m,m'}. \tag{9.12}$$

Note that the angular eigenfunctions, unlike the radial functions below, are independent of the form of the potential, $V(r)$, as long as it is spherically symmetric.

The radial part of the wave function satisfies the equation

$$\tfrac{1}{2}\frac{d^2R_{nl}}{dr^2} + \left[E - V(r) - \frac{l(l+1)}{2r^2}\right]R_{nl} = 0. \tag{9.13}$$

We see that R depends on l but not on m. The index n labels the energy states. Generally for a given value of l, the states in increasing order of energy are labeled:

$$n = l+1,\ l+2,\ l+3,\ldots.$$

The radial functions have the normalization

$$\int_0^\infty R_{nl}(r) R_{n'l}(r)\, dr = \delta_{n,n'}. \tag{9.14}$$

(We have not put a complex conjugation here, since the Rs can always be chosen as real). In addition to the above discrete eigenfunctions, there is also a continuous set of eigenfunctions, corresponding to unbound states.

The solutions for the pure Coulomb case, when $V(r) = -Z/r$, are

$$R_{nl}(r) = -\left\{\frac{Z(n-l-1)!}{n^2[(n+l)!]^3}\right\}^{1/2} e^{-\rho/2}\rho^{l+1} L_{n+l}^{2l+1}(\rho), \tag{9.15a}$$

$$E_n = -Z^2/2n^2, \tag{9.15b}$$

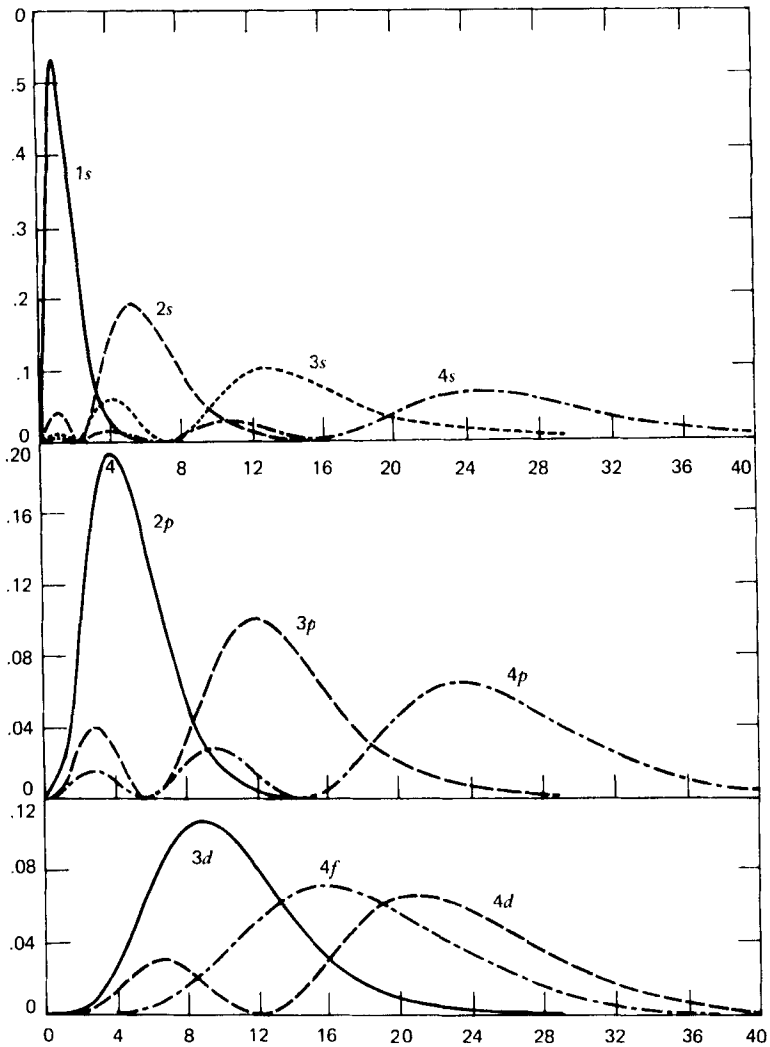

Figure 9.1 Radial probability distribution for an electron in several of the lowest levels of hydrogen. The abscissa is the radius in atomic units. (Taken from Condon, E. and Shortley, G. 1963, The Theory of Atomic Spectra, Cambridge, Cambridge University Press.)

where $\rho = 2Zr/n$. The functions L_{n+l}^{2l+1} are the associated Laguerre polynomials. The first three radial functions are:

$$R_{10} = 2Z^{3/2} r e^{-Zr}, \tag{9.16a}$$

$$R_{20} = \left(\frac{Z}{2}\right)^{3/2} (2 - Zr) r e^{-Zr/2}, \tag{9.16b}$$

$$R_{21} = \left(\frac{Z}{2}\right)^{3/2} \frac{Zr^2}{\sqrt{3}} e^{-Zr/2}. \tag{9.16c}$$

The quantity R_{nl}^2 is the probability that the electron is between r and $r + dr$. Figure 9.1 shows the probability distribution for the lowest states of hydrogen.

Spin

The electron possesses an intrinsic angular momentum s, with $|s| = \frac{1}{2}$. There are thus two states, $m_s = \pm\frac{1}{2}$, for the spin. To incorporate spin into the theory in a completely satisfactory way one should use the relativistic Dirac equation. However, for nonrelativistic cases it is usually sufficient to treat the spin in terms of wave functions with two components. The wave functions corresponding to the values $m_s = \pm\frac{1}{2}$ are defined as

$$|\tfrac{1}{2}\rangle \equiv \alpha = \begin{pmatrix} 1 \\ 0 \end{pmatrix} \qquad |-\tfrac{1}{2}\rangle \equiv \beta = \begin{pmatrix} 0 \\ 1 \end{pmatrix}. \tag{9.17}$$

A single particle state must now include specification of m_s as well as n, l, and m.

9.3 MANY-ELECTRON SYSTEMS

Statistics: The Pauli Principle

We now have a set of single-particle states specified by n, l, m, and m_s. (These are called *orbitals*). From these we want to construct states of the whole system. As a first step let us form products of the sort

$$u_a(1) u_b(2) \cdots u_k(N),$$

where each subscript $a, b \cdots k$ represents the set of values (n, l, m, m_s) and the numbers $1, 2, \ldots, N$ represent the space and spin coordinates of the 1st,

2nd,..., Nth particle. The functions u are the orbitals with spatial part ψ_{nlm}, multiplied by a spin part α or β.

Such products are satisfactory from one point of view: they form a complete set in terms of which any state of the system of N electrons can be represented. They fail, however, to satisfy a basic principle of quantum mechanics, namely, that all electrons are *identical* and that it should not be possible to say that particle 1 is in orbital a, particle 2 is in orbital b, and so on. We may avoid this by forming linear combinations of the above products, including every permutation P of the particles among the orbitals. Since there are $N!$ permutations, the weight we choose must have magnitude $(N!)^{-\frac{1}{2}}$. Its phase is determined by the *Pauli exclusion principle*, which states that no two electrons can occupy the same orbital. Thus we choose the phase as

$$\epsilon_p = \pm 1$$

according as the permutation is an even or odd permutation of some standard ordering. Thus if two electrons are put into the same orbital, the linear combination will vanish, so that no physical (normalizable) state exists. Therefore, the basis states for the whole system are

$$(N!)^{-\frac{1}{2}} \sum_p \epsilon_p P u_a(1) u_b(2) \cdots u_k(N). \tag{9.18}$$

This may be conveniently written as the *Slater determinant*

$$\frac{1}{\sqrt{N!}} \begin{vmatrix} u_a(1) & u_a(2) & \cdots & u_a(N) \\ u_b(1) & u_b(2) & \cdots & u_b(N) \\ \vdots & & & \\ u_k(1) & u_k(2) & \cdots & u_k(N) \end{vmatrix}. \tag{9.19}$$

In this form it is clear that when two electrons occupy the same orbital, two rows of this determinant are equal and it therefore vanishes.

Particles with the above symmetry for their wave functions are called *Fermi–Dirac* particles or simply *fermions*. There is complete antisymmetry of the wave function under interchange of two particles, $\psi(1,2,\ldots N) = \epsilon_p P\psi(1,2,\ldots N)$, as can be seen by interchanging two columns in the above determinant.

Hartree–Fock Approximation: Configurations

An important method for choosing the orbitals used to construct atomic states is based on a variational principle for the expectation value of the energy. The *exact* energy states of the system are determined by the variational condition

$$\delta\langle H\rangle = \delta\int \psi^* H\psi\, d(1)d(2)\cdots d(N) = 0,$$

where δ is an arbitrary variation of the normalized trial wave function ψ. We now can determine approximate energy states by using a restricted variation in which ψ is a properly antisymmetrized product of orbitals (a Slater determinant) and considering only variations with respect to a choice of these orbitals. When the details of this variation are carried out one obtains the *Hartree–Fock equations* for each orbital. These are Schrodinger equations with two types of potentials: (1) a term representing the electrostatic potential of the nucleus and of the averaged charge density of all other electrons and (2) a term having no classical analogue, called the *exchange potential*. This exchange term has its origin in the Pauli principle and may be regarded as an expression of an effective repulsion of electrons with the same spin (see Problem 9.1).

There is no real "potential" in the N-electron problem corresponding to this exchange repulsion, only the antisymmetry of the wave functions, which prevents two electrons with the same spin from occupying the same volume element. It is only when one formulates the N-electron problem in terms of single-particle states that the repulsion manifests itself by means of an effective potential in the equations. The essentially nonclassical nature of the exchange potential is clear, since it takes a "nonlocal" form, which cannot easily be interpreted classically.

If the Hartree–Fock potentials are averaged over all angles, one obtains a central potential, which is used to compute the orbitals. It is found that these orbitals give a fair description of the gross structure of atomic systems, including the main features of the periodic table.

The *configuration* of an atomic system is defined by specifying the nl values of all the electron orbitals: nl^x means x electrons in the orbital defined by n and l. There are $2(2l+1)$ electron states available to each l value because m has $2l+1$ values for each l and there are two possible spins. A fairly complete table of ground-level configurations is given in Table 9.1. We see here the regular filling of shells up to the case of Ar($Z=18$). Then there is a nonuniformity in that $K(Z=19)$ fills the $4s$ orbital rather than the $3d$ orbital. This is because the effective potential

Table 9.1

Neutral atoms

Atom		K	L	M	N	O	Ground level
		$1s$	$2s\,2p$	$3s\,3p\,3d$	$4s\,4p\,4d$	$5s$	
H	1	1					$^2S_{\frac{1}{2}}$
He	2	2					$^1S_0$
Li	3	2	1				$^2S_{\frac{1}{2}}$
Be	4	2	2				$^1S_0$
B	5	2	2 1				$^2P^o_{\frac{1}{2}}$
C	6	2	2 2				$^3P_0$
N	7	2	2 3				$^4S^o_{1\frac{1}{2}}$
O	8	2	2 4				$^3P_1$
F	9	2	2 5				$^2P^o_{1\frac{1}{2}}$
Ne	10	2	2 6				$^1S_0$
Na	11	2	2 6	1			$^2S_{\frac{1}{2}}$
Mg	12			2			$^1S_0$
Al	13			2 1			$^2P^o_{\frac{1}{2}}$
Si	14		10	2 2			$^3P_0$
P	15			2 3			$^4S^o_{1\frac{1}{2}}$
S	16		Ne core	2 4			$^3P_2$
Cl	17			2 5			$^2P^o_{1\frac{1}{2}}$
Ar	18			2 6			$^1S_0$
K	19	2	2 6	2 6	1		$^2S_{\frac{1}{2}}$
Ca	20				2		$^1S_0$
Sc	21				1 2		$^2D_{1\frac{1}{2}}$
Ti	22				2 2		$^3F_2$
V	23		18		3 2		$^4F_{1\frac{1}{2}}$
Cr	24				5 1		$^7S_3$
Mn	25		A core		5 2		$^6S_{2\frac{1}{2}}$
Fe	26				6 2		$^5D_4$
Co	27				7 2		$^4F_{4\frac{1}{2}}$
Ni	28				8 2		$^3F_4$
Cu	29	2	2 6	2 6 10	1		$^2S_{\frac{1}{2}}$
Zn	30				2		$^1S_0$
Ga	31				2 1		$^2P^o_{\frac{1}{2}}$
Ge	32		28		2 2		$^3P_0$
As	33				2 3		$^4S^o_{1\frac{1}{2}}$
Se	34				2 4		$^3P_2$
Br	35				2 5		$^2P^o_{1\frac{1}{2}}$
Kr	36				2 6		$^1S_0$
Rb	37	2	2 6	2 6 10	2 6	1	$^2S_{\frac{1}{2}}$
Sr	38					2	$^1S_0$
Y	39					1 2	$^2D_{1\frac{1}{2}}$
Zr	40					2 2	$^3F_2$
Nb	41			36		4 1	$^6D_{\frac{1}{2}}$
Mo	42					5 1	$^7S_3$
Tc	43			Kr core		5 2	$^6S_{2\frac{1}{2}}$
Ru	44					7 1	$^5F_5$
Rh	45					8 1	$^4F_{4\frac{1}{2}}$
Pd	46					10	$^1S_0$

Atom		K L M N	N	O			P		Q	Ground level
			$4f$	$5s$	$5p$	$5d$ $5f$	$6s$	$6p$ $6d$	$7s$	
Ag	47			1						$^2S_{\frac{1}{2}}$
Cd	48			2						$^1S_0$
In	49			2	1					$^2P^o_{\frac{1}{2}}$
Sn	50			2	2					$^3P_0$
Sb	51			2	3					$^4S^o_{1\frac{1}{2}}$
Te	52			2	4					$^3P_2$
I	53			2	5					$^2P^o_{1\frac{1}{2}}$
Xe	54			2	6					$^1S_0$
Cs	55			2	6		1			$^2S_{\frac{1}{2}}$
Ba	56				8		2			$^1S_0$
La	57					1	2			$^2D_{1\frac{1}{2}}$
Ce	58		1	2	6	1	2			$^1G^o_4$
Pr	59		3				2			$^4I^o_{4\frac{1}{2}}$
Nd	60		4				2			$^5I_4$
Pm	61		5				2			$^6H^o_{2\frac{1}{2}}$
Sm	62		6				2			$^7F_0$
Eu	63		7				2			$^8S^o_{3\frac{1}{2}}$
Gd	64		7	8		1	2			$^9D_2$
Tb	65		9				2			$^6H^o_{7\frac{1}{2}}$
Dy	66		10				2			$^5I_8$
Ho	67		11				2			$^4I^o_{7\frac{1}{2}}$
Er	68		12				2			$^3H_6$
Tm	69		13				2			$^2F^o_{3\frac{1}{2}}$
Yb	70		14				2			$^1S_0$
Lu	71		14			1	2			$^2D_{1\frac{1}{2}}$
Hf	72		14	2	6	2	2			$^3F_2$
Ta	73					3	2			$^4F_{1\frac{1}{2}}$
W	74					4	2			$^5D_0$
Re	75		46+22			5	2			$^6S_{2\frac{1}{2}}$
Os	76					6	2			$^5D_4$
Ir	77					7	2			$^4F_{1\frac{1}{2}}$
Pt	78					9	1			$^3D_3$
Au	79		14	2	6	10	1			$^2S_{\frac{1}{2}}$
Hg	80						2			$^1S_0$
Tl	81						2	1		$^2P^o_{\frac{1}{2}}$
Pb	82		46+32				2	2		$^3P_0$
Bi	83						2	3		$^4S^o_{1\frac{1}{2}}$
Po	84						2	4		$^3P_2$
At	85						2	5		$^2P^o_{1\frac{1}{2}}$
Rn	86						2	6		$^1S_0$
Fr	87		14	2	6	10	2	6	1	$^2S_{\frac{1}{2}}$
Ra	88								2	$^1S_0$
Ac	89		46+32					1	2	$^2D_{2\frac{1}{2}}$
Th	90							2	2	$^3F_2$
Pa	91					2		1	2	$^4K_{5\frac{1}{2}}$
U	92					3		1	2	$^5L^o_6$

K L M N

N $4s\,4p\,4d$, M $3s\,3p\,3d$, L $2s\,2p$, (K $1s$, Pd core 46)

due to the electron cloud gives more binding to electrons that penetrate closer to the nucleus and thus feel the higher Coulomb field; such electrons are just the low-l electrons.

Closed shells generally are not much influenced by changes in the outer, partially filled shells, so that often one will only specify the configuration of the outer shell, such as: $Al-3s^2 3p$. Radiative transitions, at least at optical frequencies, usually affect only outer electrons.

By using the Pauli principle in this way, one can understand qualitatively the building up of the periodic table of elements.

The Electrostatic Interaction; *LS* Coupling and Terms

The specification of the electron configuration, the n, l values of all electrons, leaves a great deal of unspecified information, since we are not given the values of m_l and m_s. Note that in the central field approximation all of these states are degenerate, since the central field Hamiltonian is spherically symmetric and does not depend on spin. To proceed further we write the exact Hamiltonian as

$$H=\sum_i \frac{P_i^2}{2m} - Z\sum \frac{1}{r_i} + \sum V_i(r_i) + H_1 \equiv H_0 + H_1. \tag{9.20}$$

We have added and subtracted the central field potentials due to the smeared-out electrons. We regard this as a perturbation problem in which H_0 is the zeroth-order potential, whose states are just the configurations we have been discussing. The perturbation part H_1 is

$$H_1=\sum_{i>j} \frac{1}{r_{ij}} - \sum_i V_i(r_i) + H_{so} \equiv H_{es} + H_{so} + \cdots, \tag{9.21}$$

where H_{so} is the spin-orbit interaction to be discussed later, and where there are additional terms that are to be regarded as negligible. The first two terms represent the residual electrostatic interaction between the electrons after the averaged central field has been subtracted. This is what we simply call the *electrostatic interaction*, H_{es}.

For the present we are concerned with the splitting of the configurations by the electrostatic interaction. We note first of all that the individual orbital angular momenta will not remain constant under this interaction, although their total $\mathbf{L}=\Sigma_i \mathbf{l}_i$ will be constant. Also the sum of the spin angular momenta, $\mathbf{S}=\Sigma \mathbf{s}_i$, will be constant.

According to degenerate perturbation theory the first-order energy corrections must be found by evaluating the diagonal matrix elements between the particular linear combinations of the unperturbed states that

diagonalize the perturbation. Another way of characterizing these linear combinations is that they are eigenstates of operators that commute with the perturbation. We note that two such operators are **L** and **S** so that the whole perturbation problem is simplified (and in many cases completely solved) by forming those linear combinations of unperturbed states that represent states of total spin and total orbital angular momenta.

In this way we find the configurations split into *terms* with particular values of L and S (the magnetic numbers m_S and m_L do not enter by rotational symmetry arguments). These terms then split further by the action of the spin-orbit interaction. The fact that the electrostatic interaction is the dominant splitting interaction of a configuration for many atoms (especially of low Z) and that the remaining spin-orbit splitting is much smaller makes this perturbation scheme and its attendant characterization and labeling of states a very useful one. It is called *LS coupling* or *Russell–Saunders coupling*.

Let us discuss the origin of this electrostatic splitting from a physical point of view. The electrons repel each other, and therefore their mutual electrostatic energy is positive. The farther away the electrons get, the lower will be the contribution of the electrostatic energy to the total energy. This leads to an important set of rules governing the splitting of the configuration energies as a function of spin and orbital angular momentum. First we note that a large spin implies that the individual spins are aligned in the same direction. By the nature of the Pauli principle, we have that the electrons will be further apart on the average. Thus the rule: *terms with larger spin tend to lie lower in energy*. There is a similar effect regarding the orbital angular momentum L. A large L implies that the individual $\mathbf{l}_i$ are aligned so that the sense of orbiting around the atom is the same for most electrons. Such a pattern lends itself to the electrons keeping farther apart on the average than when they orbit in opposite directions. This effect is usually smaller than the preceding, thus the rule: *of those terms of a given configuration with a given spin those with largest L tend to lie lower in energy*. These two rules are known as *Hund's rules* and apply strictly only to the ground configuration.

9.4 PERTURBATIONS, LEVEL SPLITTINGS, AND TERM DIAGRAMS

Equivalent and Nonequivalent Electrons and Their Spectroscopic Terms

A problem of great importance is the evaluation of the possible spectroscopic terms that can arise from a given configuration of single particle states. This is a matter of listing the possible values of m_l and m_s for the

electrons outside of the closed shells and then determining what values of S and L can be constructed from them, subject to limitations imposed by indistinguishability and the Pauli exclusion principle. The reason that only the electrons in the closed shells need be considered is the following: Closed shells are spherically symmetric ($L=0$) and have very little interaction with external electrons. This fact results from a property of the spherical harmonics: for given n and l, if all possible electron states are filled, the total electron density distribution is precisely spherically symmetric. For example, for $l=1$,

$$|Y_{10}|^2+|Y_{1-1}|^2+|Y_{11}|^2=\frac{3}{4\pi}\cos^2\theta+\frac{3}{8\pi}\sin^2\theta+\frac{3}{8\pi}\sin^2\theta=\frac{3}{4\pi}.$$

It is useful to distinguish the cases of *nonequivalent* electrons and *equivalent* electrons. Nonequivalent electrons are those differing in either n or l values, whereas equivalent electrons have the same n and l values. For two equivalent s electrons, for example, we write s^2; if they are nonequivalent, we write $s{\cdot}s$ or ss'.

The terms of nonequivalent electrons are fairly simple to find. For sample, the configuration $1s2s$ can only have $L=0$, since both electrons have $l=0$. The spin can be $S=0,1$, corresponding to the two ways of orienting the spins. Thus we have the two possible terms ^1S and ^3S, where the letter refers to the total L value and the superscript refers to the number of m_s values, namely, $(2S+1)$. The $S=0$ and $S=1$ total spin states are called *singlet* and *triplet* states, respectively, in accordance with the number of m_s values. If the electrons are equivalent, say $1s^2$, then the triplet term cannot occur, since this would imply both spins are the same, and all sets of quantum numbers would be identical. Thus the only term for the equivalent electrons is ^1S.

The distinction between the spectroscopic combination of equivalent and nonequivalent electrons can be seen in the following illustration. Consider the combination of two p electrons. If they have different values of n, so that they are nonequivalent, the possible L-S combinations are $S=0,1$, $L=0,1,2$, leading to the spectroscopic terms ^1S, ^1P, ^1D, ^3S, ^3P, ^3D and $1+3+5+3+9+15=36$ distinguishable states, corresponding to the 6×6 product of the one-electron states. Now, suppose the two p electrons have the same n values and are thus equivalent. Then all the 36 states are not available: some are ruled out by the Pauli exclusion principle, and some are ruled out because they are not distinguishable from others. To count the distinguishable permitted states, we construct Table 9.2, giving possible combinations of m_{l_1}, m_{l_2}, m_{s_1}, m_{s_2}, marking OUT for Pauli excluded states and labeling only distinguishable states. We find there are 15 distinguishable states allowed.

Table 9.2

m_{l1}	m_{l2}	m_{s1}	m_{s2}	Label	m_{l1}	m_{l2}	m_{s1}	m_{s2}	Label
+1	+1	+½	+½	OUT	0	−1	+	+	11
		+	−	1			+	−	12
		−	+	1			−	+	13
		−	−	OUT			−	−	14
+1	0	+	+	2	−1	+1	+	+	6
		+	−	3			+	−	8
		−	+	4			−	+	7
		−	−	5			−	−	9
+1	−1	+	+	6	−1	0	+	+	11
		+	−	7			+	−	13
		−	+	8			−	+	12
		−	−	9			−	−	14
0	+1	+	+	2	−1	−1	+	+	OUT
		+	−	4			+	−	15
		−	+	3			−	+	15
		−	−	5			−	−	OUT
0	0	+	+	OUT					
		+	−	10					
		−	+	10					
		−	−	OUT					

Which spectroscopic terms do these combinations correspond to? We simply use the fact that

$$m_L = m_{l_1} + m_{l_2}, \tag{9.22a}$$

$$m_S = m_{s_1} + m_{s_2}. \tag{9.22b}$$

Since the combination $m_L = \pm 2$, $m_S = \pm 1$ does not occur, the ^3D state can be ruled out. On the other hand, state 2 requires a ^3P configuration. State 1 requires a $^1D_2$ configuration. These two configurations take up $3\times 3+1\times 5 = 14$ of the 15 distinguishable states. The only remaining configuration can be ^1S, with one associated state. Thus the allowed terms for two equivalent p electrons are

$$^1S,\ ^3P,\ ^1D.$$

When more than two equivalent electrons are involved, the counting is straightforward, but more tedious.

Table 9.3

TERMS OF NON-EQUIVALENT ELECTRONS

Electron Configuration	Terms
$s\ s$	$^1S, {}^3S$
$s\ p$	$^1P, {}^3P$
$s\ d$	$^1D, {}^3D$
$p\ p$	$^1S, {}^1P, {}^1D, {}^3S, {}^3P, {}^3D$
$p\ d$	$^1P, {}^1D, {}^1F, {}^3P, {}^3D, {}^3F$
$d\ d$	$^1S, {}^1P, {}^1D, {}^1F, {}^1G, {}^3S, {}^3P, {}^3D, {}^3F, {}^3G$
$s\ s\ s$	$^2S, {}^2S, {}^4S$
$s\ s\ p$	$^2P, {}^2P, {}^4P$
$s\ s\ d$	$^2D, {}^2D, {}^4D$
$s\ p\ p$	$^2S, {}^2P, {}^2D, {}^2S, {}^2P, {}^2D, {}^4S, {}^4P, {}^4D$
$s\ p\ d$	$^2P, {}^2D, {}^2F, {}^2P, {}^2D, {}^2F, {}^4P, {}^4D, {}^4F$
$p\ p\ p$	$^2S(2), {}^2P(6), {}^2D(4), {}^2F(2), {}^4S(1), {}^4P(3), {}^4D(2), {}^4F(1)$
$p\ p\ d$	$^2S(2), {}^2P(4), {}^2D(6), {}^2F(4), {}^2G(2), {}^4S(1), {}^4P(2), {}^4D(3), {}^4F(2), {}^4G(1)$
$p\ d\ f$	$^2S(2), {}^2P(4), {}^2D(6), {}^2F(6), {}^2G(6), {}^2H(4), {}^2I(2)$ $^4S(1), {}^4P(2), {}^4D(3), {}^4F(3), {}^4G(3), {}^4H(2), {}^4I(1)$

Similar arguments can be used to obtain the terms for other configurations, although the details become quite tedious for complicated cases. In these cases tables such as Table 9.3 may be consulted.

A useful rule concerning the terms of equivalent electrons is that the terms for a shell more than half filled are the same as for the complementary number of electrons needed to fill the shell. Since 6 electrons are required to fill the p shell, the terms corresponding to p and p^5 are the same; also p^2 and p^4. This rule is simply proved by noting that the total spin and orbital angular momentum of a closed shell are both zero, as mentioned previously. In enumerating the various values of m_L and m_S it makes no difference if we use m_l and m_s of the missing electrons, since only the magnitudes of the sums Σm_{l_i} and Σm_{s_i} are relevant. This is sometimes stated as the equivalence of electrons and holes in a shell.

Parity

Besides the quantum numbers L and S there is another important quantum number called the *parity* of the configuration. This is simply ± 1 or (even, odd) according to the even or oddness of the sum Σl_i extended over all the electrons of the configuration. Since the sum of the l_i for a closed shell is even, we may restrict the sum to incomplete shells. Physically the

parity corresponds to the symmetry or antisymmetry of the wave function when all spatial coordinates are reflected: $x \to -x$, $y \to -y$, $z \to -z$. For even parity $\psi \to \psi$, and for odd parity $\psi \to -\psi$. Since this property of the wave function is maintained under the usual interactions with which we deal, if a wave function has a certain parity at one time, it will keep that parity for all times. It should be noted that although the individual orbital angular momenta l_i do not in general have meaning, the evenness or oddness of their sum does. Note also that the sum Σl_i does not, in general, equal the total L of the configuration.

The parity of a configuration is usually given as a superscript "O" on the terms arising from this configuration when the parity is odd; when the parity is even no superscript appears. Thus a *s-p* configuration leads to terms ${}^1P^O$ and ${}^3P^O$, whereas *s-d* leads to terms ${}^1D$ and ${}^3D$. (Sometimes the parity is not indicated at all, so that the absence of a superscript does not always mean even parity).

Spin-Orbit Coupling

The next step in the resolution of the degenerate levels of a configuration is through the *spin-orbit* coupling. In *L-S* coupling this is assumed to be much smaller than the electrostatic interaction. The effect is to split each term into a set of *levels*, each of which is labeled by the one remaining quantum number, the total angular momentum J. The magnetic quantum number M_J, or simply M, does not participate in the splitting, unless there are external fields to break the rotational symmetry of the internal interactions.

The basic spin-orbit interaction may be illustrated by an individual electron moving in a central electrostatic force field. In the rest frame of the electron this electric field will be perceived as having a magnetic field component

$$\mathbf{B} = -\frac{1}{c}\mathbf{v} \times \mathbf{E} = \frac{\mathbf{l}}{mecr}\frac{dU}{dr}. \tag{9.23}$$

Here $\mathbf{v}$ is the electron's velocity, $\mathbf{l} = m\mathbf{v} \times \mathbf{r}$ is its orbital angular momentum, and $U(r)$ is the equivalent electrostatic potential. This magnetic field interacts with the electron's magnetic moment, which is

$$\boldsymbol{\mu} = -\frac{e}{mc}\mathbf{s}. \tag{9.24}$$

This is twice the value one obtains by considering the electron to be a classical charge and mass distribution of the same shape, and it requires

the Dirac equation of relativistic quantum mechanics for its derivation. (See, e.g., Bjorken and Drell, 1964.)

From the above, we might expect the interaction energy to be $U_{\text{int}} = -\boldsymbol{\mu}\cdot\mathbf{B}$. However, an exact derivation from the Dirac equation yields a value of one-half this. The discrepancy can be traced to the use of the instantaneous rest frame of the electron, which is constantly changing as the electron orbits. The effect of this acceleration can be described by *Thomas precession* (see Leighton, 1959), which is one-half the naively expected rate, but in the opposite direction, leading to the final result

$$H_{so} = \frac{1}{2m^2c^2}\mathbf{s}\cdot\mathbf{l}\frac{1}{r}\frac{dU}{dr}. \tag{9.25}$$

This is often written, for the sum of the interactions of all electrons,

$$H_{so} = \sum_i \xi_i(r_i)\mathbf{s}_i\cdot\mathbf{l}_i, \tag{9.26a}$$

where

$$\xi_i(r_i) = \frac{1}{2m^2c^2r}\frac{dU(r_i)}{dr}. \tag{9.26b}$$

When we find matrix elements of this H_{so} between states of S and L, the individual spin and orbital angular momenta become averaged over in such a way that an equivalent interaction for our purposes is simply

$$H_{so} = \xi\mathbf{S}\cdot\mathbf{L}, \tag{9.27a}$$

where

$$\mathbf{S} = \sum \mathbf{s}_i, \qquad \mathbf{L} = \sum \mathbf{l}_i \tag{9.27b}$$

and ξ is an appropriate average of the ξ_i. (For details see Bethe and Jackiw, 1968.)

With this simplified spin-orbit term we are in a position to find the splittings of a given term as a function of the total angular momentum quantum number J. To do this we note that

$$\mathbf{J}^2 = (\mathbf{L}+\mathbf{S})\cdot(\mathbf{L}+\mathbf{S}) = \mathbf{L}^2 + \mathbf{S}^2 + 2\mathbf{L}\cdot\mathbf{S}, \tag{9.28}$$

so that

$$H_{so} = \tfrac{1}{2}\xi(\mathbf{J}^2 - \mathbf{L}^2 - \mathbf{S}^2). \tag{9.29}$$

Note also that $\mathbf{J}^2$, $\mathbf{L}^2$ and $\mathbf{S}^2$ are mutually commuting operators, since $\mathbf{L}$ commutes with $\mathbf{L}^2$ and $\mathbf{S}$ commutes with $\mathbf{S}^2$. Therefore, when we take diagonal elements of this quantity between states of given L, S, and J we obtain

$$\langle H_{so} \rangle = \tfrac{1}{2} C\big[J(J+1) - L(L+1) - S(S+1)\big], \tag{9.30}$$

where C is a constant related to the average of $\xi(r)$ over the spatial part of the wave function.

For fixed L and S, that is, for a given term, the energy shift is proportional to $J(J+1)$, so that the consecutive splittings are given by

$$\begin{aligned} E_{J+1} - E_J &= \tfrac{1}{2} C\big[(J+1)(J+2) - J(J+1)\big] \\ &= C(J+1). \end{aligned} \tag{9.31}$$

Therefore, we have the *Lande interval rule*: *the spacing between two consecutive levels of a term is proportional to the larger of the two J values involved.* This rule is very useful in determining the J values of levels empirically.

The J value of a level is given as a subscript on the term symbol: $^3P_2$, $^2S_{\frac{1}{2}}$. Often the allowed values of J are given on the term symbol, separated by commas, for example, $^2P_{1/2,3/2;}$ $^3D_{1,2,3}$. The number of J values in any term is equal to the smaller of $(2L+1)$ and $(2S+1)$.

The ordering of the energies within the levels of a term are with increasing J if the shell is less than half-full, that is, the constant C above is positive. Such a term is called *normal*. On the other hand for shells more than half full the ordering is with decreasing J. Such terms are called *inverted*. An illustration of this is the two cases of the ground levels of carbon and oxygen. Each has the same terms, as the configurations p^2 and p^4, respectively. The ground term is a ^3P in both cases, but the ground level is $^3P_0$ for C, and a $^3P_2$ for O.

The progressive splitting of a configuration into terms and levels is illustrated by Fig. 9.2.

The degeneracy of each of the levels is $(2J+1)$, corresponding to the values of the magnetic quantum numbers $M_J = -J, \ldots -1, 0, 1, \ldots J$. These levels remain degenerate, unless external fields are applied, for example, a magnetic field (Zeeman effect) or an electric field (Stark effect). It is easily verified from Fig. 9.2a that for the case of the $4p4d$ configuration the total number of states represented by the final fine structure levels is 60. This is the same as the number of states represented by the configuration: $2\cdot(2l+1)\cdot 2(2l'+1) = 60$, where $l=1$, $l'=2$.

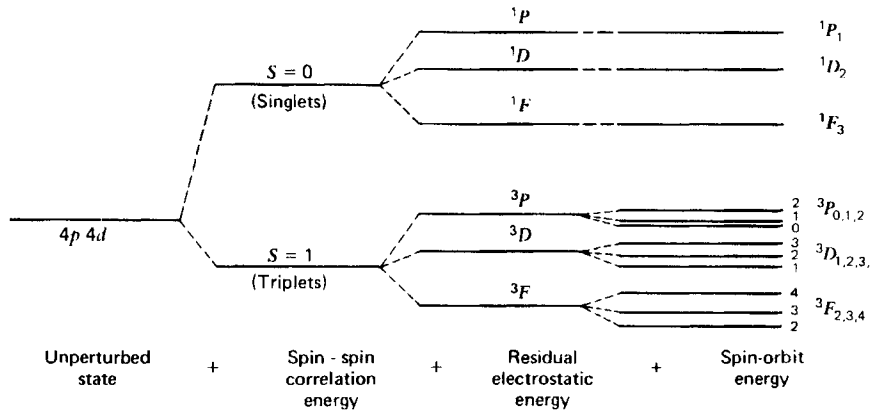

(*a*)

Figure 9.2a Schematic diagram illustrating the terms of energy levels generated by a 4p4d configuration in L-S coupling.

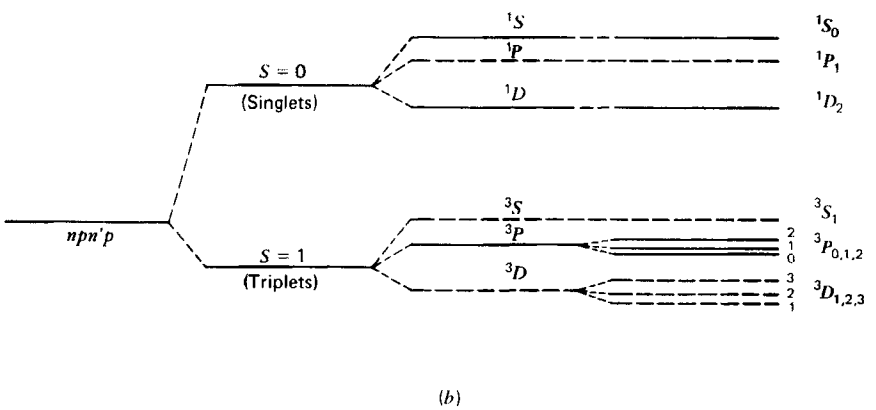

(*b*)

Figure 9.2b Same as a, but for two p electrons. Dashed levels are absent from the multiplet if the electrons are equivalent (n = n'). (Taken from Leighton, R., 1959, Principles of Modern Physics, McGraw-Hill, New York.)

The usual mode of presentation of this information is in a *term diagram*, which separates the terms of different S values, and within each group separates according to L values. The energies are represented by lines drawn on the proper vertical scale.

Zeeman Effect

As is shown in Chapter 3, electrical particles of charge e, mass m, oscillating at frequency ω_0 radiate dipole radiation of frequency ω_0. As is easily shown (Leighton, 1959), a classical analysis indicates that in the presence of a magnetic field of strength B, the radiation is split into three separate frequencies, $\omega_+ \equiv \omega_0 + eB/2mc$, ω_0, and $\omega_- \equiv \omega_0 - eB/2mc$. This splitting, due to the Lorentz force on the electron, also has well-defined polarization properties: If the radiation is viewed at right angles to **B**, all three components are visible, with the component ω_0 plane polarized and $\omega_\pm$ circularly polarized. If the radiation is viewed along the magnetic field, the undeviated component ω_0 is no longer visible. These classical line patterns are termed *normal* Zeeman lines.

Unfortunately, the observed Zeeman splittings are generally *anomalous*; that is, they disagree with the classical prediction because of quantum mechanical effects. As in the spin-orbit coupling discussed previously, the interaction energy between the electrons of total magnetic moment μ and the external magnetic field is

$$U_B = -\mu \cdot \mathbf{B}. \tag{9.32}$$

The total magnetic moment is the sum over all electrons of the orbital and spin magnetic moments of the individual electrons

$$\mu = -\sum \left[\tfrac{1}{2}\left(\frac{e}{mc}\right)\mathbf{l}_i + \left(\frac{e}{mc}\right)\mathbf{s}_i \right]. \tag{9.33}$$

The different proportionality factors multiplying $\mathbf{l}_i$ and $\mathbf{s}_i$ result from the quantum mechanical nature of intrinsic spin, [cf. Eq. (9.24)]. Now, since the energy of Zeeman splitting is generally much smaller than that of the fine-structure levels, we may treat the former as a perturbation, with L and S remaining good quantum numbers. Thus Eq. (9.33) becomes, using Eqs. (9.27b) and (9.28)

$$\begin{aligned} \mu &= -\tfrac{1}{2}\left(\frac{e}{mc}\right)(\mathbf{L} + 2\mathbf{S}) \\ &= -\tfrac{1}{2}\left(\frac{e}{mc}\right)(\mathbf{J} + \mathbf{S}). \end{aligned} \tag{9.34}$$

The torque of the external magnetic field causes the magnetic moment $\boldsymbol{\mu}$ to precess around **B**. However, this precession frequency is much smaller than the precession frequency of **S** around **J** (because of the much more energetic $\mathbf{L}\cdot\mathbf{S}$ coupling). Thus the component of $\boldsymbol{\mu}$ along **J** can be considered fixed, with the component along **S** precessing around. The time-averaged component of $\boldsymbol{\mu}$ along **B** (assumed to lie along the z axis) can be approximated by the component along **J** multiplied by the component of **J** along **B**:

$$U_B \approx \tfrac{1}{2}\left(\frac{e}{mc}\right)[(\mathbf{J}+\mathbf{S})\cdot\mathbf{J}]\frac{(\mathbf{J}\cdot\mathbf{B})}{|\mathbf{J}|^2}$$

$$= \tfrac{1}{2}\left(\frac{e\hbar B}{mc}\right)gM_J, \tag{9.35a}$$

where

$$M_J = J_Z$$

and

$$g(J,L,S) \equiv 1 + \frac{J(J+1)+S(S+L)-L(L+1)}{2J(J+1)}. \tag{9.35b}$$

Here we have used Eq. (9.28) to evaluate Eq. (9.35). The quantity g is called the Lande g factor; if the proportionality factors multiplying $\mathbf{l}_i$ and $\mathbf{s}_i$ in Eq. (9.33) were equal, g would be independent of J, L and S.

The frequency of a transition from level 1 to level 2 is

$$\omega_{12} = \tfrac{1}{2}\left(\frac{eB}{mc}\right)(g_1 M_{J_1} - g_2 M_{J_2}). \tag{9.36}$$

If $\Delta M_J = 0, \pm 1$ (see Chapter 10) and if $g_1 = g_2$, the splittings would agree with the classical theory. However, in general J, L and S change in the transition in such a way that g also changes, leading to a variety of different splittings.

Role of the Nucleus; Hyperfine Structure

Up to this point we have made several simplifying assumptions concerning the nucleus: (1) infinite mass; (2) point particle; (3) interaction with electrons only through the Coulomb field of its total charge Ze. The

violations of these assumptions produce small effects on the atomic electron states called *hyperfine structure*. The small effects on the states are not so important in themselves as are the splittings of the states into several substates, since this is much easier to observe. The splittings may be divided into two groups which have rather different origins:

I—*Isotope Effect:* An atomic nucleus of charge Ze can have a number of different masses, depending on the total number of neutrons it possesses. The various species of nuclei with the same atomic number Z are called *isotopes*. Each isotope will have a slightly different set of atomic energy levels, because of finite (noninfinite) mass and finite (nonzero) size effects, which differ for each isotope. In any naturally occurring material there will be a distribution over the various isotopes in proportions that depend on the origin, age, and history of the material. The spectra produced by such an isotopic mixture show splittings of lines, each component of which comes from a different isotope.

One may regard isotope splittings as due purely to the production of spectra by differing atomic species, where the differences are extremely small. The splittings as such do not occur in a single atom, and it would be meaningless to speak of an atomic transition between the split states, as this would require a nuclear transformation.

II—*Nuclear Spin:* Like electrons, other subatomic particles possess spin and associated magnetic moments. The nucleus therefore also has a total spin angular momentum **I**, with eigenvalues $I(I+1)$ for its square and M_I for its z component. We may express the magnetic moment μ_N by means of a nuclear g factor:

$$\mu_N = g\frac{e}{2Mc}\mathbf{I}. \tag{9.37}$$

For the proton, for example, where $M \sim 1840\ m_e$, we have $g = 5.5855$. (Recall that for the electron $g = 2.00232$.) Since g factors are normally of order unity we see that nuclear magnetic moments are about 10^{3-4} smaller than that of the electron.

The nuclear magnetic moment interacts with the magnetic moments of the atomic electrons, and each previously described atomic state is further split by this interaction. In analogy with the L-S coupling scheme we now introduce the total angular momentum vector $\mathbf{F} = \mathbf{J} + \mathbf{I}$ and label the hyperfine states by the quantum number F. For example, when $I = 2$ for a $^3D_3$ state, we have five splittings, corresponding to $F = 1$ to 5.

In contrast to the isotope effect, the nuclear spin effects produce splittings within a single atom, and the states so produced may be reached

by an appropriate atomic electron transition, such that the orientation of $\mathbf{J}=\mathbf{L}+\mathbf{S}$ changes relative to $\mathbf{I}$.

An example of extreme importance in astrophysics is the ground level of neutral atomic hydrogen, which is a ${}^2S_{\frac{1}{2}}$ level. The proton spin is $\frac{1}{2}$ so that two hyperfine states occur, the ground state with $F=0$ and an excited state with $F=1$. The energy difference between these states corresponds to a frequency of 1420 MHz, or a wavelength of 21 cm. Radiative transitions from $F=1$ to $F=0$ are extremely rare for a given atom, that is, about once every 10^7 years, but with the enormous abundance of neutral hydrogen this nonetheless gives rise to an observable 21-cm line.

9.5 THERMAL DISTRIBUTION OF ENERGY LEVELS AND IONIZATION

Thermal Equilibrium: Boltzmann Population of Levels

The relative populations of the various atomic levels is a difficult question in general, since it depends on the detailed processes by which any level becomes populated or depopulated. An exception is the case of *thermal equilibrium*, where the populations are completely determined by the temperature T. Then in any collection of atoms of a specific type the number in any given level is proportional to $ge^{-\beta E}$, where $\beta \equiv 1/kT$, $k=$ Boltzmann's constant, and $g=$ statistical weight (degeneracy) of the level. In L-S coupling the g factors are simply $g=(2J+1)$. It is customary to measure energies using the ground level as a zero point; let us call these energies E_i for the ith level. If N_i is the population (number per unit volume) of the ith level and N is the total population of the atom we have the *Boltzmann law*:

$$N_i = \frac{N}{U} g_i e^{-\beta E_i}. \tag{9.38}$$

Here U is the constant of proportionality; it is called the *partition function*. We may find U by demanding that

$$N = \sum N_i,$$

where the sum is over all levels. This yields

$$U = \sum g_i e^{-\beta E_i}. \tag{9.39}$$

At sufficiently low temperatures only the first term in the sum is significant, and we obtain

$$U = g_0,$$

where g_0 is the degeneracy of the ground level.

At finite temperatures we run into a mathematical difficulty: the sum $\sum g_i e^{-\beta E_i}$ diverges. This occurs because $g = 2J + 1$ approaches infinity while $e^{-\beta E_i}$ approaches a constant as the ionization continuum is approached. Physically this is resolved by recognizing that in an actual gas the atoms are not at infinite distances, so that the idealized model of an atom extending to infinity is not valid. The high principal quantum number n values that cause the divergence are just those states that are affected by the presence of the neighboring atoms. These high-n electrons can be easily ripped off by perturbations from the neighbors, so that an atom reaches its effective ionization potential at some large but finite value of the principal quantum number, $n_{\max}$. This lowering of the ionization potential can be taken into account approximately by cutting off the summation over levels at the value $n = n_{\max}$. One limit on $n_{\max}$ may be deduced from the condition that the Bohr orbit corresponding to $n = n_{\max}$ be of order of the interatomic distances

$$n_{\max}^2 a_0 Z^{-1} \sim N^{-1/3},$$

$$n_{\max} \sim \left(\frac{Z}{a_0}\right)^{1/2} N^{-1/6}. \tag{9.40}$$

For hydrogen at $N = 10^{12}$ cm^{-3}, for example, we would have $n_{\max} \sim 10^2$. Actually, there are other effects operating here as well (e.g., Debye shielding) which depend on temperature as well, so that the computation of $n_{\max}$ is quite involved. A really basic understanding of the cutoff has probably not yet been achieved. Fortunately, for many cases of interest the precise value of the cutoff is not too critical. In the range of temperatures up to 10^4K, U is in most cases equal to g_0, the exceptions being low-ionization potential elements like the alkali metals.

The Saha Equation

So far we have considered the distribution among the levels of a single atom in thermal equilibrium. Now we want to determine the distribution of an atomic species among its various stages of ionization. The resulting equation is called the *Saha equation*. We now derive this equation for the case of a neutral atom and its first stage of ionization.

We start with the generalization of the Boltzmann law:

$$\frac{dN_0^+(v)}{N_0} = \frac{g}{g_0}\exp\left[-\frac{\left(\chi_I + \frac{1}{2}m_e v^2\right)}{kT}\right], \tag{9.41}$$

where χ_I is the ionization potential. Here $dN_0^+(v)$ is the differential number of ions in the ground level with the free electron in velocity range $(v, v+dv)$, and N_0 is the number of atoms in the ground level. The statistical weight of the atom in its ground state is g_0. The statistical weight g is the product of the statistical weight of the ion in its ground state g_0^+ and the differential electron statistical weight g_e:

$$g = g_0^+ \cdot g_e. \tag{9.42}$$

The statistical weight g_e is given by

$$g_e = \frac{2dx_1dx_2dx_3dp_1dp_2dp_3}{h^3}, \tag{9.43}$$

where the factor 2 comes about from the two spin states. The volume element satisfies $dx_1dx_2dx_3 = 1/N_e$, where N_e = electron density, since we are applying Boltzmann's law to a region containing one electron. Since the electrons have an isotropic velocity distribution, we have

$$dp_1dp_2dp_3 = 4\pi m_e^3 v^2 dv.$$

Thus Eq. (9.41) becomes

$$\frac{dN_0^+(v)}{N_0} = \frac{8\pi m_e^3}{h^3}\frac{g_0^+}{N_e g_0}\exp\left[-\frac{\left(\chi_I + \frac{1}{2}m_e v^2\right)}{kT}\right]v^2 dv. \tag{9.44}$$

To find the total N_0^+, irrespective of the electron's velocity, we integrate over all v:

$$\frac{N_0^+ N_e}{N_0} = \frac{8\pi m_e^3}{h^3}\frac{g_0^+}{g_0}e^{-\chi_I/kT}\left(\frac{2kT}{m_e}\right)^{3/2}\int_0^\infty e^{-x^2}x^2\,dx,$$

where the substitution $x \equiv (m_e/2kT)^{1/2}v$ has been made. The integral has the value $\pi^{1/2}/4$. Thus we obtain

$$\frac{N_0^+ N_e}{N_0} = \left(\frac{2\pi m_e kT}{h^2}\right)^{3/2}\frac{2g_0^+}{g_0}e^{-\chi_I/kT}. \tag{9.45}$$

To find the number of atoms or ions in any state, not just the ground state, we use the Boltzmann laws [cf. Eqs. (9.38)],

$$\frac{N_0}{N} = \frac{g_0}{U(T)}, \qquad \frac{N_0^+}{N^+} = \frac{g_0^+}{U^+(T)}. \tag{9.46}$$

We then obtain *Saha's equation*:

$$\frac{N^+ N_e}{N} = \frac{2U^+(T)}{U(T)} \left(\frac{2\pi m_e kT}{h^2} \right)^{3/2} e^{-\chi_1/kT}. \tag{9.47}$$

Here N and N^+ are the total number densities of neutral atoms and first ionized atoms, respectively, and U and U^+ are the corresponding partition functions.

A similar derivation shows that there is a Saha equation connecting any two successive stages of ionization:

$$\frac{N_{j+1} N_e}{N_j} = \frac{2U_{j+1}(T)}{U_j(T)} \left(\frac{2\pi m_e kT}{h^2} \right)^{3/2} e^{-\chi_{j,j+1}/kT}, \tag{9.48}$$

where the subscripts here refer to stages of ionization. These equations are often stated in terms of pressures rather than number densities. The ideal gas law is

$$P = NkT,$$

so that

$$\frac{P_{j+1} P_e}{P_j} = \frac{2U_{j+1}(T)}{U_j(T)} \left(\frac{2\pi m_e}{h^2} \right)^{3/2} (kT)^{5/2} e^{-\chi_{j,j+1}/kT}. \tag{9.49}$$

To calculate the ionizational equilibrium of a mixture of various elements, some further equations must be used. First there must be an equation giving the conservation of nuclei

$$\sum N_j^{(i)} = N^{(i)}, \tag{9.50a}$$

where $N_j^{(i)}$ is the number density of species i in the jth stage of ionization, and $N^{(i)}$ is the total number density over all stages of ionization (the number density of nuclei of that species). Also, there is an equation for conservation of charge (number of electrons):

$$N_e = \sum_i \sum_j Z_j N_j^{(i)}. \tag{9.50b}$$

Here Z_j is the charge (in units of e) of the jth stage of ionization.

The actual solution to these equations must proceed numerically, in most cases by an iterative procedure. For many cases of physical interest, most of a given species is found in a few (one to three) ionization stages for any one set of conditions (see Problem 9.4). This reduces the numerical problems considerably, so that a solution can usually be obtained after a few iterations.

The ionization equilibrium of pure hydrogen can be worked out analytically (neglecting the H^- ion as unimportant) (see Problem 9.5), but this is an exception. Also, one must be quite careful in such situations to take into consideration species that have a low ionization potential, even if such species are not abundant. This is because the electron density may be completely determined by ionization of these trace constituents. Because of this, a "pure" hydrogen case rarely occurs in nature.

It is common in astrophysics to denote neutral and ionized hydrogen by HI and HII, respectively. In general, an element Q which is in its nth ionization state is denoted by Q followed by the Roman numeral for $n+1$.

PROBLEMS

9.1—Consider two electronic orbitals u_a and u_b occupied by two electrons, 1 and 2. Neglect the electrostatic repulsion of the two electrons.

a. Show that the mean square distance, $\langle R^2 \rangle$, between the two electrons is

$$\langle R^2 \rangle = (\mathbf{r}^2)_a + (\mathbf{r}^2)_b - 2|\mathbf{r}_a||\mathbf{r}_b| + 2|\mathbf{r}_{ab}|^2$$

where

$$\mathbf{r}_a \equiv \int u_a^* \mathbf{r} u_a d^3r,$$

$$(\mathbf{r}^2)_a \equiv \int u_a^* \mathbf{r}^2 u_a d^3r,$$

$$\mathbf{r}_{ab} \equiv \int u_a^* \mathbf{r} u_b d^3r.$$

(The integration here also imply a summation over spins.)

b. For states a and b defined by n, l, m, m_s show that $\mathbf{r}_a = \mathbf{r}_b = 0$, so that

$$\langle R^2 \rangle = (\mathbf{r}^2)_a + (\mathbf{r}^2)_b + 2|\mathbf{r}_{ab}|^2.$$

c. For electrons having different spins show that

$$\mathbf{r}_{ab} = 0$$

so that for such electrons

$$\langle R^2 \rangle = (\mathbf{r}^2)_a + (\mathbf{r}^2)_b,$$

which is the same as for the classical uncorrelated motion of two particles.

d. Thus show that electrons having the same spins are on the average further apart than electrons having different spins. This is an example of an *electron correlation effect*.

9.2—Give the spectroscopic terms arising from the following configurations, using L-S coupling. Include parity and J values. Give your arguments in detail for deriving these results.

a. $2s^2$

b. $2p3s$

c. $3p4p$

Find the terms corresponding to the following configuration.

d. $2p^4 3p$

9.3—For each of the *configurations* in the problem above evaluate its degeneracy from the l values involved [you may omit (d) here]. Next evaluate the degeneracy of each of the terms from the L and S values. Finally, evaluate the degeneracy of each of the levels from the J values. Show that these degeneracies are consistent, in that the degeneracy of any configuration is equal to the sum of the degeneracies of the terms it generates, and that the degeneracy of any term is equal to the sum of the degeneracies of the levels it generates.

9.4—The thermal de Broglie wavelength of electrons at temperature T is defined by $\lambda = h/(2\pi mkT)^{1/2}$. The degree of degeneracy of the electrons can be measured by the number of electrons in a cube λ on a side:

$$\xi \equiv N_e \lambda^3 = 4.1 \times 10^{-16} N_e T^{-3/2}.$$

For many cases of physical interest the electrons are very nondegenerate,

the quantity $\gamma \equiv \ln \xi^{-1}$ being of order 10 to 30. We want to investigate the consequences for the Boltzmann and Saha equations of γ being large and only weakly dependent on temperature. For the present purposes assume that the partition functions are independent of temperature and of order unity.

a. Show that the value of temperature at which the stage of ionization passes from j to $j+1$ is given approximately by

$$kT \sim \frac{\chi}{\gamma}$$

where χ is the ionization potential between stages j and $j+1$. Therefore, this temperature is much smaller than the ionization potential expressed in temperature units.

b. The rapidity with which the ionization stage changes is measured by the temperature range ΔT over which the ratio of populations N_j/N_{j+1} changes substantially. Show that

$$\frac{\Delta T}{T} \sim \left[\frac{d \log(N_{j+1}/N_j)}{d \log T} \right]^{-1} \sim \gamma^{-1}$$

Therefore, ΔT is much smaller than T itself, and the change occurs rapidly.

c. Using the Boltzmann equation and result (a) above, show that when γ is large, an atom or ion stays mostly in its ground state before being ionized.

9.5—A cold neutral hydrogen gas of density ρ resides inside a metal container. The container walls are then heated to temperature T. Find the equilibrium value of the ratio δ of ionized to neutral hydrogen as a function of ρ and T.

a. Find a single, dimensionless parameter $\Delta(\rho, T)$ that determines δ (cf. 9.4 above).

b. Derive an explicit algebraic expression for $\delta(\Delta)$. You may assume that the partition function is constant and equal to the ground state statistical weight.

REFERENCES

Bethe, H. A., and Jackiw, R., 1968. *Intermediate Quantum Mechanics* 2nd ed., (Benjamin, Reading, Mass.).
Bjorken, J. D., and Drell, S. D. 1964, *Relativistic Quantum Mechanics*, (McGraw-Hill, New York).
Kuhn, H., 1962, *Atomic Spectra* (Academic, New York).
Leighton, R. 1959, *Principles of Modern Physics*, (McGraw-Hill, New York).
Mihalas, D., 1978, *Stellar Atmospheres* 2nd ed., (Freeman, San Francisco).

10

RADIATIVE TRANSITIONS

10.1 SEMI-CLASSICAL THEORY OF RADIATIVE TRANSITIONS

So far we have looked only at those properties of atomic systems—such as ionization potentials and statistical mechanics—that depend solely on the energies of the various states. Now we want to investigate the nature of the light produced in transitions between these states. There are two major objectives here: first, to give so-called *selection rules* for radiative transitions and second, to determine the *strengths* of the radiation. The first of these is in some sense a special case of the second, but we shall regard it separately. The rules we give will be mostly applicable to L-S coupling and, additionally, to electric dipole transitions, although we do discuss some generalizations.

We use the so-called *semi-classical* theory of radiation, in which the atom is treated quantum mechanically, but the radiation field is treated classically. It is found that this theory correctly predicts the induced radiation processes, that is, those processes described by Einstein B coefficients, but that it fails to predict the spontaneous process, described by the Einstein A coefficient. This is not a great difficulty, because the Einstein coefficients are related, and any one can be used to derive the

other two. The physical argument used to justify the semi-classical approach is the following: the classical limit of radiation is the one in which the number of photons per photon state is large. Thus the induced processes, which are proportional to the number of photons, dominate the spontaneous process, which is independent of the number of photons. Because of the linearity of the induced processes in the number of photons, these processes may be extrapolated to small photon numbers, i.e. the quantum regime. The spontaneous rate can then be found by the Einstein relations.

The Electromagnetic Hamiltonian

The relativistic generalization of the Hamiltonian for a particle in an external electromagnetic field is

$$H = \left[(c\mathbf{p} - e\mathbf{A})^2 + m^2c^4\right]^{1/2} + e\phi. \tag{10.1}$$

If we expand this in the nonrelativistic limit, ignoring the (constant) rest mass, we obtain

$$\begin{aligned} H &= \frac{1}{2m}\left(\mathbf{p} - \frac{e\mathbf{A}}{c}\right)^2 + e\phi \\ &= \frac{p^2}{2m} - \frac{e}{mc}\mathbf{A}\cdot\mathbf{p} + \frac{e^2A^2}{2mc^2} + e\phi. \end{aligned} \tag{10.2}$$

In Eq. (10-2) we have used the "Coulomb gauge," (see §2.5 for a discussion of Gauge transformations),

$$\nabla\cdot\mathbf{A} = \phi = 0, \tag{10.3}$$

so that the momentum operator $\mathbf{p}$ commutes with $\mathbf{A}$ in their scalar product:

$$\mathbf{p}\cdot\mathbf{A} = \mathbf{A}\cdot\mathbf{p}.$$

We may estimate the ratio of the two terms in $\mathbf{A}$:

$$\eta \equiv \frac{epA/mc}{e^2A^2/2mc^2} \simeq \frac{2ev/c}{\alpha^2 a_0 A},$$

where α is the *fine-structure* constant

$$\alpha \equiv \frac{e^2}{\hbar c} \simeq \frac{1}{137}. \tag{10.4}$$

Since $v/c \sim \alpha$ [cf. Eqs. (9.6) and (9.7)] for atoms and $A \sim \lambda E$, where E is the electric field and λ is the wavelength, we have

$$\eta^2 \sim \frac{4\hbar\omega}{2\pi\alpha a_0^2 \lambda E^2}.$$

Since $\lambda \sim a_0/\alpha$ and $n_{ph} \sim E^2/\hbar\omega$ is the photon density, we have

$$\eta^2 \sim \left(n_{ph} a_0^3\right)^{-1} \gg 1 \tag{10.5}$$

as the condition that the linear term in A dominates the quadratic one. In other words, the number of photons inside the atom at one time is small. In fact, the term quadratic in A contributes to two-photon processes, which we ignore here under the assumption that the number of photons is sufficiently small. Note that the photon density at which this assumption fails is $n_{ph} \sim 10^{25}$ cm^{-3}, whereas at the sun's surface we have only $n_{ph} \sim 10^{12}$ cm^{-3}. Ordinarily, the neglect of the A^2 term is justified.

We now want to apply this to an atomic system of electrons. To do this we regard the sum of terms of the sort $(-e/mc)\mathbf{p}\cdot\mathbf{A}$ as a perturbation to the atomic Hamiltonian, and we use time-dependent perturbation theory to calculate the transition probabilities between the atomic states. (We continue to work in the Coulomb gauge, so that $\phi = 0$ and $\nabla \cdot \mathbf{A} = 0$.)

The Transition Probability

First, we split the Hamiltonian of Eq. (10.2) into a time-independent and a time-dependent piece:

$$H = H^0 + H^1. \tag{10.6}$$

Here H^0 is the atomic Hamiltonian, assumed independent of time, and H^1 is the perturbation due to the external electromagnetic field. The atomic eigenvalues E_k and eigenfunctions ϕ_k of H^0 are given by

$$H^0 \phi_k = E_k \phi_k. \tag{10.7}$$

Therefore, the zeroth-order time dependent wave functions are $\phi_k \exp(-iE_k t/\hbar)$. We may expand the actual wave function in this complete set

$$\psi(t) = \sum a_k(t) \phi_k \exp(-iE_k t/\hbar). \tag{10.8}$$

It is now straightforward to show from the Schrodinger equation (e.g.,

Merzbacher, 1961) that the probability per unit time for a transition from state i to state f, w_{fi}, is given by

$$w_{fi} = \frac{4\pi^2}{\hbar^2 T} |H_{fi}^1(\omega_{fi})|^2 \tag{10.9}$$

where

$$H_{fi}^1(\omega) \equiv (2\pi)^{-1} \int_0^T H_{fi}^1(t') e^{i\omega t'} dt' \tag{10.10a}$$

$$H_{fi}^1(t) \equiv \int \phi_f^* H^1 \phi_i \, d^3x, \tag{10.10b}$$

$$\omega_{fi} \equiv \frac{E_f - E_i}{\hbar}. \tag{10.10c}$$

Here the perturbation is assumed to be active only during the time interval 0 to T.

For a number of atomic electrons we have the perturbation from an external field

$$H^1 = \frac{-e}{mc} \sum \mathbf{A} \cdot \mathbf{p}_j = \frac{ie\hbar}{mc} \mathbf{A} \cdot \sum \nabla_j, \tag{10.11}$$

since $\mathbf{p}_j \rightarrow -i\hbar\nabla_j$. We assume that $\mathbf{A}(\mathbf{r}, t)$ has the form

$$\mathbf{A}(\mathbf{r}, t) = \mathbf{A}(t) e^{i\mathbf{k}\cdot\mathbf{r}},$$

where $\mathbf{A}(t)$ vanishes outside the interval $0 < t < T$. T is assumed to be large enough that a well-defined frequency of the wave exists. Then we obtain

$$H_{fi}^1(\omega_{fi}) = \mathbf{A}(\omega_{fi}) \cdot \frac{ie\hbar}{mc} \left\langle f \middle| e^{i\mathbf{k}\cdot\mathbf{r}} \sum \nabla_j \middle| i \right\rangle, \tag{10.12}$$

where

$$\left\langle f \middle| e^{i\mathbf{k}\cdot\mathbf{r}} \sum \nabla_j \middle| i \right\rangle \equiv \int \phi_f^* e^{i\mathbf{k}\cdot\mathbf{r}} \sum \nabla_j \phi_i \, d^3x,$$

which does not depend on time. Here d^3x denotes integration over the coordinates of all particles. $\mathbf{A}(\omega)$ is defined in the same manner as $H_{fi}^1(\omega)$, [cf. Eq. (10.10a)]. The transition rate is then

$$w_{fi} = \frac{4\pi^2 e^2}{m^2 c^2 T} |A(\omega_{fi})|^2 \left| \left\langle f \middle| e^{i\mathbf{k}\cdot\mathbf{r}} \mathbf{1} \cdot \sum \nabla_j \middle| i \right\rangle \right|^2, \tag{10.13}$$

where $\mathbf{l}$ is a unit vector specifying the polarization of the wave: $\mathbf{A} = A\mathbf{l}$. We want to express $A(\omega_{fi})$ in terms of the intensity of the electromagnetic wave traveling in direction $\mathbf{n}$. This intensity is [cf. §2.3]

$$I = \langle \mathbf{S} \cdot \mathbf{n} \rangle = \frac{c}{4\pi T} \int_{-\infty}^{\infty} E^2(t)\, dt = \frac{c}{T} \int_0^{\infty} |E(\omega)|^2 d\omega. \tag{10.14}$$

Also, for the monochromatic intensity we have [cf. Eq. (2.34)]

$$\frac{dW}{dA\, d\omega\, dt} \equiv \mathcal{I}(\omega) = \frac{c|E(\omega)|^2}{T}.$$

But since $\mathbf{E} = -c^{-1}\partial \mathbf{A}/\partial t$ we have $\mathbf{E}(\omega) = -i\omega c^{-1}\mathbf{A}(\omega)$ so that

$$\mathcal{I}(\omega) = \frac{\omega^2}{cT} |\mathbf{A}(\omega)|^2. \tag{10.15}$$

Thus we obtain

$$w_{fi} = \frac{4\pi^2 e^2}{m^2 c} \frac{\mathcal{I}(\omega_{fi})}{\omega_{fi}^2} \left| \left\langle f \left| e^{i\mathbf{k}\cdot\mathbf{r}} \mathbf{l} \cdot \sum \nabla_j \right| i \right\rangle \right|^2. \tag{10.16a}$$

This formula applies equally to absorption or to induced emission. The two processes can be simply related. The probability rate for the inverse process is the same, except w_{fi} is replaced by w_{if}, and the integral is replaced by $\langle i|e^{i\mathbf{k}\cdot\mathbf{r}}\mathbf{l}\cdot\Sigma\nabla_j|f\rangle$. If we interchange labels f and i integrate by parts, noting $\mathbf{l}\cdot\mathbf{k} = 0$ for a plane wave, we have

$$w_{if} = \frac{4\pi^2 e^2}{m^2 c} \frac{\mathcal{I}(\omega_{fi})}{\omega_{fi}^2} \left| \left\langle f \left| e^{-i\mathbf{k}\cdot\mathbf{r}} \mathbf{l} \cdot \sum \nabla_j \right| i \right\rangle^* \right|^2, \tag{10.16b}$$

which is the same as (10.16a). Thus we have

$$w_{fi} = w_{if}, \tag{10.17}$$

the "principle of detailed balance."

10.2 THE DIPOLE APPROXIMATION

The transition probabilities contain terms of the form

$$\int \phi_f^* e^{i\mathbf{k}\cdot\mathbf{r}} \mathbf{l} \cdot \nabla_j \phi_i \, d^3x. \tag{10.18}$$

We now wish to justify an expansion of the exponential

$$e^{i\mathbf{k}\cdot\mathbf{r}} = 1 + i\mathbf{k}\cdot\mathbf{r} + \tfrac{1}{2}(i\mathbf{k}\cdot\mathbf{r})^2 + \cdots$$

This is appropriate, since

$$\mathbf{k}\cdot\mathbf{r} \sim ka_0 \sim \frac{a_0 \Delta E}{\hbar c} \sim \frac{Z\alpha}{2} \ll 1,$$

at least for moderate Z. The lowest order of this approximation, in which $e^{i\mathbf{k}\cdot\mathbf{r}}$ is set equal to unity, gives rise to the *dipole approximation*. When the results of this approximation yield a zero result for certain transition rates, however, one needs to go to the higher terms in the expansion to derive the actual rates. These higher order terms give rise to *electric quadrupole*, *octupole*, and so on and *magnetic dipole*, *quadrupole*, and so on. Since the quantity $Z\alpha$ is also the order of magnitude estimate for v/c of the electrons in an atom [cf. Eq. (9.15b)], therefore, an equivalent condition for the applicability of the dipole approximation is

$$\frac{v}{c} \ll 1.$$

The expansion in $\mathbf{k}\cdot\mathbf{r}$ may be regarded as an expansion in v/c. Note that as higher order terms in v/c are retained, one must also add correction terms of these orders to the nonrelativistic form of the Schrodinger equation, Eq. (10.2). The reason that electric quadrupole and magnetic dipole radiation have roughly the same order of magnitude is that the magnetic force is already down by a factor v/c from the electric force.

By setting $e^{i\mathbf{k}\cdot\mathbf{r}} = 1$, the integral (10.18) becomes

$$\int \phi_f^* (\mathbf{l}\cdot\nabla_j)\phi_i \, d^3x = i\hbar^{-1}(\mathbf{l}\cdot\mathbf{p}_j)_{fi} \tag{10.19}$$

where $(\ )_{fi}$ denotes the matrix elements between states f and i. A useful alternative expression may be found by using the commutation relations

$$\mathbf{r}_j\mathbf{p}_j^2 - \mathbf{p}_j^2\mathbf{r}_j = 2i\hbar\mathbf{p}_j.$$

It follows that $\mathbf{r}_j$ commutes with the Hamiltonian

$$H^0 = \frac{1}{2m}\sum \mathbf{p}_j^2 + V(\mathbf{r}_1, \mathbf{r}_2, \ldots, \mathbf{r}_N) \tag{10.20}$$

in the following way:

$$\hbar^{-2}(\mathbf{r}_j H_0 - H_0 \mathbf{r}_j) = i\hbar^{-1}\mathbf{p}_j.$$

Using this to replace $i\hbar^{-1}\mathbf{p}_j$ in the matrix element yields

$$\begin{aligned} i\hbar^{-1}(\mathbf{l}\cdot\mathbf{p}_j)_{fi} &= m\hbar^{-2}\int \phi_f^* \mathbf{l}\cdot(\mathbf{r}_j H_0 - H_0\mathbf{r}_j)\phi_i\, d^3x \\ &= m\hbar^{-2}(E_i - E_f)\int \phi_f^* \mathbf{l}\cdot\mathbf{r}\phi_i\, d^3x, \end{aligned} \tag{10.21}$$

where we have used the fact that H_0 acting on its eigenfunctions yields the corresponding eigenvalues. Thus the transition rate is

$$w_{fi} = \frac{4\pi^2}{\hbar^2 c}|(\mathbf{l}\cdot\mathbf{d})_{fi}|^2 \mathcal{G}(\omega_{fi}), \tag{10.22}$$

where

$$\mathbf{d} \equiv e\sum_j \mathbf{r}_j \tag{10.23}$$

is the *electric dipole operator*.

Often we are only concerned with unpolarized radiation from atoms with random orientations. We then average the above formula over all angles, which gives

$$\langle|(\mathbf{l}\cdot\mathbf{d})_{fi}|^2\rangle = \frac{1}{3}|d_{fi}|^2,$$

since

$$\langle\cos^2\theta\rangle = \frac{1}{3}.$$

Here we interpret the quantity $|d_{fi}|^2$ to mean the combination

$$\mathbf{d}_{fi}^*\cdot\mathbf{d}_{fi} = |(d_x)_{fi}|^2 + |(d_y)_{fi}|^2 + |(d_z)_{fi}|^2. \tag{10.24}$$

Thus the average transition rate is

$$\langle w_{fi}\rangle = \frac{4\pi^2}{3c\hbar^2}|d_{fi}|^2 \mathcal{G}(\omega_{fi}). \tag{10.25}$$

10.3 EINSTEIN COEFFICIENTS AND OSCILLATOR STRENGTHS

We can relate this to our previous discussion in terms of the Einstein B coefficients (§1.6). Letting u and l refer to the upper and lower-states, respectively, we have

$$\langle w_{lu} \rangle = B_{lu} J_{\nu_{ul}}. \tag{10.26a}$$

Note that $J_{\nu_{ul}} = (4\pi)^{-1} \mathcal{J}(\nu_{ul})$, since the intensity considered here is undirectional. Also, we have the relation that $\mathcal{J}(\nu_{ul}) = 2\pi \mathcal{J}(\omega_{ul})$ so that

$$\langle w_{lu} \rangle = \frac{1}{2} B_{lu} \mathcal{J}(\omega_{ul}). \tag{10.26b}$$

Comparing this with the above expression gives

$$B_{lu} = \frac{8\pi^2 |d_{lu}|^2}{3c\hbar^2} = \frac{32\pi^4 |d_{lu}|^2}{3ch^2}. \tag{10.27}$$

From the Einstein relations (Eqs. 1.72) we have for nondegenerate levels

$$B_{lu} = B_{ul}$$

$$A_{ul} = \frac{4\omega_{fi}^3}{3c^3\hbar} |d_{ul}|^2 = \frac{64\pi^4 \nu_{ul}^3 |d_{ul}|^2}{3c^3 h}. \tag{10.28a}$$

If the levels are *degenerate*, the transition rate is found by averaging over the initial states and summing over the final states. Thus the Einstein A coefficient is given by

$$A_{ul} = \frac{64\pi^4 \nu_{ul}^3}{3hc^3} \frac{1}{g_u} \sum |d_{ul}|^2, \tag{10.28b}$$

where the sum is over all substates of the upper and lower levels. In this case the Einstein relations have their usual statistical weight factors.

It is convenient to define the *absorption oscillator strength* f_{lu} by the relationship

$$B_{lu} = \frac{4\pi^2 e^2}{h\nu_{ul} mc} f_{lu}, \tag{10.29a}$$

$$f_{lu} = \frac{2m}{3\hbar^2 g_l e^2} (E_u - E_l) \sum |d_{lu}|^2. \tag{10.29b}$$

The reason for naming it such is that the B coefficient associated with a classical oscillator can be defined in terms of the total energy extracted from a beam of radiation [cf. Eqs. (3.65), (1.66), and (1.74)]

$$\int_0^\infty \sigma(\nu)\,d\nu = \frac{\pi e^2}{mc} = B_{lu}^{\text{classical}} \frac{h\nu_{lu}}{4\pi}, \tag{10.30}$$

so that

$$B_{lu}^{\text{classical}} = \frac{4\pi^2 e^2}{h\nu_{lu} mc}. \tag{10.31}$$

The oscillator strength (or *f value*) is just that factor which corrects this classical result. One can in this way picture the quantum mechanical process as being due to a number (usually fractional) f_{lu} of equivalent classical electron oscillators of the same frequency ν. Normally f_{lu} is of order unity, so that it is a particularly useful quantity to characterize the strengths of transitions.

It is also convenient to define an *emission oscillator strength* by the formula

$$B_{ul} = \frac{4\pi^2 e^2}{h\nu_{lu} mc} f_{ul}. \tag{10.32}$$

Since $g_l B_{lu} = g_u B_{ul}$ and $\nu_{ul} = -\nu_{lu}$, we have the general relation

$$g_l f_{lu} = -g_u f_{ul}. \tag{10.33}$$

Thus emission oscillator strengths are *negative*. We may write the A coefficient in terms of the emission and absorption oscillator strengths:

$$g_u A_{ul} = -\frac{8\pi^2 e^2 \nu_{ul}^2}{mc^3} g_u f_{ul} = \frac{8\pi^2 e^2 \nu_{ul}^2}{mc^3} g_l f_{lu}. \tag{10.34}$$

One modification of the oscillator strength concept is necessary when the upper state happens to lie in a continuum. In this case it is meaningless to talk about the probability of a transition to a single state, but rather we need to define the *probability per unit energy (or frequency) range*. With this in mind we define the derivatives of f such that $(df/d\epsilon)d\epsilon$ is the strength for a transition from state i to a set of continuum states in an energy range $d\epsilon$. The frequency of the emitted photon is given by $h\nu = \epsilon + \chi$ where χ is the ionization potential from the state i. This is illustrated in Fig. 10.1.

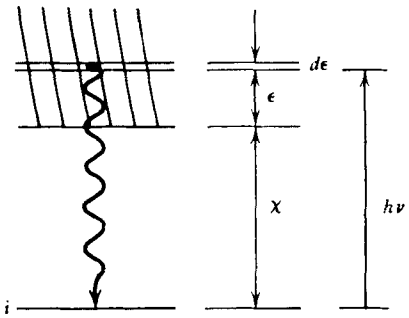

Figure 10.1 Transition between level i and the continuum (shaded). Here χ is the ionization potential.

The *continuum oscillator strength* f_c is the total oscillator strength to all continuum states:

$$f_c = \int_0^\infty \frac{df}{d\epsilon}\, d\epsilon = \int_{\nu_0}^\infty \frac{df}{d\nu}\, d\nu \tag{10.35}$$

where $h\nu_0 = \chi$.

The oscillator strengths must be found by direct calculation or by experiment. The theoretical determination of f values (or A values) is difficult, but with the advent of large computers, much can now be done to obtain accurate, reliable results. The basic difficulty is that most approximate wave functions for complex atoms, such as Hartree–Fock, tend to be most accurate at small radii where the associated contribution to the total energy is most important. However, the transition probabilities depend more critically on the wave functions at large radii. We can see this simply by noting that the energies depend on averages of *inverse distances*,

$$\int \psi^* r^{-1} \psi\, d^3\mathbf{r},$$

while the dipole operator depends on averages of *distance*,

$$\int \psi^* r \psi\, d^3\mathbf{r}.$$

For this reason one needs better wave functions than those ordinarily available.

There are a number of general result relating oscillator strengths, known as *sum rules*. They are of great value in determining approximate values or

bounds for f values that cannot easily be measured or calculated, and also in obtaining absolute f values from relative f values. The simplest and most general sum rule is the *Thomas–Reiche–Kuhn sum rule*:

$$\sum_{n'} f_{nn'} = N, \tag{10.36}$$

where N is the total number of electrons in the atom, and the summation is over all states of the atom. For each initial state this rule gives a relation involving transitions to all other states. Equation (10.36) follows from the expressions for f_{if} Eqs. (10.23) and (10.29b), and the easily proved identity

$$\frac{2m}{3\hbar^2} \sum_{k} (E_k - E_s)|\mathbf{r}_{sk}|^2 = 1.$$

In many cases, such as when there is a closed shell and a smaller number q of electrons outside the closed shells that are involved in a more limited set of transitions, we also have

$$\sum_{n'} f_{nn'} = q, \tag{10.37}$$

where the sum is now only over those states which involve transitions of these outer electrons.

The sum can be split into two sums, depending on whether n' is a state above or below n:

$$\sum_{\substack{n' \\ E_{n'} > E_n}} f_{nn'} + \sum_{\substack{n' \\ E_{n'} < E_n}} f_{nn'} = q. \tag{10.38}$$

The first sum gives the contribution due to absorption from the state n, and the second sum gives the contribution due to emission from state n to all lower states. Since in the second sum these emission oscillator strengths are negative, we have

$$\sum_{\substack{n' \\ E_{n'} > E_n}} f_{nn'} \geqslant q, \tag{10.39}$$

the equality holding only for the ground state or for an excited state that cannot radiate by a dipole transition (metastable state).

Other types of sum rules also exist under more restrictive assumptions about the nature of the atomic states (e.g., single configuration, L-S coupling, j-j coupling, single electron).

10.4 SELECTION RULES

In general, there will always be some probability for radiative transition between two states, but in some cases this probability can be exceedingly small. This occurs when the states involved fall approximately into a classification scheme (like L-S coupling) for which the transition probability would be strictly zero if that scheme held rigorously. For example, a transition probability may be strictly zero in the dipole approximation but nonzero for higher order multipole radiation or two-photon emission.

The precise statements of when a transition probability vanishes under some specified set of assumptions are called *selection rules*. We are primarily concerned with dipole selection rules, so that the crucial question involves when the dipole matrix element $\mathbf{d}_{fi}$ vanishes. The most general result is *Laporte's rule*: *there are no transitions between states of the same parity*. This is easily proved by recalling the definition

$$\mathbf{d}_{fi} \equiv e \int \phi_f^* \sum_j \mathbf{r}_j \phi_i \, d^3x.$$

If we reflect all coordinates we note $\Sigma \mathbf{r}_j \rightarrow -\Sigma \mathbf{r}_j$ while $\phi_f^* \phi_i$ is unchanged if f and i have the same parity. Thus the integral is equal to its negative, and vanishes.

For states with a specific configuration assignment the parity is $(-1)^{\Sigma l_i}$ where the l_i are the angular momentum quantum numbers of the individual orbitals. Thus we deduce that the configuration must change by at least one orbital, from Laporte's rule. There are no dipole transitions between states of the same configuration.

A sharpened selection rule applies to the transitions between configurations: The configuration must change by precisely one orbital. This is proved by noting that a given configuration may be expressed as a superposition of determinental wave functions, which in turn are superpositions of products of one-particle orbitals. The dipole operator is a sum of the $\mathbf{r}_j$ over all electrons, so that ultimately one can write the matrix element $\mathbf{d}_{fi}$ as a sum of matrix elements of a single $\mathbf{r}_j$ between product wave functions corresponding to the two configurations:

$$\int u_a^* u_b^* \cdots u_k^*(\mathbf{r}_j) u_{a'} u_{b'} \cdots u_{k'} \, d^3x.$$

The particular one-particle wave functions having the coordinates $\mathbf{r}_j$ will integrate out to some result (in general nonzero), but all the other integrals will be simply the orthonormality integrals of the functions u; therefore, in order not to give a zero result, all the corresponding functions must be the same, except for the one involving $\mathbf{r}_j$. The only way to ensure that all the

terms in the grand summation will not vanish is to make all orbitals the same except for one. This selection rule is known as the *one-electron jump rule*. It can be violated by states that are superpositions of several configurations (configuration interaction), but it will be obeyed for L-S coupling, which assumes no such configuration interaction.

As indicated above, under the assumption of configuration assignments we may evaluate the dipole matrix element by evaluating a simplified matrix element that connects states of the jumping electron orbitals only. Recall these orbitals have a very simple representation (Eq. 9.9) times a spin function. Since **r** and **s** commute, we see that the spin cannot change, so that $m_s = m_{s'}$; thus we may deal with the space parts alone. The dipole matrix element between two such orbitals will involve the integral

$$\int r R_{nl} R_{n'l'} dr,$$

which is called the *radial integral*. It will also involve an integral over spherical harmonics. An examination of this latter integral, using the fact that the dipole operator is a vector, leads to the selection rules (see Problem 10.6)

$$\Delta l = \pm 1, \tag{10.40a}$$

$$\Delta m = 0, \pm 1. \tag{10.40b}$$

In a multielectron atom these rules apply to the jumping electron. These rules completely determine the spectra of one-electron atoms, such as HI and HeII, and also the alkali metals.

There are also selection rules for many electron atoms that involve the total quantities L, S, and J. One general result (which applies even to higher multipole radiation) is that the transition $J=0$ to $J=0$ is *forbidden*, because the photon carries off one unit of angular momentum. In L-S coupling we find that we must have

$$\Delta S = 0 \tag{10.41a}$$

$$\Delta L = 0, \pm 1, \tag{10.41b}$$

$$\Delta J = 0, \pm 1. \qquad (\text{except } J=0 \text{ to } J=0) \tag{10.41c}$$

The rule $\Delta S = 0$ follows from the fact that the dipole operator does not involve spin. We note that $\Delta L = 0$ is allowed here but that $\Delta l = 0$ is not. This is because there is no direct relation of L to the parity; for example, for two equivalent p electrons we have the state ^3P which has odd L but even parity, and ^1S which has even L and even parity.

For higher multipole radiation the selection rules for J remain unchanged ($\Delta J = 0, \pm 1$, except $J=0$ to $J=0$), but the parity rule becomes: for magnetic dipole and electric quadrupole radiation, parity is unchanged.

For magnetic dipole transitions *the configuration does not change*. This allows for many of the forbidden lines in the ground configurations of C, N, O, for example, and for the important 21-cm lines.

10.5 TRANSITION RATES

One case in which a fairly complete discussion of transition rates can be given purely theoretically is the pure Coulomb case of hydrogen (and for other hydrogen-like ions, such as HeII and LiIII). The frequency of a photon absorbed or emitted in a transition between two discrete levels with principal quantum numbers n' and n' is given by

$$h\nu = Ry(n^{-2} - n'^{-2}), \tag{10.42a}$$

where

$$Ry \equiv \frac{e^2}{2a_0} = 13.6 \text{ eV}. \tag{10.42b}$$

When the upper level is in the continuum, so that there is a free electron with energy $\epsilon = \frac{1}{2}mv^2$, we have

$$h\nu = Ry/n^2 + \epsilon. \tag{10.43}$$

To liberate a free electron one needs a photon of at least the *threshold energy*, $h\nu_n = \chi_n$ = ionization potential from the initial state n.

Bound-bound Transitions for Hydrogen

To calculate the dipole oscillator strength we must evaluate the dipole operator matrix element. This will involve integrals over the radial wave functions $R_{nl}(r)$ of the form

$$\int R_{nl} R_{n'(l-1)} r\, dr. \tag{10.44}$$

By the selection rule (10.40a) we know that $\Delta l = 1$. Since these radial functions are analytically known [Laguerre polynomials; see Eq. (9.15a)], the integrals of Eq. (10.44) can be performed, but are complicated (Gordon, 1929.) When the integral is performed, it can then be summed over all l appropriate to a given n and n'. The Lyman-α transition ($n = 1$ $n' = 2$) in hydrogen is treated explicitly in Problem 10.3 and yields the f value

$$gf = \frac{2^{14}}{3^9} = 0.8324. \tag{10.45}$$

For other members of the Lyman series ($n'=1$), the result is (Menzel and Pekeris, 1935)

$$g_1 f_{1n} = \frac{2^9 n^5 (n-1)^{2n-4}}{3(n+1)^{2n+4}}. \tag{10.46}$$

In general, the expression for f can be reduced to a closed form. Note that for high values of n the oscillator strengths decrease rapidly

$$g_1 f_{1n} = \frac{2^9}{3n^3} \frac{\left(1-\frac{1}{n}\right)^{2n-4}}{\left(1+\frac{1}{n}\right)^{2n-4}}$$

$$\sim \frac{2^9}{3n^3} \frac{e^{-2}}{e^2} \sim 3.1 \frac{1}{n^3}. \tag{10.47}$$

Further values of oscillator strengths for the bound-bound transitions can be obtained from Table 10.1.

Table 10.1

n / n'	1	2	3	n / n'	1	2	3
2	4.162×10^{-1}			19	2.295×10^{-4}	5.167×10^{-4}	8.364×10^{-4}
3	7.910×10^{-2}	6.408×10^{-1}		20	1.966×10^{-4}	4.418×10^{-4}	7.117×10^{-4}
4	2.899×10^{-2}	1.193×10^{-1}	8.420×10^{-1}	21	1.698×10^{-4}	3.803×10^{-4}	6.111×10^{-4}
5	1.394×10^{-2}	4.467×10^{-2}	1.506×10^{-1}	22	1.476×10^{-4}	3.302×10^{-4}	5.286×10^{-4}
6	7.800×10^{-3}	2.209×10^{-2}	5.585×10^{-2}	23	1.276×10^{-4}	2.885×10^{-4}	4.608×10^{-4}
7	4.814×10^{-3}	1.271×10^{-2}	2.768×10^{-2}	24	1.137×10^{-4}	2.534×10^{-4}	4.040×10^{-4}
8	3.184×10^{-3}	8.037×10^{-3}	1.604×10^{-2}	25	1.005×10^{-4}	2.240×10^{-4}	3.558×10^{-4}
9	2.216×10^{-3}	5.429×10^{-3}	1.023×10^{-2}	26	8.931×10^{-5}	1.987×10^{-4}	3.155×10^{-4}
10	1.605×10^{-3}	3.851×10^{-3}	6.981×10^{-3}	27	7.963×10^{-5}	1.772×10^{-4}	2.809×10^{-4}
11	1.201×10^{-3}	2.836×10^{-3}	4.996×10^{-3}	28	7.138×10^{-5}	1.587×10^{-4}	2.513×10^{-4}
12	9.215×10^{-4}	2.150×10^{-3}	3.711×10^{-3}	29	6.431×10^{-5}	1.427×10^{-4}	2.243×10^{-4}
13	7.226×10^{-4}	1.672×10^{-3}	2.839×10^{-3}	30	5.809×10^{-5}	1.288×10^{-4}	2.034×10^{-4}
14	5.774×10^{-4}	1.326×10^{-3}	2.223×10^{-3}	31	5.260×10^{-5}	1.167×10^{-4}	1.840×10^{-4}
15	4.687×10^{-4}	1.070×10^{-3}	1.776×10^{-3}	32	4.784×10^{-5}	1.060×10^{-4}	1.670×10^{-4}
16	3.855×10^{-4}	8.770×10^{-4}	1.443×10^{-3}	33	4.359×10^{-5}	9.654×10^{-5}	1.521×10^{-4}
17	3.211×10^{-4}	7.273×10^{-4}	1.189×10^{-3}	34	3.982×10^{-5}	8.829×10^{-5}	1.389×10^{-4}
18	2.703×10^{-4}	6.098×10^{-4}	9.914×10^{-4}	35	3.656×10^{-5}	8.084×10^{-5}	1.272×10^{-4}

Bound-free Transitions (Continuous Absorption) for Hydrogen

When the upper state lies in the continuum, there can be absorption in a continuous range of frequencies. Since the absorption results in an electron being liberated from the atom, this process is also called *photoionization*. We express our results in terms of the cross section for the transition. The differential transition rate, dw, for a transition from bound state i to a continuum state f, with electron in momentum range dp and solid angle range $d\Omega$, is

$$dw = \frac{4\pi^2 e^2}{m^2 c} \frac{\mathcal{J}(\omega)}{\omega^2} |\langle f | e^{i\mathbf{k}\cdot\boldsymbol{\eta}} \cdot \nabla | i \rangle|^2 \left[\frac{dn}{dp\, d\Omega} dp\, d\Omega \right]. \tag{10.48}$$

Here the term in brackets is the number of free electron states available, that is, the "density of states" $dn/dp\,d\Omega$ multiplied by the differential range $dp\,d\Omega$, and the remaining factor is identical to our expression for the transition rate for bound-bound transitions, Eq. (10.16). By energy conservation, we have that the frequency interval $d\omega$ of incident photons is related to the momentum interval dp of nonrelativistic electrons by

$$\hbar\, d\omega = \frac{p\, dp}{m}. \tag{10.49}$$

We also have, by definition, that the number of photons per unit area per unit time per unit frequency in the incident beam satisfies

$$\frac{dN}{dA\, dt\, d\omega} = \frac{\mathcal{J}(\omega)}{\hbar\omega}. \tag{10.50}$$

If the final electron is localized to a volume V, then the density of states for a given final spin state is [cf. Eq. (9.43)]

$$\frac{dn}{dp\, d\Omega} = \frac{p^2 V}{h^3}. \tag{10.51}$$

Combining Eqs. (10.48) to (10.51), we obtain for the differential bound-free cross section,

$$\frac{d\sigma_{bf}}{d\Omega} = \frac{\alpha v V}{2\pi\omega} |\langle f | e^{i\mathbf{k}\cdot\boldsymbol{\eta}} \cdot \nabla | i \rangle|^2, \tag{10.52}$$

where $v = p/m$ is the final electron velocity.

For the simple case of a bound-free transition from the ground state of hydrogen, ionized by a photon of frequency ω, this differential cross

section is evaluated explicitly for $\hbar\omega \gg Ry$ in Problem 10.4. The total cross section, $\sigma_{bf} = \int (d\sigma / d\Omega) d\Omega$, is

$$\sigma_{bf}(\hbar\omega \gg Ry) \approx \frac{(2\alpha)^{9/2} \pi Z^5 c^{7/2}}{3 a_0^{3/2} \omega^{7/2}}. \tag{10.53}$$

For the more general case of a bound-free transition from state n and l, a detailed calculation (Karzas and Latter, 1961) gives

$$\sigma_{bf} = \frac{512\pi^7 m e^{10} Z^4}{3\sqrt{3}\, ch^6 n^5} \frac{g(\omega, n, l, Z)}{\omega^3}, \tag{10.54}$$

where g is the bound-free Gaunt factor. If χ_n is the ionization potential for the initial level, σ_{bf} is zero for $\omega < \omega_n$ where

$$\omega_n \equiv \frac{\chi_n}{\hbar} = \frac{\alpha^2 mc^2 Z^2}{2\hbar n^2}, \tag{10.55}$$

rises abruptly to Eq. (10.54) at threshold $\omega = \omega_n$ and then decreases roughly as ω^{-3}. Near threshold, the Gaunt factor g is unity, to within 20%.

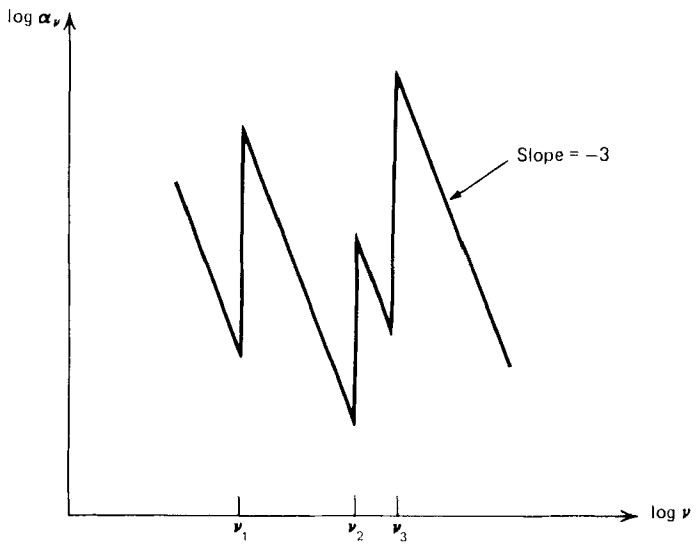

***Figure 10.2** Schematic illustration of the frequency dependence of the absorption coefficient. The sharp rises, absorption edges, occur at the frequency of ionization of a particular level.*

For convenience, Eq. (10.54) can also be written in the form

$$\sigma_{bf} = \left(\frac{64\pi ng}{3\sqrt{3}\, Z^2} \right) \alpha a_0^2 \left(\frac{\omega_n}{\omega} \right)^3. \tag{10.56}$$

We can also write our results in terms of the absorption coefficient, $\alpha_\nu = N_n \sigma$, where N_n is the atomic density at the absorbing level. The total absorption coefficient equals the sum of terms of this form and is illustrated schematically in Fig. 10.2. The *absorption edges* correspond to the onset of absorption from different levels. The relative strength of these edges depends on the number of atoms in each level. For example, if the material is in thermodynamic equilibrium, these numbers are given by the Boltzmann law.

Radiative Recombination; Milne Relations

The process inverse to photoionization is *radiative recombination*, in which an electron is captured by an ion into a bound state n with emission of a photon. There are connections between rates for photoionization and recombination, analogous to the Einstein relations. These are called the *Milne relations* and are examples of general *detailed balancing* relations. If we want to apply these directly to a single capture event we first have to consider the distribution function for the electrons, that is, how many electrons are moving in each speed range. However, it is also quite useful, and usually sufficient, to deal with a *thermal distribution* of electrons. The detailed balance relations can then be obtained by the simple requirement that the radiation field in equilibrium is the Planck function $B_\nu(T)$. Since the coefficients refer to atomic properties, they then can be used for any distributions of electrons and radiation.

Let $\sigma_{fb}(v)$ be the cross section for recombination for electrons of velocity v. Then the number of recombinations per unit time per unit volume due to thermal electrons in speed range dv is

$$N_+ N_e \sigma_{fb} f(v) v \, dv, \tag{10.57}$$

where N_e is the electron density, N_+ is the ion density, and $f(v)$ is the Maxwellian velocity distribution. The number of photoionizations per time per volume for a blackbody radiation field ($I_\nu = B_\nu$) in frequency range $d\nu$ is, (cf. Problem 1.2), with N_n the neutral atom density,

$$\frac{4\pi}{h\nu} N_n \sigma_{bf} (1 - e^{-h\nu/kT}) B_\nu \, d\nu, \tag{10.58}$$

where the factor $(1-e^{-h\nu/kT})$ now gives the net photoionization rate when "stimulated recombinations" are subtracted out. Then equating (10.57) and (10.58) and using the Planck function and Eq. (10.49), we obtain

$$\frac{\sigma_{bf}}{\sigma_{fb}} = \frac{N_+ N_e}{N_n} e^{h\nu/kT} \frac{f(v)c^2 h}{8\pi m \nu^2}. \tag{10.59}$$

But, we also know

$$f(v) = 4\pi \left(\frac{m}{2\pi kT}\right)^{3/2} v^2 \exp\left(\frac{-mv^2}{2kT}\right), \tag{10.60}$$

and from Saha's equation [cf. Eq. (9.47)]

$$\frac{N_+ N_e}{N_n} = \left(\frac{2\pi mkT}{h^2}\right)^{3/2} \frac{g_e g_+}{g_n} e^{-\chi/kT}.$$

Using the result

$$h\nu = \tfrac{1}{2} mv^2 + \chi, \tag{10.61}$$

we obtain the Milne relation:

$$\frac{\sigma_{bf}}{\sigma_{fb}} = \frac{m^2 c^2 v^2}{\nu^2 h^2} \frac{g_e g_+}{2g_n}. \tag{10.62}$$

Since we have already found σ_{bf}, we can compute σ_{fb}.

In this way recombination coefficients can be computed for given velocity distribution, say Maxwellian. We have the following results for the thermal recombination coefficient onto the nth level of hydrogen: (Gaunt factor = 1)

$$\langle v\sigma_{fb} \rangle = \int v f(v) \sigma_{fb} \, dv \tag{10.63}$$

where $f(v)$ is the speed distribution of the thermal electrons, Eq. (10.60). Substitution of Eqs. (10.56), (10.61), and (10.62) into (10.63) then yields (Cillié 1932)

$$\langle v\sigma_{fb} \rangle = 3.262 \times 10^{-6} M(n, T), \tag{10.64a}$$

where

$$M(n,T)=\frac{e^{\chi_n/kT}}{n^3T^{3/2}}E_1\left(\frac{\chi_n}{kT}\right), \tag{10.64b}$$

and where

$$E_1(x)\equiv\int_x^\infty \frac{e^{-t}}{t}\,dt. \tag{10.64c}$$

In evaluating Eqs. (10.64) we have used $g_e=2$, $g_+=1$, $g_n=2n^2$ as the values for the statistical weight factors.

Also of interest is the recombination coefficient summed over all bound states n. A convenient approximation is (Seaton, 1959)

$$\sum_n \langle v\sigma_{fb}\rangle = 5.197\times10^{-14}\lambda^{1/2}\left(0.4288+\tfrac{1}{2}\ln\lambda+0.469\lambda^{-1/3}\right) \tag{10.65a}$$

where

$$\lambda\equiv 1.579\times10^5/T. \tag{10.65b}$$

Recombination can proceed in other ways besides radiative recombination. *Three-body recombination* is usually quite slow at astrophysical densities, since it requires a close encounter of three bodies simultaneously. However, *dielectronic recombination* (see, e.g., Massey and Gilbody 1974) can be very important for some ions.

The Role of Coupling Schemes in the Determination of f Values

When particular coupling schemes are appropriate, it is possible to relate the f values for different transitions by means of formulas (or tables). For L-S coupling (Russell–Saunders coupling) we can interrelate the f values of all lines between two given terms; this set of lines is called a *multiplet*. The relative strengths of the lines within a multiplet depend only on the term types of the two terms involved. For example, if we have an upper ^2P term and a lower ^2S term, the transition $^2S_{1/2}-{}^2P_{3/2}$ is twice as strong as the transition $^2S_{1/2}-{}^2P_{1/2}$. The factor of 2 is due to there being two times the number of states in $J=3/2$ as in $J=1/2$. This is the situation with the Lyman $-\alpha$ ($Ly\alpha$) transition in HI. If we know the *total* strength of the multiplet, we can then find the strengths of the individual line components.

Thus since the total gf is 0.8324 [cf (10.45)], we have $(gf)\ 1/2-3/2=0.5549$, $(gf)\ 1/2-1/2=0.2775$. Tables to deduce the relative strength of lines within a multiplet can be found in Allen (1974) and Aller (1963).

Another use of the L-S coupling scheme is to deduce the relative strengths of *multiplets* between two *configurations*. This kind of calculation is affected more by deviations from L-S coupling than the preceding, so that it is not as reliable. The set of multiplets arising out of transitions between two configurations is called a *transition array*, and the relative strengths of multiplets within a transition array is discussed in the above references.

Other coupling schemes give their own rules for relating f values, but we do not discuss these here. In cases where a particular coupling scheme is not applicable, or its applicability is dubious, we must obtain f values for the desired transitions either directly by experiment or by a more sophisticated theoretical calculation.

10.6 LINE BROADENING MECHANISMS

Atomic levels are not infinitely sharp, nor are the lines connecting them. This was already recognized in our discussion of the Einstein coefficients, where we introduced the line profile function $\phi(\nu)$ to account for the nonzero width of the line. Many physical effects determine the line shape, and we can only deal with a few here (see, e.g., Griem 1974; Mihalas 1978).

Doppler Broadening

Perhaps the simplest mechanism for line broadening is the Doppler effect. An atom is in thermal motion, so that the frequency of emission or absorption in its own frame corresponds to a different frequency for an observer. Each atom has its own Doppler shift, so that the net effect is to spread the line out, but not to change its total strength.

The change in frequency associated with an atom with velocity component v_z along the line of sight (say, z axis) is, to lowest order in v/c, given by Eq. (4.12)

$$\nu-\nu_0=\frac{\nu_0 v_z}{c}. \tag{10.66}$$

Here ν_0 is the rest-frame frequency. The number of atoms having velocities

in the range v_z to $v_z + dv_z$ is proportional to the Maxwellian distribution

$$\exp\left(-\frac{m_a v_z^2}{2kT}\right) dv_z$$

where m_a is the mass of an atom. From the above we have the relations

$$v_z = \frac{c(\nu - \nu_0)}{\nu_0}, \tag{10.67a}$$

$$dv_z = \frac{c\, d\nu}{\nu_0}. \tag{10.67b}$$

Therefore, the strength of the emission in the frequency range ν to $\nu + d\nu$ is proportional to

$$\exp\left[-\frac{m_a c^2(\nu - \nu_0)^2}{2\nu_0^2 kT}\right] d\nu,$$

and the profile function is

$$\phi(\nu) = \frac{1}{\Delta\nu_D \sqrt{\pi}}\, e^{-(\nu-\nu_0)^2/(\Delta\nu_D)^2}. \tag{10.68}$$

Here the *Doppler width* $\Delta\nu_D$ is defined by

$$\Delta\nu_D = \frac{\nu_0}{c}\sqrt{\frac{2kT}{m_a}}. \tag{10.69}$$

The constant $(\Delta\nu_D\sqrt{\pi})^{-1}$ in the formula for $\phi(\nu)$ is determined by the normalization condition $\int\phi(\nu)\,d\nu = 1$ under the (reasonable) assumption that $\Delta\nu_D \ll \nu_0$. The *line-center* cross section for each atom, neglecting stimulated emission, is therefore

$$\sigma_{\nu_0} = B_{12}\frac{h\nu_0}{4\pi}\phi(\nu_0) = \frac{1}{\Delta\nu_D\sqrt{\pi}}\frac{h\nu_0}{4\pi}B_{12}$$

$$= \frac{\pi e^2}{mc} f_{12}\frac{1}{\Delta\nu_D\sqrt{\pi}} \tag{10.70}$$

for the case of Doppler broadening. Numerically this is

$$\sigma_{\nu_0} = 1.16 \times 10^{-14} \lambda_0 \sqrt{A/T}\, f_{12} \text{ cm}^2, \tag{10.71}$$

where λ_0 is in $\mathring{A}$, T in K, and A is the atomic weight for the atom.

In addition to thermal motions there can also be turbulent velocities associated with macroscopic velocity fields. When the scale of the turbulence is small in comparison with a mean free path (called *microturbulence*) these motions are often accounted for by an effective Doppler width

$$\Delta\nu_D = \frac{\nu_0}{c}\left(\frac{2kT}{m_a} + \xi^2\right)^{1/2}, \tag{10.72}$$

where ξ is a root mean-square measure of the turbulent velocities. This assumes that the turbulent velocities also have a Gaussian distribution.

Natural Broadening

A certain width to the atomic level is implied by the uncertainty principle, namely, that the spread in energy ΔE and the duration Δt in the state must satisfy $\Delta E\, \Delta t \sim \hbar$. We note that the spontaneous decay of an atomic state n proceeds at a rate

$$\gamma = \sum_{n'} A_{nn'},$$

where the sum is over all states n' of lower energy. If radiation is present, we should add the induced rates to this. The coefficient of the wave function of state n, therefore, is of the form $e^{-\gamma t/2}$ and leads to a decay of the electric field by the same factor. (The energy then decays proportional to $e^{-\gamma t}$.) Therefore, we have an emitted spectrum determined by the decaying sinusoid type of electric field, as given in §2.3 and Fig. 2.3. Thus the profile is of the form

$$\phi(\nu) = \frac{\gamma/4\pi^2}{(\nu - \nu_0)^2 + (\gamma/4\pi)^2}. \tag{10.73}$$

This is called a *Lorentz* (or *natural*) *profile*.

Actually, the above result applies to cases in which only the upper state is broadened (e.g., transitions to the ground state). If both the upper and

lower state are broadened, then the appropriate definition for γ is

$$\gamma = \gamma_u + \gamma_l, \tag{10.74}$$

where γ_u and γ_l are the widths of the upper and lower states involved in the transition. Thus, for example, we can have a weak but broad line if the lower state is broadened substantially.

Collisional Broadening

The Lorentz profile applies even more generally to certain types of collisional broadening mechanisms. For example, if the atom suffers collisions with other particles while it is emitting, the phase of the emitted radiation can be altered suddenly (see Fig. 10.3). If the phase changes completely randomly at the collision times, then information about the emitting frequencies is lost. If the collisions occur with frequency ν_{col}, that is, each atom experiences ν_{col} collisions per unit time on the average, then the profile is (see Problem 10.7).

$$\phi(\nu) = \frac{\Gamma/4\pi^2}{(\nu - \nu_0)^2 + (\Gamma/4\pi)^2}, \tag{10.75a}$$

where

$$\Gamma = \gamma + 2\nu_{\text{col}}. \tag{10.75b}$$

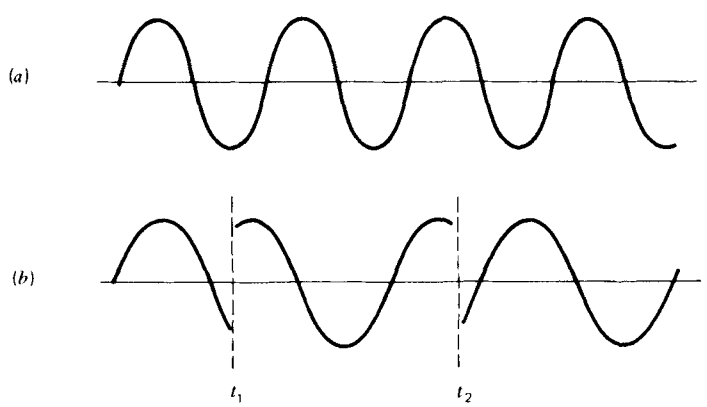

***Figure 10.3** Time-dependence of the electric field of emitted radiation which is (a) purely sinusoidal and (b) subject to random phase interruptions by atomic collisions.*

Combined Doppler and Lorentz Profiles

Quite often an atom shows both a Lorentz profile plus the Doppler effect. In these cases we can write the profile as an average of the Lorentz profile over the various velocity states of the atom:

$$\phi(\nu)=\frac{\Gamma}{4\pi^2}\int_{-\infty}^{\infty}\frac{(m/2\pi kT)^{1/2}\exp(-mv_z^2/2kT)}{(\nu-\nu_0-\nu_0 v_z/c)^2+(\Gamma/4\pi)^2}\,dv_z. \tag{10.76}$$

We can write this more compactly using the definition of the *Voigt function*

$$H(a,u)\equiv\frac{a}{\pi}\int_{-\infty}^{\infty}\frac{e^{-y^2}dy}{a^2+(u-y)^2}. \tag{10.77}$$

Then Eq. (10.76) can be written as

$$\phi(\nu)=(\Delta\nu_D)^{-1}\pi^{-1/2}H(a,u), \tag{10.78}$$

where

$$a\equiv\frac{\Gamma}{4\pi\Delta\nu_D}, \tag{10.79a}$$

$$u\equiv\frac{\nu-\nu_0}{\Delta\nu_D}. \tag{10.79b}$$

For small values of a, the center of the line is dominated by the Doppler profile, whereas the "wings" are dominated by the Lorentz profile. (See problem 10.5).

PROBLEMS

10.1—What radiative transitions are allowed between the fine structure levels of a ^3P term and those of a ^3S term? Draw a diagram showing the levels with spacings determined by the Lande interval rule. How many spectral lines will be produced, and how will they be spaced relative to one another? Consider the different possibilities of ^3P being normal or inverted and being the upper or lower term.

10.2—Which of the following transitions are allowed under L-S coupling selection rules for electric dipole radiation and which are not? Explain which rules, if any, are violated.

a. $3s\ ^2S_{1/2} \leftrightarrow 4s\ ^2S_{1/2}$

b. $2p\ ^2P_{1/2} \leftrightarrow 3d\ ^2D_{5/2}$

c. $3s3p\ ^3P_1 \leftrightarrow 3p^2\ ^1D_2$

d. $2p3p\ ^3D_1 \leftrightarrow 3p4d\ ^3F_2$

e. $2p^2\ ^3P_0 \leftrightarrow 2p3s\ ^3P_0$

f. $3s2p\ ^1P_1 \leftrightarrow 2p3p\ ^1P_1$

g. $2s3p\ ^3P_0 \leftrightarrow 3p4d\ ^3P_1$

h. $1s^2\ ^1S_0 \leftrightarrow 2s2p\ ^1P_1$

i. $2p3p\ ^3S_1 \leftrightarrow 2p4d\ ^3D_2$

j. $2p^3\ ^2D_{3/2} \leftrightarrow 2p^3\ ^2D_{1/2}$

10.3—Derive Eq. (10.45) for the Lyman-α oscillator strength.

10.4—Derive Eq. (10.53) for the bound-free cross section, using the nonrelativistic Born approximation.

10.5—Line radiation is emitted from an optically thin, thermal source. Assuming that the only broadening mechanisms are Doppler and natural broadening, show that the observed half-width of the line is independent of the temperature T for $T \ll T_c$ and increases as the square root of T for $T \gg T_c$, where T_c is some critical temperature. For the Lyman-α line of hydrogen estimate T_c in terms of fundamental constants, and give its numerical value.

10.6—Derive the simple dipole selection rule, Eq. (10.40).

10.7—Derive the profile function, Eq. (10.75), when phase-destroying collisions occur with frequency ν_{col}.

REFERENCES

Allen, C. W., 1974, *Astrophysical Quantities*, (Althone Press, London).
Aller, L. H., 1963, *The Atmospheres of the Sun and Stars*, (Ronald, New York).

Bethe, H. A., and Jackiw, R., op. cit.
Bethe, H. A., and Salpeter, E. E., 1957, *Quantum Mechanics of One- And Two-Electron Atoms*, (Springer-Verlag, Berlin).
Cillié, G., 1932, *Mon. Not. Roy. Astr. Soc.* **92**, 820.
Gordon, W., 1929, *Ann. Phys.*, **2**, 1031.
Griem, H. R., 1974, *Spectral Line Broadening by Plasmas*, (Academic, New York).
Karzas, W. J., and Latter, R., 1961, *Astrophys. J. Suppl.*, **6**, 167.
Massey, H. S. W., and Gilbody, H. B., 1974, *Electronic and Ionic Impact Phenomena, vol. IV*, (Clarendon, Oxford).
Menzel, D. H., and Pekeris, C. L., 1935, *Mon. Not. Roy. Astr. Soc.*, **96**, 77.
Merzbacher, E., 1961, *Quantum Mechanics*, (Wiley, New York).
Mihalas, D., 1978, *Stellar Atmospheres*, (Freeman, San Francisco).
Seaton, M., 1959, *Mon. Not. Roy. Astr. Soc.*, **119**, 81.

11

MOLECULAR STRUCTURE

When two or more atoms join together into a molecule there is considerable complexity, as compared to a single atom. Many of the simple symmetries of the atom, such as complete rotational symmetry about the nucleus, are lost, and this means fewer quantum numbers are available to help sort out the molecular states. On the other hand, there are a few consolations:

1. For *diatomic* molecules (to which we restrict ourselves exclusively) there is still rotational symmetry about a line.
2. Some of the most important transitions in molecules involve *rotation* and/or *vibration* of the nuclei with respect to each other; these transitions do not occur in atoms and are actually quite a bit simpler than any atomic transitions. The primary difficulties in understanding molecules are *electronic* states.

11.1 THE BORN–OPPENHEIMER APPROXIMATION: AN ORDER OF MAGNITUDE ESTIMATE OF ENERGY LEVELS

A great simplification in the understanding of molecules was made when it was realized that the motions of the electrons and nuclei could be treated

separately. This comes about because of the great disparity between the masses of the electron and a typical nucleus, which have ratios m/M in the range $\sim 10^{-4} - 10^{-5}$. From the uncertainty relations we see that this implies that the electrons are much faster than the nuclei and characteristically have much higher energies. Let a be a typical molecular size. Then the momentum of an electron is of order $\hbar/a$ and will have energy states with typical spacings

$$E_{\text{elect}} \sim \frac{\hbar^2}{ma^2}. \tag{11.1}$$

For typical molecular sizes ($\sim 10^{-8}$ cm) this amounts to about a few eV.

The slowly moving nuclei only sense the electrons as a kind of smoothed-out cloud. Therefore, as the nuclei move the electrons have sufficient time to adjust adiabatically to the new nuclear positions. The nuclei then feel only an *equivalent potential* that depends on the internuclear distance and on the particular electronic state. This separation of nuclear and electronic motions is called the *Born–Oppenheimer approximation.*

For stable molecules the internuclear potential has a minimum at some point (see Fig. 11.1). Vibrations about the minimum can occur and can be estimated roughly by comparing to a harmonic oscillator. We can approximate the potential as $\frac{1}{2}M\omega^2\xi^2$, where ξ is the displacement of the

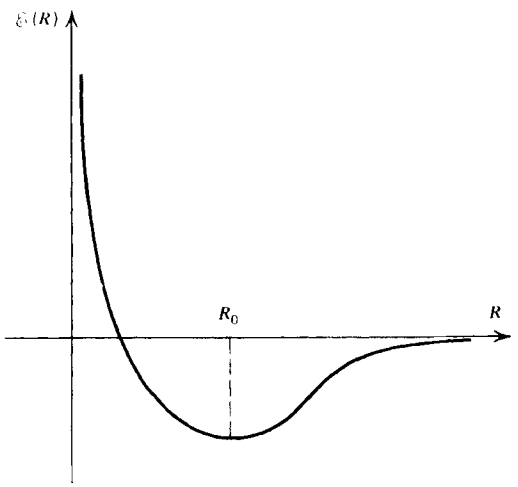

Figure 11.1 Potential between two atoms in a molecule as a function of their separation R.

nucleus from its equilibrium position and ω is the frequency of vibration. When ξ is of order a the electronic energies must change to something of order $\hbar^2/2ma^2$, so we set

$$\frac{1}{2}M\omega^2a^2 \sim \frac{\hbar^2}{2ma^2},$$

so that

$$E_{\text{vib}} \sim \hbar\omega \sim \left(\frac{m}{M}\right)^{1/2}\frac{\hbar^2}{ma^2} \sim \left(\frac{m}{M}\right)^{1/2}E_{\text{elect}}. \tag{11.2}$$

These energies are typically tenths or hundredths of an eV, lying in the *infrared.*

The nuclei can also rotate about each other. Let us estimate the energies involved in such motions. If the angular momentum of this motion is $l\hbar$ ($l=0,1,2,\ldots$), then the energy of rotation is

$$E_{\text{rot}} \sim \frac{\hbar^2 l(l+1)}{2I}, \tag{11.3}$$

where I is the moment of inertia of the molecule: $I \sim Ma^2$. Thus for small values of l (low-lying rotational states)

$$E_{\text{rot}} \sim \left(\frac{m}{M}\right)E_{\text{elect}}. \tag{11.4}$$

These energies are of order 10^{-3} eV, lying in the far infrared or *radio.*

The various energies of the molecule are approximately additive

$$E = E_{\text{elect}} + E_{\text{vib}} + E_{\text{rot}}, \tag{11.5}$$

and the contributions are in the approximate ratios

$$E_{\text{elect}} : E_{\text{vib}} : E_{\text{rot}} = 1 : \left(\frac{m}{M}\right)^{1/2} : \frac{m}{M}. \tag{11.6}$$

11.2 ELECTRONIC BINDING OF NUCLEI

We give below a couple of simple examples in which approximate solutions are found for the molecular potential as a function of separation

distance of the nuclei. These solutions provide qualitative understanding of the nature of the potential minimum.

The H_2^+ Ion

The simplest molecule is H_2^+, formed when two protons are held together by one electron. The Hamiltonian for the ion is, in the same units as Eq. (9.8),

$$H = -\frac{\nabla^2}{2} - \frac{1}{|\mathbf{r}-\mathbf{R}_A|} - \frac{1}{|\mathbf{r}-\mathbf{R}_B|} + \frac{1}{|\mathbf{R}_A-\mathbf{R}_B|} \tag{11.7}$$

(see Fig. 11.2). We have neglected the kinetic energy of the nuclei and have assumed that their positions are fixed. This problem can be treated approximately by a variational method. We assume that the electron is in a state that is a superposition of two hydrogen atomic states, each centered on a different nucleus:

$$\psi(\mathbf{r}) = \alpha\psi_A(\mathbf{r}) + \beta\psi_B(\mathbf{r}), \tag{11.8}$$

where, for ψ_A and ψ_B both ground states [cf. Eq. (9.16)]

$$\psi_A(\mathbf{r}) = \pi^{-1/2}e^{-|\mathbf{r}-\mathbf{R}_A|}, \tag{11.9a}$$

$$\psi_B(\mathbf{r}) = \pi^{-1/2}e^{-|\mathbf{r}-\mathbf{R}_B|}. \tag{11.9b}$$

The potential is symmetric about the midpoint of the molecule $(\mathbf{R}_A + \mathbf{R}_B)/2$, so we can classify the states by their parities: thus either $\alpha = \beta$ or

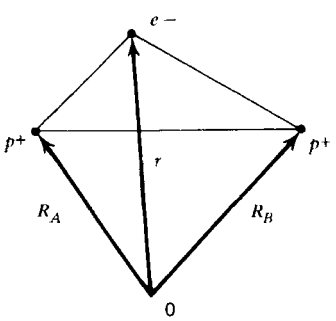

Figure 11.2 Schematic illustration of the location of particles in an H_2^+ ion.

$\alpha = -\beta$, and we can write

$$\psi_{\pm}(\mathbf{r}) = C_{\pm}\left[\psi_A(\mathbf{r}) \pm \psi_B(\mathbf{r})\right]. \tag{11.10}$$

The normalization constant $C_{\pm}$ must be found by integrating $|\psi_{\pm}(\mathbf{r})|^2$ over all space:

$$1 = \int |\psi_{\pm}(\mathbf{r})|^2 d^3\mathbf{r} = |C_{\pm}|^2 \int |\psi_A(\mathbf{r}) \pm \psi_B(\mathbf{r})|^2 d^3\mathbf{r}.$$

Thus we obtain for $C_{\pm}$

$$|C_{\pm}|^{-2} = 2 \pm 2S(R), \tag{11.11}$$

where $S(R)$ is the *overlap integral*

$$\begin{aligned} S(R) &\equiv \mathrm{Re} \int \psi_A^*(\mathbf{r}) \psi_B(\mathbf{r}) d^3r \\ &= \left(1 + R + \tfrac{1}{3}R^2\right) e^{-R}, \end{aligned} \tag{11.12}$$

and where

$$R \equiv |\mathbf{R}_A - \mathbf{R}_B|. \tag{11.13}$$

Equation (11.12) is derived in problem 11.2. A quite similar evaluation applies to the other integrals below (see Baym, 1969). Choosing $C_{\pm}$ to be real, we obtain

$$C_{\pm} = \left[2 \pm 2S(R)\right]^{-1/2}. \tag{11.14}$$

The expectation value of H is

$$\begin{aligned} \langle H_{\pm} \rangle \equiv \varepsilon_{\pm}(R) &= \int \psi_{\pm}^* H \psi_{\pm} \, d^3\mathbf{r} \\ &= \frac{\langle A|H|A\rangle + \langle B|H|B\rangle \pm 2\langle A|H|B\rangle}{2 \pm 2S(R)}, \end{aligned} \tag{11.15}$$

where

$$\begin{aligned} \langle A|H|A\rangle &\equiv \int \psi_A^*(\mathbf{r}) H \psi_A(\mathbf{r}) d^3\mathbf{r} \\ &= \langle B|H|B\rangle = -\frac{1}{2} + (1 + R^{-1}) e^{-2R}. \end{aligned} \tag{11.16}$$

Note the $1/R$ term, arising from the repulsive force of the nuclei at small distances and causing large positive energies at small R. The term $-\frac{1}{2}$ is the energy of the $1s$ state of atomic hydrogen (in atomic units). Also, we have the result

$$\langle A|H|B\rangle \equiv \mathrm{Re}\int \psi_A^* H\psi_B\, d^3r$$

$$= \left(-\tfrac{1}{2} + R^{-1}\right)S(R) - \mathrm{Re}\int \psi_A^* |\mathbf{r}-\mathbf{R}_B|^{-1}\psi_B\, d^3\mathbf{r}. \quad (11.17)$$

The integral here is the *exchange integral*

$$\int \psi_A^* |\mathbf{r}-\mathbf{R}_B|^{-1}\psi_B\, d^3\mathbf{r} = (1+R)e^{-R}. \quad (11.18)$$

Plotting the sum of all these terms we have two curves of $\varepsilon_{\pm}(R)$, one for even, one for odd parity (see Fig. 11.3). We seek a minimum of these curves with respect to R. The odd parity state has no minimum, and therefore, there is no bound molecular state with odd parity. However, an even parity state does exist at internuclear separation 1.3 Å and at a relative binding of -1.76 eV. Experimentally, it is found that $R_0 = 1.03$ Å and $\Delta E = -2.8$ eV, which is some indication of the crudeness of our approximations.

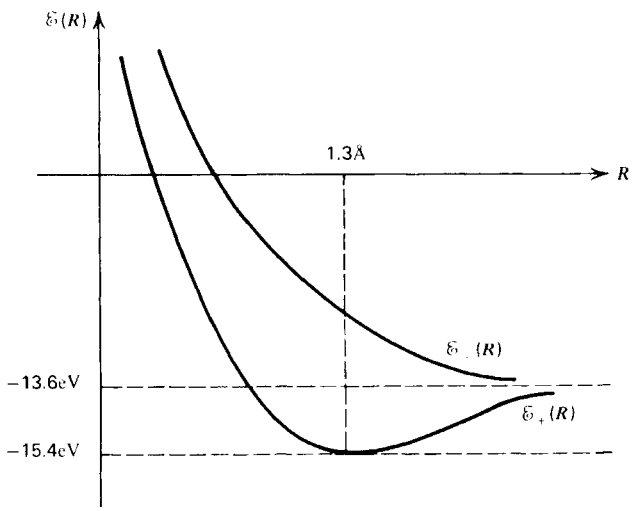

***Figure 11.3** Energy of an H_2^+ ion as a function of the proton separation R. ε_+ and ε_- denote the even and odd parity solutions.*

A single electron wave function is called a molecular *orbital.* In particular, a molecular orbital such as $\psi_{\pm}$, chosen to be a *l*inear *c*ombination of *a*tomic *o*rbitals, is called *LCAO.* Orbitals such as ψ_+ are called *bonding orbitals*, and orbitals such as ψ_- are called *antibonding orbitals.*

In this case we can understand the reason why ψ_+ is a bonding orbital and ψ_- is not. Since ψ_- has odd parity, it vanishes at the midpoint of the molecule; but even stronger, it vanishes everywhere on the midplane because of rotational symmetry around the internuclear line. Thus the electron has a low probability of being between the two nuclei where it can perform a bonding function. On the other hand, ψ_+ is larger along the midplane, which leads to a higher concentration of the electron there, and this in turn produces the bonding.

When R is large, we simply have a wave function that is a superposition of two separated hydrogen atoms in $1s$ states. Since the wave functions do not overlap, this is equivalent to saying that the electron can be bound to either proton with equal probability. The energy of this state is correctly given by the above wave functions, since we have constructed it out of exact $1s$ functions, having the exponential form $e^{-|\mathbf{r}-\mathbf{R}|}$.

In the opposite limit, when $R \to 0$, the two protons come together, and we have a He^+ atom. The electronic energy of this case is not well approximated by our wave function, because the exponential for He^+ should be $e^{-2|\mathbf{r}-\mathbf{R}|}$. For this reason the binding of the electrons to the protons is underestimated by our wave functions near $R=0$. This explains why we obtained a binding energy significantly less than the experimental value. Some account of this can be made by taking modified atomic orbitals that have an arbitrary scaling factor η, $\psi_A(r) \to \psi_A(\eta r)$ and by using η as a variational parameter. In our case this makes the wave functions correct at $R=0$ and improves the binding energy estimate.

The H_2 Molecule

The next simplest molecule is the neutral hydrogen molecule H_2. Because of the two electrons, we must take account of the Pauli principle. As a first approximation let us take two molecular orbitals for the H_2^+ molecule and form a wave function from these. Since we are concerned with finding the ground state, we expect that we want two *binding* orbitals of the type ψ_+. The space part of the wave function will then be symmetric; thus we must choose an antisymmetric spin part, that is, the singlet spin state. Thus choose

$$\psi_s(1,2) = \frac{1}{2[1+S(r)]}[\psi_A(\mathbf{r}_1)+\psi_B(\mathbf{r}_1)][\psi_A(r_2)+\psi_B(\mathbf{r}_2)]\chi_s.$$

There is a difficulty with this wave function that can be seen when we expand out the space parts:

$$\psi_s \propto [\psi_A(\mathbf{r}_1)\psi_A(\mathbf{r}_2)+\psi_B(\mathbf{r}_1)\psi_B(\mathbf{r}_2)]+[\psi_A(\mathbf{r}_1)\psi_B(\mathbf{r}_2)+\psi_A(\mathbf{r}_2)\psi_B(\mathbf{r}_1)].$$

Let us examine the meaning of these terms as $R\to\infty$. The first set of terms correspond to a proton plus a H^- ion, while the second set corresponds to two separated H atoms. We know that the binding of the H^- ion is very weak, so that we expect that it is the second set of terms that will lead to strong binding in H_2, and not the first set. Since we are doing a variational calculation of sorts, we are at liberty to use any information we have to bring to bear on the selection of trial functions. Thus we simply eliminate the first set of terms; this gives the *valence bond* or *London–Heiter* method (as opposed to the molecular orbital method):

$$\psi_s(1,2)=\frac{1}{\sqrt{2(1+S^2)}}[\psi_A(\mathbf{r}_1)\psi_B(\mathbf{r}_2)+\psi_A(\mathbf{r}_2)\psi_B(\mathbf{r}_1)]\chi_s. \qquad (11.19)$$

Note that the normalization is now dependent on the square of the overlap integral S. Note also that this state has even parity. A similar result

$$\psi_t(1,2)=\frac{1}{\sqrt{2(1-S^2)}}[\psi_A(\mathbf{r}_1)\psi_B(\mathbf{r}_2)-\psi_A(\mathbf{r}_2)\psi_B(\mathbf{r}_1)]\chi_t \qquad (11.20)$$

holds for the triplet states. This state has odd parity.

With these trial functions the internuclear potentials can be computed as before. The details are complicated, however, and are omitted. The results are quite similar in form to Fig. 11.3. The curve $\varepsilon_+(R)$ has a minimum at a value less than -27.2 eV, which is the value for two separated H atoms. Thus a H_2 molecule can exist in the singlet spin state.

Similar problems to those in the H_2^+ molecule occur here when we go to the limit $R\to 0$. The electronic states should approach the ground state of the He atom, but because our wave functions have been defined in terms of H-like functions, this limit is rather badly approximated. Similar rescaling can be used to improve the results. Extensive variational calculations have been done on H_2, and the results compare extremely well to experiment.

One seeming contradiction implied by the above results is that for atoms we argued that electrons with aligned spins (large total spin) led to the lowest Coulomb energies and thus to the tightest binding. Now we find that it is the low spin (singlet) state that binds, while the triplet state does not. This paradox is explained by the fact that for molecules it is the

electron density between the nuclei that leads to binding and this effect outweighs the lower interelectron Coulomb energy in the high spin states.

Another point of interest involves the large R behavior of the internuclear potential. In a second-order perturbation expansion it is found that two H-atoms will attract each other with a R^{-6} *Van der Waals* potential. Thus the triplet curve eventually becomes attractive at large R. However, the depth of the resulting potential is insufficient to lead to binding in H_2, although it can lead to binding in other molecules.

11.3 PURE ROTATION SPECTRA

Energy Levels

In the ground state a diatomic molecule is very near to the bottom of the potential between two nuclei. (Because of zero point motions we cannot say that they are precisely at the bottom.) In this state the easiest way to excite it into higher energy states is to cause the molecule to rotate. This follows from the discussion of §11.1, where it was shown that the energy required to excite a vibrational mode or an electronic state was much greater than typical rotation energies. Therefore, it is possible to have transitions solely among the rotational states when the molecule is in its lowest vibrational and electronic states. Such transitions give rise to a *pure rotational spectrum*, which typically lies in the radio or far-IR regimes.

Since the moment of inertia of a diatomic molecule around the line connecting the nuclei is negligible, the appropriate axis of rotation to consider is perpendicular to this line, through the center of mass of the two nuclei. The moment of inertia about this axis is

$$I = \mu r_0^2, \tag{11.21}$$

where r_0 is the equilibrium internuclear distance, and μ is the reduced mass, defined below. If we denote by $\mathbf{K}$ the angular momentum operator for rotation, then the Hamiltonian is $H = (1/2I)\mathbf{K}^2$, which leads to the energy eigenvalues

$$E_K = \frac{\hbar^2}{2I} K(K+1). \tag{11.22}$$

Corrections to this essentially classical formula can be found by considering the radial wave equation for the nuclei of a diatomic molecule,

$$\frac{1}{r^2}\frac{d}{dr}\left(r^2\frac{d\psi}{dr}\right) + \frac{2\mu}{\hbar^2}\left[E - V_n(r) - \frac{\hbar^2 K(K+1)}{2\mu r^2}\right]\psi = 0, \tag{11.23}$$

where μ is the reduced mass of the diatomic molecule

$$\mu \equiv \frac{M_1 M_2}{M_1 + M_2}. \tag{11.24}$$

Here M_1 and M_2 are the masses of the two nuclei and r is their separation; $V_n(r)$ is the potential of the nuclei, in electronic state n; and K is the angular momentum quantum number of the molecule.

Vibrational and rotational energy levels of the molecule may be approximately calculated by expanding the "effective potential"

$$U_n \equiv V_n + \frac{\hbar^2 K(K+1)}{2\mu r^2} \equiv V_n + V_K \tag{11.25}$$

about its minimum in a Taylor series. Letting r_0 and r_K be the equilibrium radii of V_n and U_n respectively, that is, $\partial V/\partial r|_{r_0} = 0$ and $\partial U_n/\partial r|_{r_K} = 0$ and letting the " spring constant" k_{n0}, A_n and V_{n0} be defined by

$$V(r) \sim V_{n0} + \tfrac{1}{2} k_{n0}(r - r_0)^2 + A_n(r - r_0)^3 + \cdots, \tag{11.26}$$

one obtains for r_K

$$r_K = r_0 + \frac{\hbar^2 K(K+1)}{k_n \mu r_0^3} + O\left(\frac{V_k}{V_n}\right)^2. \tag{11.27}$$

An approximate expression for $U_n(r)$ is then

$$\begin{aligned} U_n(r) = V_{n0} &+ \frac{\hbar^2 K(K+1)}{2\mu r_K^2} \\ &+ \tfrac{1}{2}\left[k_{n0} + \frac{3\hbar^2 K(K+1)}{\mu r_K^4}(1 + 2A_n r_K/k_n)\right](r - r_K)^2 + \cdots \end{aligned} \tag{11.28}$$

Note that Eq. (11.22), derived classically, has the same form as the first two terms of $U_n(r)$, which define *rotational energy levels* E_{nk} satisfying [cf. Eq. (11.28)]

$$\begin{aligned} E_{nk} &= V_{n0} + \frac{\hbar^2 K(K+1)}{2\mu r_k^2} \\ &\approx V_{n0} + \frac{\hbar^2 K(K+1)}{2\mu r_0^2}\left[1 - \frac{2\hbar^2 K(K+1)}{k_n \mu r_0^4}\right]. \end{aligned} \tag{11.29}$$

The second term in brackets [cf. Eqs. (11.28) and (11.29)] corresponds to a stretching of the molecule in response to centrifugal forces, which increases the moment of inertia and therefore decreases the kinetic energy of rotation for fixed angular momentum.

Selection Rules and Emission Frequencies

Whether a transition between two K values can be accompanied by the emission or absorption of radiation is governed by *selection rules*. For dipole radiation there are two such rules:

1. $d \neq 0$ (11.30a)
2. $\Delta K = -1$ (emission) or $\Delta K = +1$ (absorption). (11.30b)

Here d is the *permanent dipole moment* of the molecule:

$$d \equiv Z_1 e r_1 + Z_2 e r_2 + d_e, \tag{11.31}$$

where d_e is the electronic contribution.

These selection rules can be understood physically. A rotating system will radiate classically only if its dipole moment changes. Clearly, if $d = 0$, it cannot radiate classically, which explains the first rule. The second

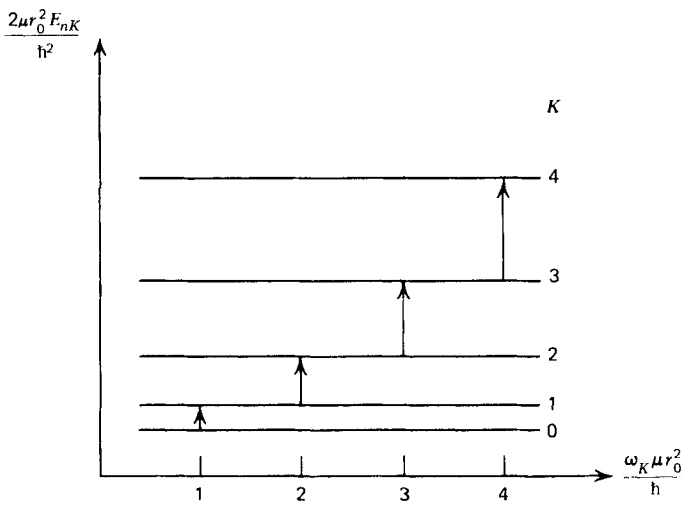

***Figure 11.4** Term diagram for energy levels and frequencies in pure rotational transitions.*

follows from angular momentum considerations, essentially identical to those leading to the selection rule of Eq. (10.40). See also Problem 10.6.

An immediate consequence of rule 1 is that a *homonuclear diatomic molecule cannot show pure rotation spectrum in the dipole approximation* [cf. Eq. (11.31)]. This rules out molecules such as H_2, O_2, C_2, although weak pure rotation spectra due to higher order radiation have been observed.

Rule 2 allows us to immediately write down the emission frequencies for rotational transitions [cf. Eqs. (11.29)]:

$$\omega_K \equiv \frac{E_{nK+1} - E_{nK}}{\hbar} = \frac{\hbar(K+1)}{\mu r_0^2}\left[1 - \frac{4\hbar^2(K+1)^2}{k_n \mu r_0^4}\right]. \tag{11.32}$$

This can also be depicted in a term diagram in Fig. 11.4. The frequencies are almost equidistant, but get slightly closer together with high K.

11.4 ROTATION-VIBRATION SPECTRA

Energy Levels and the Morse Potential

Because the energies required to excite vibrational modes are much larger than those required to excite rotation, it is unlikely to have a pure vibrational spectrum in analogy to the pure rotational spectrum. There is, instead, what is called a *rotation-vibration spectrum*, in which both the vibrational state and the rotational state can change together. We can, however, consider cases in which the electronic state remains the same.

The third term in $U_n(r)$ of Eq. (11.28) is the potential of a harmonic oscillator, leading to *vibrational energy* levels

$$E_{nv} = \hbar\omega_{nK}\left(v + \tfrac{1}{2}\right)$$

$$\omega_{nK} \approx \mu^{-\frac{1}{2}}\left[k_{n0} + \frac{3\hbar^2 K(K+1)}{\mu r_0^4}(1 + 2A_n r_K/k_n)\right]^{1/2}. \tag{11.33}$$

Here v is the harmonic oscillator quantum number, $v = 0, 1, 2, \ldots$

The above vibrational energy levels are those of a harmonic oscillator and result from the approximate expansion of the potential up to quadratic displacements from equilibrium. A more exact treatment clearly must include cubic, quartic, and higher order terms in the potential. Alternatively, the potential $U_n(r)$ may be approximated by a closed analytic expression which is both accurate and simple. An expression of this form

has been proposed by Morse (1929):

$$U_n(r) = U_{n0} + B_n\{1 - \exp[-\beta_n(r - r_0)]\}^2, \tag{11.34}$$

where B_n, β_n, and r_0 are three parameters that must be properly chosen to fit the observed potential curve. The energy eigenvalues (relative to the potential minimum U_{n0}) corresponding to this potential may be solved for exactly and are

$$E_{nv} = \hbar\omega_{n0}\left(v + \tfrac{1}{2}\right) - \frac{\hbar^2\omega_0^2}{4B_n}\left(v + \tfrac{1}{2}\right)^2, \tag{11.35a}$$

where

$$\omega_{n0} = \beta_n\left(\frac{2B_n}{\mu}\right)^{1/2}. \tag{11.35b}$$

Note that the first term in E_{nv} corresponds to a simple harmonic oscillator, coming from the first nonconstant term in an expansion of the Morse potential about its minimum. The vibrational quantum number v is an integer lying in the range

$$0 \leqslant v \leqslant \frac{(2\mu B_n)^{1/2}}{\beta_n\hbar} - \tfrac{1}{2}. \tag{11.36}$$

The upper limit corresponds to the condition $\partial E/\partial v = 0$. Two properties of vibrational levels correctly predicted by Eqs. (11.35) and (11.36) of the Morse potential are that there are a finite number of discrete vibrational levels below B_n and that the energy levels are more closely spaced with increasing v.

Selection Rules and Emission Frequencies

The selection rules for vibration-rotation transitions are:

1. $d \neq 0$ (11.37a)
2. $\left.\dfrac{d(d)}{dr}\right|_{r=r_0} \neq 0$ (11.37b)
3. $v = -1$ (emission) or $v = +1$ (absorption) (11.37c)
4. $K = \pm 1$ for $\Lambda = 0$
   $K = \pm 1, 0$ for $\Lambda \neq 0$. (11.37d)

Here Λ is the component of electronic orbital angular momentum along the internuclear axis (figure axis). The electronic states $\Lambda = 0, 1, 2, 3, \ldots$ are denoted by Σ, Π, Δ, $\Phi, \ldots$, respectively, in analogy with atomic spectroscopic notation.

The second of these rules requires that d change during a change in vibrational state. The third is the familiar rule from quantum theory for harmonic oscillators. The fourth rule is more complicated. Changes in the vibrational state of the molecule do not affect its parity, which must change in a dipole transition (§10.4). For $\Lambda = 0$, the parity is determined completely by the rotational quantum number K, and we obtain the same selection rule as in the pure rotational transitions, Eq. (11.30b). For $\Lambda \neq 0$,

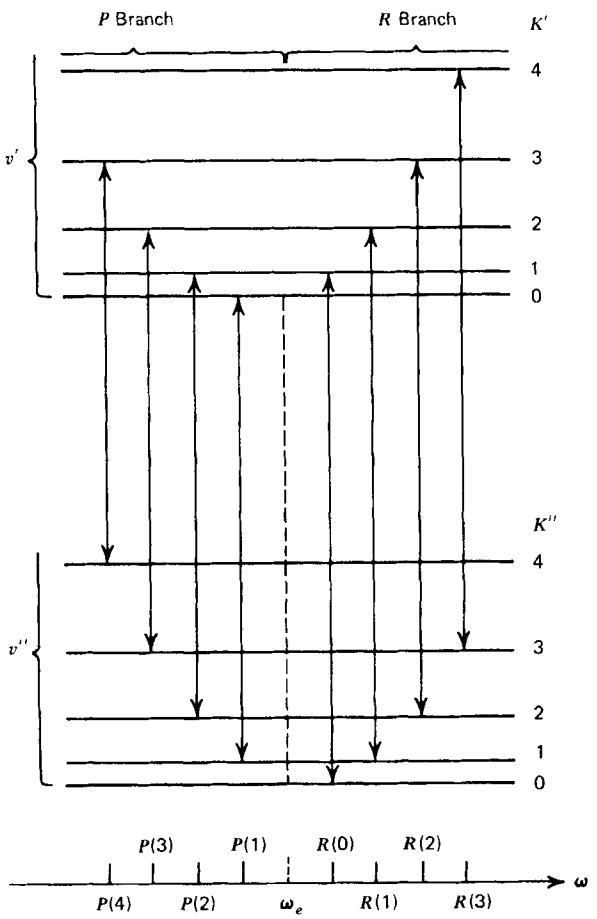

Figure 11.5 Term diagram for P and R branches in vibrational transitions. Here v and K are vibrational and rotational quantum numbers.

however, each rotational level splits into two almost degenerate levels, corresponding to the two possible signs of Λ. This is called Λ *doubling*. These two levels have opposite parity, thus allowing an overall change of parity even when $\Delta K = 0$.

Note that in either emission or absorption, both $\Delta K = +1$ and $\Delta K = -1$ are allowed, because the majority of the total energy change is in the vibrational transition. This allows a classification of the rotational "fine-structure" according to the change in K as follows

$$\Delta K = -1 : R \text{ branch} \tag{11.38a}$$

$$\Delta K = +1 : P \text{ branch} \tag{11.38b}$$

$$\Delta K = 0 : Q \text{ branch (when allowed).} \tag{11.38c}$$

Here $\Delta K = K'' - K'$, where K' refers to the upper state, and K'' to the lower state. The P and R branches are illustrated in Fig. 11.5.

11.5 ELECTRONIC-ROTATIONAL-VIBRATIONAL SPECTRA

Energy Levels

An approximate expression for the energy levels of electronic states is

$$E_{n\upsilon J} = V_{n0} + \gamma_n \hbar^2 \Lambda^2 + \alpha_n \hbar J(J+1) + \left(\upsilon + \tfrac{1}{2}\right)\hbar\omega_n, \tag{11.39}$$

where Λ is the component of electron angular momentum $\mathbf{L}$ along the axis separating the two nuclei, $\mathbf{J} = \mathbf{K} + \mathbf{L}$ is the total angular momentum, and V_{n0}, γ_n, α_n, and ω_n are all constant for a given electronic state of quantum number n. The rotational and vibrational energies in Eq. (11.39) are similar to the forms discussed previously and are quite adequate approximations when electronic transitions occur (change in n).

Selection Rules and Emission Frequencies

The selection rules governing *electronic dipole transitions* in a diatomic molecule are:

1. $\Delta\Lambda = -1, 0, +1$ (11.40a)
2. $\Delta J = -1, 0, +1$, but $J = 0 \rightarrow J = 0$ is not allowed and $\Delta J = 0$ is not allowed if $\Lambda = 0 \rightarrow \Lambda = 0$. (11.40b)
3. $\Delta\upsilon =$ any positive or negative integer. (11.40c)

Since the dipole transition is an electronic one, there is no restriction on υ.

Again, as in vibrational spectra, we can consider emission frequencies for transitions in which $\Delta J = -1$, the R branch, $\Delta J = 0$, the Q branch, and $\Delta J = +1$, the P branch:

$$\omega_{n\upsilon J} = \frac{E_{n\upsilon J} - E_{n'\upsilon'(J+\Delta J)}}{\hbar}$$

$$\equiv \omega_{nn'} + \upsilon\omega_n - \upsilon'\omega_{n'} + H(J), \tag{11.41}$$

$$H(J) = \begin{cases} (J+1)[J\alpha_n - (J+2)\alpha_{n'}], & P \quad \text{(11.42a)} \\ (\alpha_n - \alpha_{n'})J(J+1), & Q \quad \text{(11.42b)} \\ J[(J+1)\alpha_n - (J-1)\alpha_{n'}], & R. \quad \text{(11.42c)} \end{cases}$$

The dominant term in Eq. (11.41) is $\omega_{nn'}$, a frequency corresponding to the difference in a potential energy of the minima of two curves of the form of Fig. 11.6. The vibrational and rotational terms are successively finer structures on the electronic levels. For given n and n' (and hence, given $\omega_{nn'}$, ω_n and $\omega_{n'}$) Eq. (11.41) indicates that the vibrational fine structure forms a *progression* of uniformly spaced frequencies. For a given n, n', υ, and υ', the rotational fine structure is superimposed on the vibrational structure to form a *band.*

Several interesting features are apparent from Eq. (11.42) and the selection rules on ΔJ. Selection rule 2. and the requirement that J be positive forbid $J = 0$ in both the Q and R branches, respectively. Furthermore, $\alpha_n/\alpha_{n'}$ is typically not an integer, so that the bracketed expression in

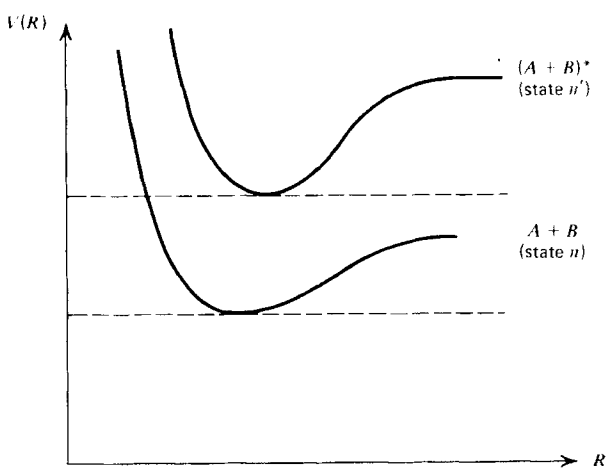

Figure 11.6 Potential energy as a function of nuclear separation of a molecule in its electronic ground state and in an excited electronic state.

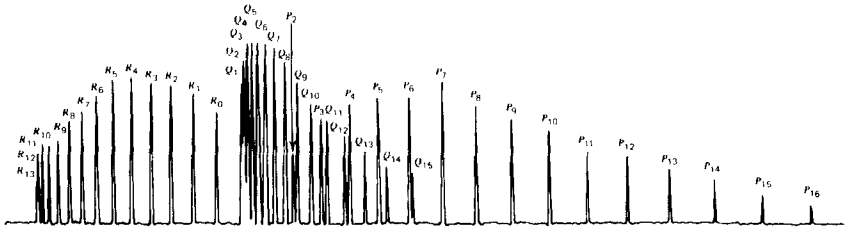

***Figure 11.7** Spectral lines observed in the molecule AlH, illustrating the P, R and Q branches. (Taken from Bingel, W. A. 1969, Theory of Molecular Spectra, Wiley, New York.)*

the P and R branch does not vanish for any value of J. Consequently, $H(J) \neq 0$ for all branches, and there is a missing line in the sequence at frequency $\omega_0 \equiv \omega_{nn'} + v\omega_n - v'\omega_{n'}$ termed, alternatively, the zero gap, null line, or band origin, as in the rotational-vibrational spectra. This is shown as the dotted line in Fig. 11.5. Since the Q and R branches converge on the null line as $J \to 0$ (the P branch converges on it as J is artificially extrapolated to -1), the null line may be used to identify the origin of J within a band.

Another striking feature of Eq. (11.42) is that the line spacing is quite nonuniform in J, in contrast to rotation-vibration levels. In the P and R

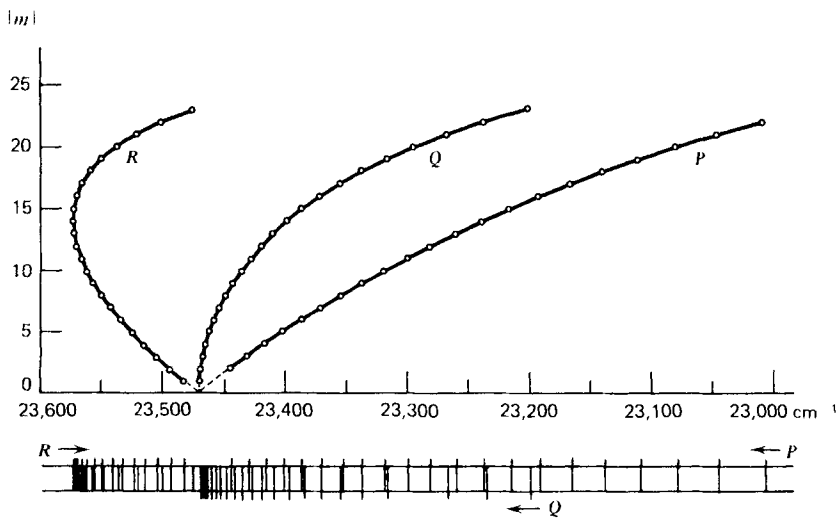

***Figure 11.8** Fortrat diagram for bands shown in Fig. 11.7. Here $|m| = J$, the total angular momentum quantum number. (Taken from Herzberg, G., 1950, Spectra of Diatomic Molecules, Van Nostrand, New York.)*

branches, the line spacing may not be montonic with J and can reverse at a particular value of $J \equiv J_{\text{head}}$, where $H(J)$ is at an extremum. Near J_{head}, the line spacing is relatively narrow; for J much bigger or smaller than J_{head}, the spacing gets broader. The result is a sharp edge at the boundary of the band, called the *band head.* It is straightforward to determine the location of the band head, and this is developed in Problems 11.3 and 11.4. Figure 11.7 below gives an observed band at 4241 Å in the spectrum of AlH. The lines are labeled according to R, Q and P, with subscripts indicating the J of the branch. Lines corresponding to R_{14}, R_{15}, and so on are not shown.

A theoretical plot of the location of the lines in the J-$\omega_{n\upsilon J}$ plane is called a *Fortrat diagram.* Figure 11.8 gives a Fortrat diagram of the same band shown in Fig. 11.7, where $|m| \equiv J$. Note that the R branch reverses at R_{13}, as is observed in the R band head of Fig. 11.7. Reversals do not occur in the Q and P branches for this spectrum, but the lowest frequency lines in the Q branch are similar in form to the band head in the R branch.

PROBLEMS

11.1—Consider an electrically neutral medium of diatomic molecules in thermal equilibrium at temperature T. Each molecule contains a nucleus of mass M_p and a nucleus of mass $2M_p$ at an equilibrium separation r_0.

a. Estimate r_0 in terms of fundamental constants.

b. Estimate the cross section σ_c for collisions between molecules.

c. It is experimentally observed that, as a function of mass density ρ of the medium, the line width of the rotational lines has the form shown in Fig. 11.9. If only Doppler and collisional broadening are present, estimate ρ_0 and show that it may be written completely in terms of fundamental constants, independent of M_p.

11.2—Derive Eq. (11.12).

11.3—Show that both the P and the R branches of the electronic-vibrational-rotational transitions, Eqs. (11.41), (11.42) may be combined into a single formula for the emission frequency of the form

$$\omega_{n\upsilon J} = \omega_{nn'} + \upsilon\omega_n - \upsilon'\omega_{n'} + j(\alpha_n + \alpha_{n'}) + j^2(\alpha_n - \alpha_{n'}),$$

where j ranges over both positive and negative integer values.

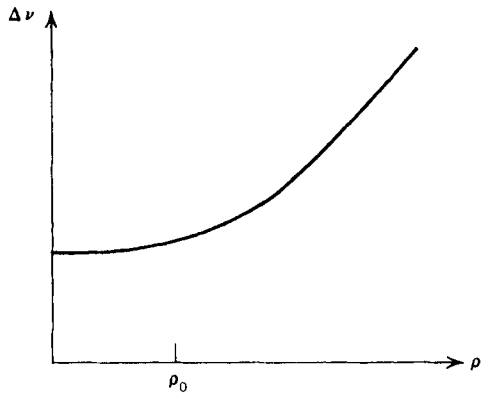

Figure 11.9 Line width as a function of density for emission from a medium of diatomic molecules.

11.4—Derive an expression for the J value and frequency of the band head in electronic-vibrational-rotational transitions, give the criteria for whether the band head occurs in the R or P branch, and give the criteria for whether the frequency of the band head lies above or below the band origin.

11.5—Show that the Q branch in electronic-vibrational-rotational transitions does not have a true band head but may have the observed appearance of one under certain conditions.

11.6—For the situation described in Problem 11.1, estimate, in terms of fundamental constants, the range in T over which purely rotational emission lines will be observed from a substantial fraction of the molecules.

REFERENCES

Baym, G. 1969, *Lectures on Quantum Mechanics*, (Benjamin, New York).
Bingel, W. A. 1969, *Theory of Molecular Spectra*, (Wiley, New York).
Leighton, R. B. 1959, *Principles of Modern Physics*, (McGraw-Hill, New York).
Herzberg, G. 1950, *Molecular Spectra and Molecular Structure, Vol.* 1, (Van Nostrand, New York).
Morse, P. M. 1929, *Phys. Rev.*, **34**, 57.